

STUDIES ON CARTILAGE AND
BONE DISEASE IN
MUCOPOLYSACCHARIDOSES
AND MUCOLIPIDOSES

Esmée Oussoren

**STUDIES ON CARTILAGE AND
BONE DISEASE IN
MUCOPOLYSACCHARIDOSES
AND MUCOLIPIDOSES**

E. Oussoren

The research presented in this thesis was financially supported by grants from ZonMw - the Netherlands Organization for Health Research and Development [projectnumbers 152001003 and 152001004], the European Union 7th Framework Programme 'Euclid' - a European Consortium for Lysosomal Storage Diseases [health F2/2008 grant agreement 201678] and the European Community's Seventh Framework Programme [FP7/2007-2013 - Meusix 304999].

Cover design and lay-out: © evelienjagtman.com

Printing: Ridderprint BV, Ridderkerk

ISBN: 978-94-6375-169-8

2018© E. Oussoren

© Copyright of the published articles is with the corresponding journal or otherwise with the author.

No parts of this thesis may be reproduced in any form by print, photo print, microfilm or any other means without permission from the author or the corresponding journal.

**STUDIES ON CARTILAGE AND
BONE DISEASE IN
MUCOPOLYSACCHARIDOSES
AND MUCOLIPIDOSES**

**Studies over kraakbeen en botziekte in
Mucopolysaccharidose en Mucolipidose**

Proefschrift

ter verkrijging van de graad van doctor aan de
Erasmus Universiteit Rotterdam
op gezag van de
rector magnificus
Prof. dr. R.C.M.E. Engels
en volgens besluit van het College voor Promoties.

De openbare verdediging zal plaatsvinden op
dinsdag 4 december 2018 om 11:30 uur

door

Esmeralda Oussoren
geboren te Zaandam

PROMOTIECOMMISSIE:

Promotor:

Prof. dr. A.T. van der Ploeg

Overige leden:

Prof. dr. I.M.J. Mathijssen

Prof. dr. R.M.W. Hofstra

Prof. dr. J.G. Leroy

Copromotoren:

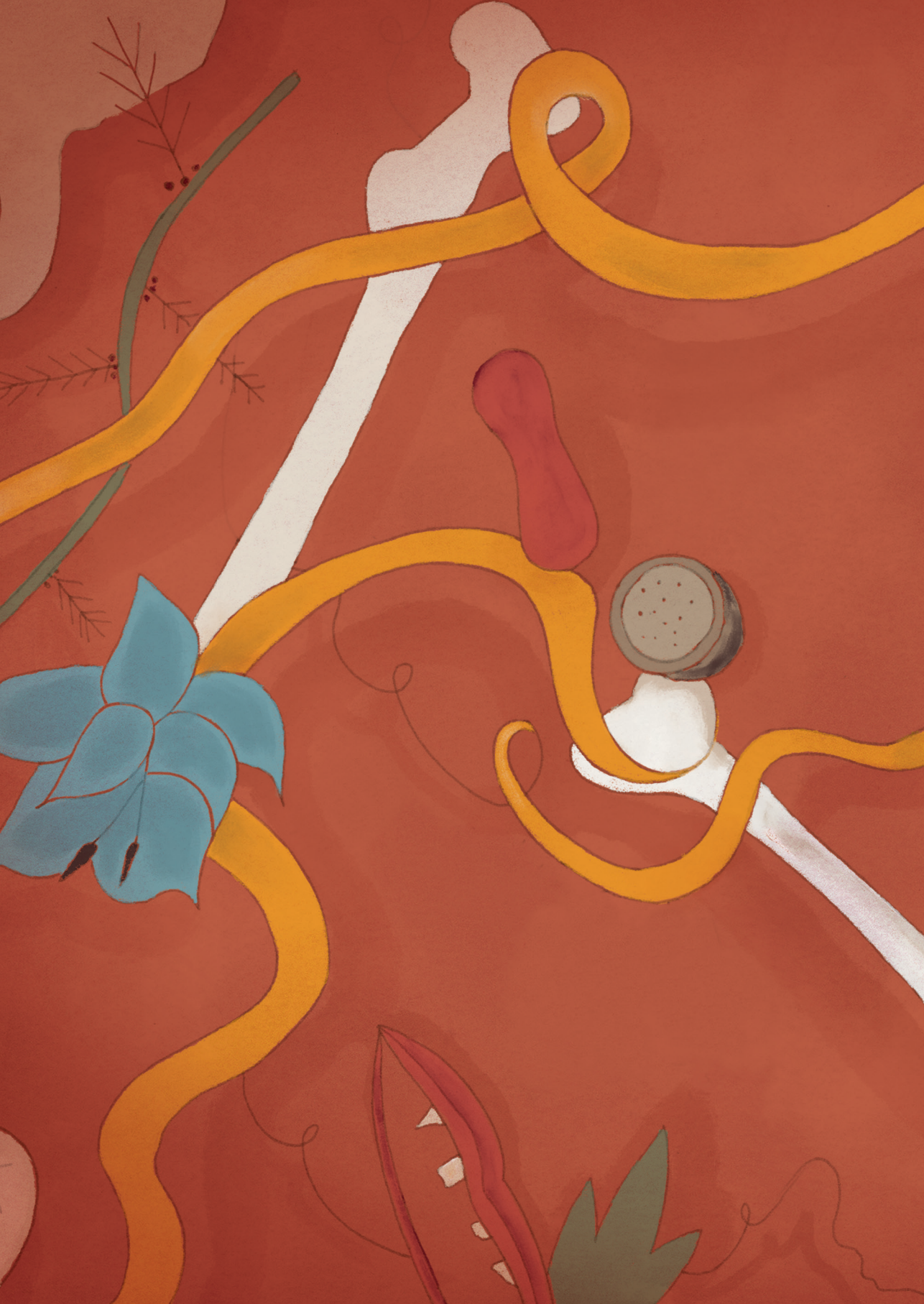
Dr. M. Langeveld

Dr. G.J.G. Ruijter

Voor mijn gezin

TABLE OF CONTENTS

Chapter 1	General Introduction	9
Chapter 2	Bones, joints and teeth development in Mucopolysaccharidoses; Relevance to therapeutic options <i>Biochim Biophys Acta</i> 2011;1812(11):1542-1556.	33
Chapter 3	A simple procedure to differentiate residual α -L-iduronidase activity in mild and severe MPS I <i>Molecular Genetics and Metabolism</i> 2013;109:377–381.	77
Chapter 4	A long term follow-up study of the development of hip disease in Mucopolysaccharidosis type VI <i>Mol Genet Metab</i> 2017;121(3):241-251.	93
Chapter 5	Mucopolipidosis type III, a series of adult patients <i>J Inherit Metab Dis.</i> 2018;41(5):839-848.	117
Chapter 6	Craniosynostosis affects the majority of mucopolysaccharidosis patients and can contribute to increased intracranial pressure <i>J Inherit Metab Dis.</i> 2018;Aug 6.	147
Chapter 7	Discussion	173
Addendum	Summary	205
	Samenvatting	211
	Acknowledgements Dankwoord	217
	Portfolio	221
	Curriculum vitae	227
	List of Publications	231

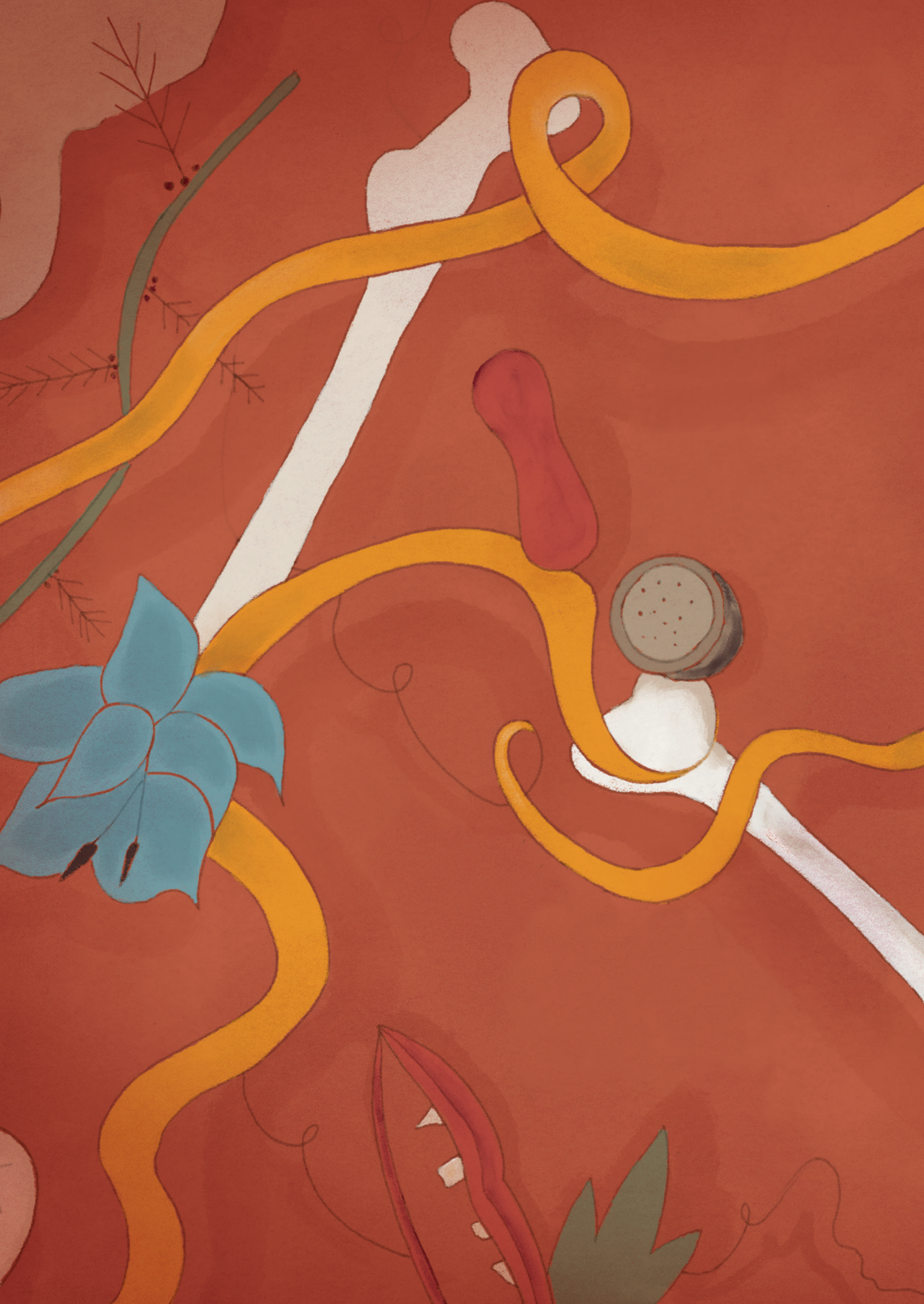


A stylized illustration on a red background. In the top left, a light-colored fetus is curled. In the center, a white skull is shown. To the right, a red flower with green leaves is depicted. In the bottom left, a white bone is visible. Yellow and orange ribbons swirl throughout the scene. The text 'CHAPTER 1' is centered in white, bold, sans-serif font.

CHAPTER 1

GENERAL
INTRODUCTION





The background is a deep red color. It features several stylized, hand-drawn illustrations. At the top left is a light-colored fetus in a curled position. Below it is a white skull. To the right of the skull is a white tooth with a red root and a green leaf. At the bottom left is a white bone. The entire scene is overlaid with thick, flowing yellow ribbons that swirl and loop across the page.

CHAPTER 2

BONES, JOINTS AND
TEETH DEVELOPMENT IN
MUCOPOLYSACCHARIDOSES;
RELEVANCE TO
THERAPEUTIC OPTIONS

E. Oussoren, M.M.M.G. Brands, G.J.G. Ruijter, A.T. van der Ploeg, A.J.J. Reuser

Biochim Biophys Acta 2011, **1812**(11):1542-1556

ABSTRACT

The mucopolysaccharidoses (MPS) are prominent among the lysosomal storage diseases. The intra-lysosomal accumulation of glycosaminoglycans (GAGs) in this group of diseases, which are caused by several different enzyme deficiencies, induce a cascade of responses that affect cellular functions and maintenance of the extra-cellular matrix. Against the background of normal tissue-specific processes, this review summarizes and discusses the histological and biochemical abnormalities reported in the bones, joints, teeth and extracellular matrix of MPS patients and animal models. With an eye to the possibilities and limitations of reversing the pathological changes in the various tissues, we address therapeutic challenges and present a model in which the cascade of pathologic events is depicted in terms of primary and secondary events.

INTRODUCTION

Mucopolysaccharidosis and glycosaminoglycans

The word Mucopolysaccharidosis (MPS) literally means “a disease in which viscous polysaccharides are being stored”. There are eleven such diseases, each caused by genetic deficiency of a different lysosomal enzyme involved in the degradation of these polysaccharides. The diseases are numbered from MPS I to MPS IX and named after the physicians who first described the syndromes or discovered the underlying enzyme deficiency (table 1) [1-9]. Chemically, the viscous polysaccharides are glycosaminoglycans (GAGs) that consist of long, un-branched chains of negatively charged amino sugars and uronic acids and have a very high capacity to bind water. Most are linked to a protein core (proteoglycan), form large complexes with hyaluronic acid and are the ground substance of connective tissues. Depending on the precise composition of the polysaccharide chain, the glycosaminoglycans have names such as dermatan sulfate, heparan sulfate, keratan sulfate, chondroitin sulfate and hyaluronic acid (table 1).

Table 1 Enzyme deficiencies and storage products in MPS

Number	Eponym	Enzyme deficiency	Storage product
I	Hurler/ Scheie	α -L-iduronidase	Heparan sulfate Dermatan sulfate
II	Hunter	Iduronate 2-sulfatase	Heparan sulfate Dermatan sulfate
III-A	Sanfilippo type A	Sulfamidase	Heparan sulfate
III-B	Sanfilippo type B	α -N-acetylglucosaminidase	Heparan sulfate
III-C	Sanfilippo type C	Acetyl-CoA; α glucosaminide N-acetyltransferase	Heparan sulfate
III-D	Sanfilippo type D	N-acetylglucosamine6-sulfatase	Heparan sulfate
IV-A	Morquio type A	Galactose 6-sulfatase	Keratan sulfate Chondroitin 6-sulfate
IV-B	Morquio type B	β -galactosidase	Keratan sulfate Chondroitin 6-sulfate
VI	Maroteaux– Lamy	N-acetylgalactosamine 4-sulfatase	Dermatan sulfate Chondroitin 4-sulfate
VII	Sly	β -glucuronidase	Heparan sulfate Dermatan sulfate Chondroitin 4-sulfate Chondroitin 6-sulfate
IX		Hyaluronidase	Hyaluronic acid

Connective tissue is composed of cells and extracellular matrix (ECM). The matrix is produced by the cells and consists of protein fibers (mainly collagen) and proteoglycans. It provides volume and function which is specified largely by its chemical composition. For instance, the connective tissue located directly under the epithelium of the skin and under the endothelium of the large blood vessels is loosely organized to provide a soft cushion that can absorb subtle transformation by pressure. In non-structural organs such as the liver, the connective tissue literally holds the hepatocytes together in a functional network of cell strains and blood sinuses. Articular cartilage (joints) is very rich in GAGs and can contain up to 80% water. This jelly-like substance is optimally structured to absorb pressure, but breaks up when traction is applied. It is thus unlike tendons, whose glycosaminoglycan content and cell density are low, but whose collagen content is high, with the collagen fibers also being laid in a single direction to transduce force. The connective tissue matrix of bone and teeth is mineralized. GAGs also serve as key biological response modifiers [10-12]. Like any other biological substance in the body, GAGs are continuously renewed. They are degraded by enzymes produced by the connective tissue cells, in part extracellularly and in part intracellularly in the lysosomes after uptake through endocytosis. Lack of degradation due to a lysosomal enzyme deficiency leads to intralysosomal GAG storage, followed by loss of cellular functions, tissue damage and organ dysfunction. This process determines the clinical symptoms observed in patients with mucopolysaccharidoses.

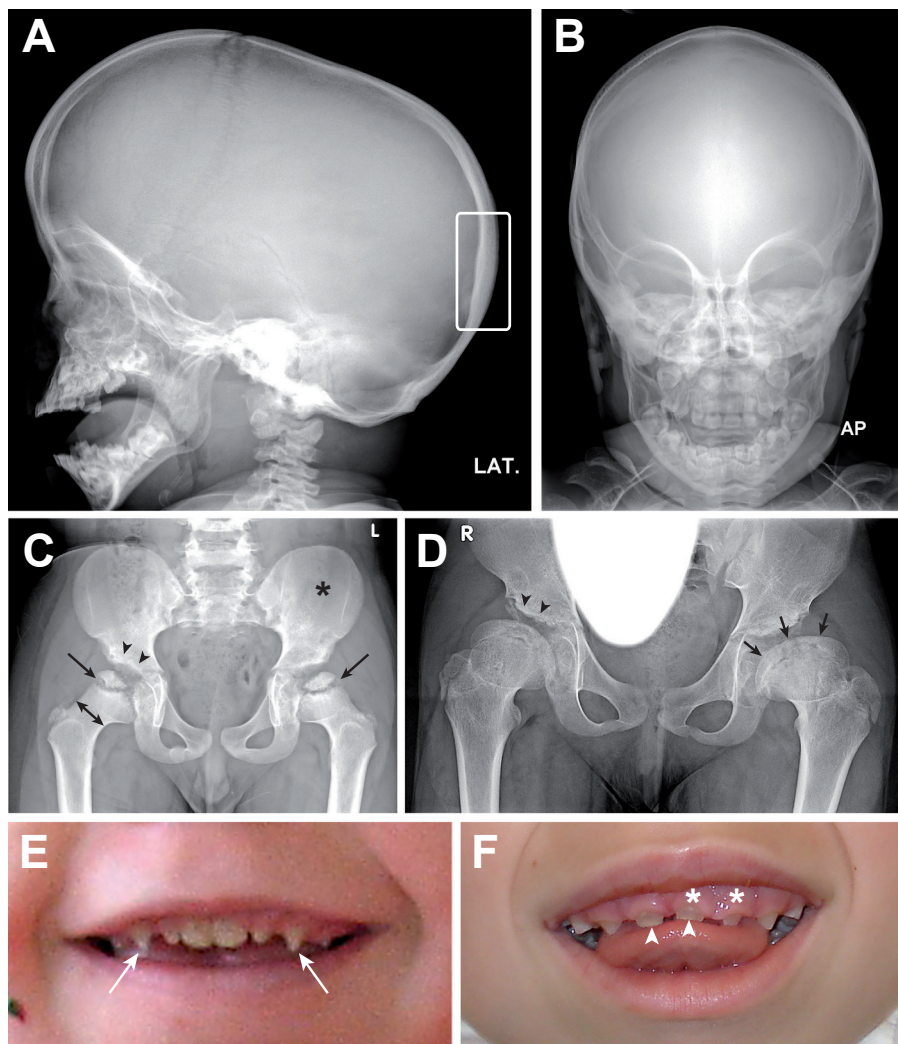
This review describes the processes underlying normal development of bone, joints and teeth in relation to abnormalities seen in MPS patients and MPS animal models and the therapeutic challenges these abnormalities present.

Bones, joints and teeth in MPS patients

As well as joint and dental problems, most patients with mucopolysaccharidoses have bone problems that cause skeletal deformities. Some of these clinical features are illustrated in figure 1. The bone and joint abnormalities were summarized recently [13].

Due mainly to lysosomal deposition of GAGs in the chondrocytes [14], the extracellular matrix (ECM) of the articular cartilage, the synovia and the surrounding tissues, MPS patients have stiff joints, contractures and poor mobility. Hyperlaxity of the joints can also occur. Together, these processes ultimately manifest as degenerative joint disease. Since the abnormalities develop early in life, they also interfere with normal growth which explains the typical short stature of most MPS patients (fig 2).

Before we introduce the pathophysiology of MPSs, the following paragraphs describe the normal development of bones, joints and teeth first.

Figure 1 Radiographs of the skull, pelvis and images of teeth in MPS**Fig.1 A and B)** Lateral and anterior-posterior radiograph of the skull of a two-year-old patient with MPS VI.

Note the atypical shape of the skull, (dolichocephalic) with partial craniosynostosis involving mainly the sagittal and the lambdoid sutures (not visible) and the thickened skull (rectangle).

C) Shows an X-ray of an eight-year-old patient with MPS VI. Note the irregularities of the epiphyses in the femoral heads. The growth plates of both femur heads are too small and lateralized (arrows). The neck of the caput femoris is broad and plump (two headed arrow) and in a valgus position. There is dysplasia of the acetabula (arrow heads); the right acetabulum is steep and shallow. The asterisk shows flaring of the wing of the os ileum.

D) Shows an X-ray of a ten-year-old patient with MPS VI. Note the deformed and flattened epiphyses of the femur (arrows) and the dysplastic acetabula (arrow heads).

E and F) Abnormal teeth in an eight-year-old and a six-year-old patient with MPS I. Both patients have hypoplastic peg-shaped teeth (arrows) and dysplastic teeth (arrow heads). The asterisks indicate gingival hyperplasia.

Figure 2 Growth chart MPS VI patient

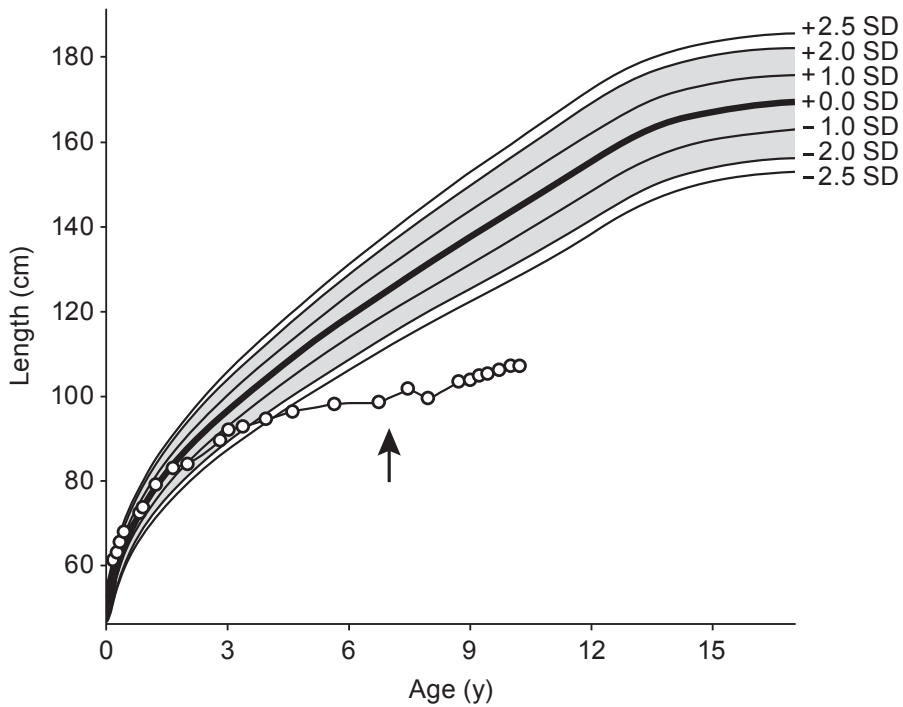


Fig. 2. The growth chart of a patient with MPS VI (open circles). Enzyme-replacement therapy was started at 7 years of age (arrow).

NORMAL DEVELOPMENT OF BONES, JOINTS AND TEETH

Bones

The human skeleton consists of bones that meet at joints and are held together by ligaments. To enable movement, tendons connect bones with muscles. Cartilage is part of the skeleton. It is found in joints and in the growth plate of immature long bones. The skeleton also serves as a scaffold and cage that supports and protects vital organs.

Bone tissue is a reservoir for calcium, phosphate and other ions and harbors the marrow, which is essential for blood-cell formation. Bone is maintained by osteocytes, each of which is directly connected to the circulatory system by thin cytoplasmic extensions running to the blood vessels through canaliculi (small tunnels in the calcified bone matrix). Together with osteoclasts, osteoblasts are instrumental in bone synthesis and bone remodeling.

In a process called endochondral ossification, long bones grow due to the proliferation and differentiation of chondroblasts in the growth plate of immature long bones; newly formed cartilage is replaced by bone as fast as it is formed. Flat bones are formed by the differentiation of mesenchymal cells to bone-forming osteoblasts in a process known as intramembranous ossification. Three types of cell are important for the formation, growth, renewal and maintenance of bone: osteoblasts, osteocytes and osteoclasts. Their roles and functions are detailed below.

Osteoblasts, the bone-forming cells, are of mesodermal origin. Originating from multipotent mesenchymal cells, they differentiate into osteocytes while synthesizing the organic components of the bone matrix (type I collagen, proteoglycans and glycoproteins). The young bone is deposited along the remnants of the cartilage of the growth plate and along pre-existing bone as an osteoid layer that turns into bone after calcification. The lifespan of an osteoblast ranges from one to two hundred days. Sixty to eighty percent die by apoptosis [15].

Osteocytes, the cells surrounded by calcified bone, have a very long lifespan of one to fifty years. Maintaining the bones throughout the skeleton, they are about ten times more numerous than the osteoblasts and a thousand times more numerous than the osteoclasts [15,16]. Housed in lacunae between lamellae of matrix, they maintain contact with each other and with cells at the bone surface through long, very thin dendritic processes that traverse the bone matrix [15]. A gel-like matrix surrounds the osteocytes and the dendritic processes. Oxygen, nutrients and waste products are transported through the canaliculi to and from the osteocytes by hydraulic vascular pressure, partly by diffusion and partly by the convection induced by mechanical forces.

Osteoclasts are created by the fusion and differentiation of cells from the monocyte macrophage cell lineage. They contain between five and fifty nuclei [17]. The lifespan of an osteoclast is approximately one to twenty-five days and they die by apoptosis [15].

Osteoclasts are bone-resorptive cells that play a crucial role in normal bone turnover. They adhere tightly to the bone surface where they create an extracellular lysosomal space [18] in which protons are secreted by the vacuolar H⁺-ATPase pump [19, 20]. The apical membrane of the polarized osteoclast opposing the bone is ruffled. It is into this membrane that lysosomal vesicles are inserted [21]. The bone minerals dissolve in the acidic environment of the extracellular space, paving the way for lysosomal proteases to degrade the organic components of the bone matrix [20, 21]. The degradation products are endocytosed at the ruffled border membrane and delivered to the basal membrane by transcytosis [22, 23].

Bone formation and remodeling

As stated briefly in the introduction, there are two ways in which bones are formed. Both processes involve the transformation of pre-existing mesenchymal tissue into bone tissue. In the process of intramembranous or desmal ossification, mesenchymal cells directly differentiate into osteoblasts that produce the bone matrix, which subsequently acquires its strength through mineralization. By contrast, endochondral ossification involves the primary deposit of a cartilage template which originates through mesenchymal cell differentiation and is gradually replaced by bone.

The growth of short bones and flat bones is achieved by intramembranous ossification. Compacted mesenchymal cells define an ossification center, which is surrounded by the periosteum, a thin layer of connective tissue with osteoprogenitor cells at the bone surface side and fibrogenic cells adjacent to the mesenchyme. The osteogenic cells differentiate into osteoblasts and continuously deposit new layers of lamellar bone against the preexisting bone [16, 24]. The formation of the skull is a typical example of intramembranous ossification (fig. 3).

The curved plates of young bone are surrounded by a single layer of osteoblasts and are deposited amid very loose mesenchymal tissue. During the process of embryonic development, the plates of bone are continuously reshaped as they grow. Osteoblasts and osteoclasts work in concert to obtain the proper curvature. Old bone is carved away from the inside and new bone is deposited on the outside. Defects in this process can lead to an abnormal shape of the skull, such as that seen in pycnodysostosis, which is caused by cathepsin K deficiency. The different plates of the skull fuse shortly after birth, forming an inflexible bony joint called synostosis.

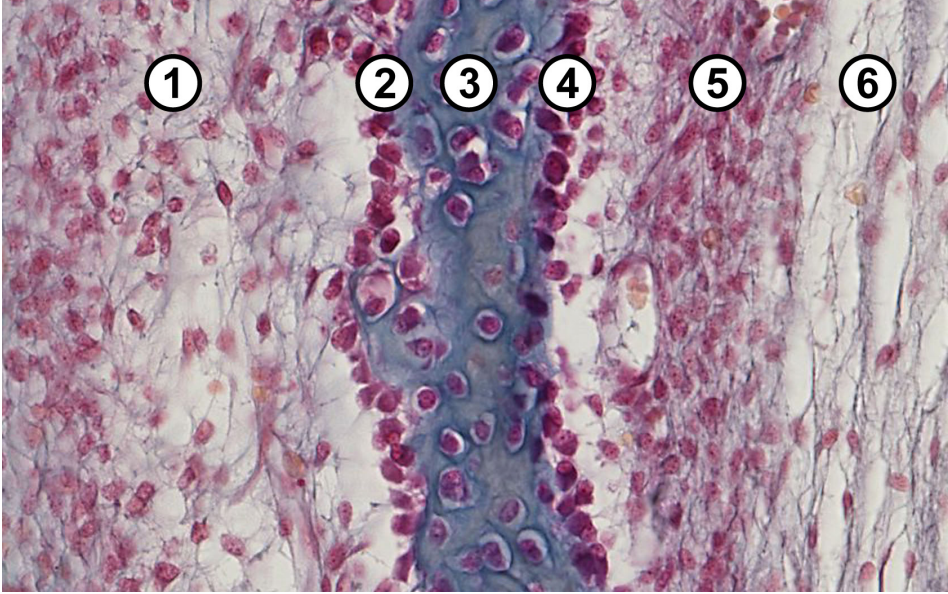
Figure 3 Intramembranous ossification

Fig. 3. Intramembranous ossification: 1 and 6) mesenchyme; 2 and 4) osteoblasts; 3) bone with osteocytes; 5) compacted mesenchyme with a blood vessel.

A role in intramembranous ossification is played by bone-morphogenetic proteins such as BMP2, BMP4 and BMP7. These are thought to activate transcription factor *Chfa1* in the mesenchymal cells, which are thus transformed into osteoblasts [25].

Rapid growth of long bones is achieved by endochondral ossification and requires the presence of a growth plate. The growth plates disappear towards adulthood, when length-wise bone growth stops, though bone widening may still occur. Skeletal long bones are initially deposited in the mesenchymal tissue as a cartilage template whose shape resembles a miniature version of the bone to be formed. When the cartilage template reaches a certain size, a collar of bone is deposited around the mid portion and blood vessels penetrate the cartilage structure.

Chondrocytes in the center enlarge and die through apoptosis. Osteoprogenitor cells, which are transported to this region by the blood vessel, differentiate into osteoblasts and form a primary ossification center which later becomes the diaphysis. Secondary ossification centers appear later at the thicker endings of the cartilage template. These become the epiphyses.

Until adolescence, the growth plate remains cartilage and separates the diaphysis from the epiphysis. Cartilage is also maintained at the endings of the bones where joints are formed. In this area, the mesenchymal cells that have formed the cartilage templates of opposing long bones migrate and differentiate, leaving either a cavity and forming a diarthrosis with free bone movement, or leaving a synarthrosis with little or no movement, such as syndesmosis, synchondrosis, or synostosis. The cavity of a diarthrosis is filled with synovial fluid produced by the synovial membrane protruding into the joint from the periphery. The fluid provides lubrication to the joint and nutrients to the avascular articular cartilage [16, 24].

The growth plate is divided into five zones: a resting zone, a proliferative zone, a hypertrophic zone, a calcified zone and an ossification zone. These start at the mid portion of the growth-plate and extend in two directions, with major growth taking place towards the diaphysis and minor growth towards the epiphysis (fig. 4) [16, 24].

The hypertrophic chondrocytes are degraded by osteoclasts. The osteoblasts, arising from osteoprogenitor cells, deposit uncalcified young bone (osteoid) against the remnants of the cartilage matrix. The mineralized bone trabeculae that are formed support the growth plate.

Many different factors are involved in endochondral ossification. GAGs have an important regulatory function. They interact in the FGFs, BMPs (as described below), TGF- β and the wiggles-type (Wnt) signaling pathways [26].

The extracellular matrix (ECM) of bone and cartilage; the role of GAGs

Fifty percent of the extracellular bone matrix consists of inorganic material: calcium, phosphorus, bicarbonate, citrate, magnesium, potassium and sodium. Calcium and phosphorus form hydroxyapatite crystals. The organic material in the matrix of bone consists of collagen type I fibers; in the cartilage, it consists of collagen type II fibers.

Large water-retaining proteoglycan aggregates (PG) fill the intervening spaces, interacting with the network of collagen fibers. The entire structure of cells and extracellular matrix is completed by various glycoproteins, such as chondronectin [16]. Homeostasis of the extracellular matrix depends on the balance between de novo synthesis and degradation of the matrix components, which is the primary responsibility of osteocytes and chondrocytes [27].

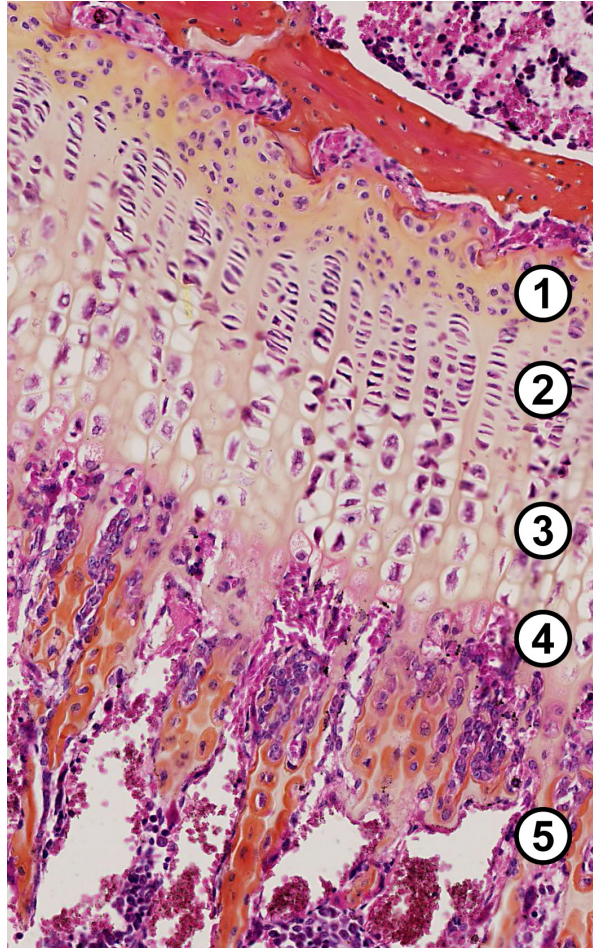
Figure 4 The epiphyseal growth plate

Fig. 4. The epiphyseal growth plate. 1) The resting zone: hyaline cartilage with chondrocyte progenitor cells. 2) The proliferative zone: chondrocytes undergo rapid mitosis and align into vertical columns. The columns are separated by septa of extracellular matrix consisting primarily of collagen (collagen type II) and proteoglycans. 3) The hypertrophic zone: chondrocytes mature and become hypertrophic. They contain large amounts of glycogen and start to secrete alkaline phosphates and collagen type X. The matrix is reduced to thin septa between the chondrocytes. 4) The calcified cartilage zone: concurrent with the death of chondrocytes, the thin septa of cartilage matrix are calcified by the deposition of hydroxyapatite. 5) The ossification zone: blood capillaries and osteoprogenitor cells invade the cavities left by the chondrocytes. The osteogenic cells form osteoblasts, which are distributed in a layer over the calcified septa. The osteoblasts deposit young bone (osteoid) on top of the three-dimensional calcified cartilage matrix (Mescher AL 'Junqueira's Basic Histology', Brighton et al. [24]). The bone matrix consists of collagen type I, GAGs and inorganic material (Ortega et al. [37]).

In cartilage, the collagen fibers are organized in a lacy network that provides tensile strength [28, 29]. Aggrecan is the most common PG in articular cartilage. Chondroitin and keratan sulfate are the side chains of aggrecan [30]. Other smaller proteoglycans are less abundant and have one or two GAG side chains, such as dermatan sulfate or heparan sulfate [31].

Proteoglycans, glycosaminoglycans and hyaluronic acid as matrix components

Proteoglycans typically consist of a protein core to which long sugar chains (glycosaminoglycans) are covalently attached. The attachment sites are formed by serine residues in the core protein that occur at an interval of 12 amino acids. Proteoglycans have a feather-like structure (fig. 5). The glycosaminoglycans linked to the serine residues consist of repeating disaccharide units of sulfated and unsulfated uronic acids and N-acetyl hexosamines. The composition of the repeating disaccharide units determines the name of the glycosaminoglycans (e.g., heparan sulfate (HS), dermatan sulfate (DS), chondroitin sulfate and keratan sulfate (KS)). KS does not contain uronic acid moieties, but galactose instead. One and the same core protein can contain different glycosaminoglycan side chains. The large proteoglycan structures are linked to a polysaccharide backbone, hyaluronic acid and together, they form an even more voluminous complex. In the extracellular matrix of articular cartilage, the long chain of hyaluronic acid is oriented in parallel with the collagen type II fibers. The featherlike structure of proteoglycans overlays the collagen fibers, forming a tight molecular network. Because the negatively charged glycosaminoglycans have a capacity to bind and retain water, they form a jelly-like structure. The tightly packed negatively charged glycosaminoglycans move apart as far as possible. They are brought together by pressure; the more pressure is put on the cartilage, the higher the repelling force will be. This enables the cartilage of the joints to absorb shocks.

An intact proteoglycan network is essential for the integrity and assembly of the functional cartilage matrix. This was demonstrated in an artificial system of cultured chondrocytes [31] which showed that inhibition of GAG incorporation in newly formed cartilage matrix not only causes the newly synthesized GAGs to diffuse further away from the chondrocytes, but also reduces the cross-linking of the collagen.

Proteoglycans, mainly those inserted into the plasma membrane and containing few glycosaminoglycan side chains, also serve as key biological response modifiers. Some of these roles are addressed below. Summarized briefly, they act as 1) stabilizers, cofactors and/or co-receptors for growth factors, cytokines and chemokines, 2) regulators of cathepsin activity, 3) signaling molecules during embryogenesis and in response to cellular damage such as wounds, infection and tumorigenesis and 4) targets for bacterial, viral and parasitic virulence factors (attachment, invasion and immune system evasion) [10-12].

Figure 5 Basic structure of aggrecan

Basic structure of aggrecan

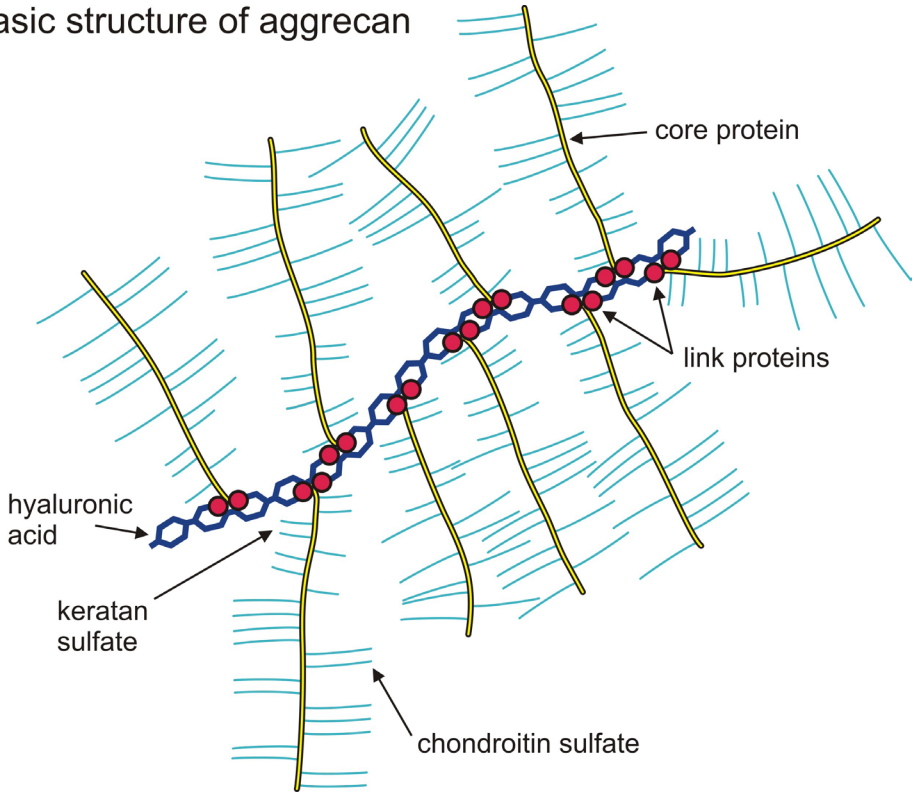


Fig. 5. Aggrecan is the complex of proteoglycans that all are connected to a central long chain of hyaluronic acid via link proteins (red dots). The proteoglycans in the large aggrecan complex are feather-like structures composed of a number of regularly spaced glycosaminoglycan chains, such as keratan sulfate and chondroitin sulfate (in light blue), which are covalently linked to a protein core (yellow).

Bone remodeling and the extracellular matrix (ECM)

Bone remodeling is a continuous process of bone resorption (osteoclasts) and bone formation (osteoblasts). The average turnover (volume replacement) of bone is 10% per year, but there are large differences dependent on age and bone regions [15].

Bone tissue is able to adapt its structure and function in response to mechanical forces and metabolic demands [32]. A change in the balance between bone resorption (osteoclast) and bone formation (osteoblast) results in a corresponding loss or gain of bone tissue. As cathepsins and matrix metalloproteinases (MMPs) are key enzymes in the turnover of the ECM, they are essential to the process of bone remodeling [27].

Cathepsin K is highly expressed by osteoclasts. It is a lysosomal enzyme that cleaves the triple helical region of type I and II collagen at multiple sites [27, 33]. During endochondral ossification, cathepsin K degrades type II collagen (cartilage) in the hypertrophic zone to create space for the deposition of young bone by osteoblasts [34]. Some evidence has been presented that certain types of GAGs modulate the cathepsin K activity depending on their concentrations [35]. According to this model, GAG storage in MPS might affect the bone remodeling [36]. Because MMPs fragment the protein core of the proteoglycans, the ECM disintegrates, resulting in a cascade of events. The release of biologically active components activates other proteases and affects processes such as cell attachment, migration, proliferation, differentiation and apoptosis [37].

MMP activity is controlled by various mechanisms. For instance, MMP transcription is upregulated via growth factors and cytokines and MMP translation and proenzyme activation are regulated by tissue inhibitors (TIMPs; tissue inhibitors of metalloproteinases), which inhibit the translation of MMPs and form complexes with MMPs that influence proenzyme activation [38-40]. Precise regulation of MMP activity is crucial for maintaining the balance between tissue remodeling and destruction. During endochondral ossification, at least three MMPs are highly expressed. When neovascularization of the cartilage anlage begins, MT1-MMP and MMP9 are expressed in the pre-osteoclasts and other chondroclastic cells of unknown origin. MMP13 is expressed in the terminal hypertrophic chondrocytes and the newly recruited osteoblasts [37].

Interaction of GAGs with bone morphogenetic proteins (BMPs) and fibroblast growth factor (FGF)

Bone morphogenetic proteins (BMPs) are multi-functional growth factors that belong to the transforming growth factor β (TGF- β) superfamily [41]. They interact with several regulatory pathways [42] and promote the differentiation of osteoclasts and chondrocytes from mesenchymal progenitor cells. In the growth plate they also promote chondrocyte hypertrophy and apoptosis. Strict regulation of the BMP activity is required to secure normal bone formation during postnatal life [41]. BMPs play an integral role in the development of the skeletal system, as well as in the heart and nervous system [43]. In humans, mutations in the BMP pathway are associated with skeletal disorders. For instance, a mutation in the Ib BMP receptor has been identified in a patient with brachydactyly and mutations in the BMP antagonist noggin have been found in patients with symphalangism and synostoses [42]. BMPs are secretory proteins with the ability to promote bone formation, but can also induce formation of ectopic cartilage. Although the activities of BMPs and their antagonists are modulated by heparan sulfate containing proteoglycans (HSPG), it is not fully understood how their activity in the MPS storage diseases is influenced by these GAGs [43]. The sulfated residues on these GAGs are thought to bind

to BMPs and their antagonists, thereby modulating receptor-mediated signaling. The growth factor regulatory role of some of the GAGs is also shown by a chondroitin-sulfate-synthesis-deficient mouse model. Mice deficient for chondroitin 4-sulfotransferase have growth plate abnormalities resembling those in MPS VI mice, in which the TGF- β signaling is upregulated and the BMP signaling down-regulated. This indicates that the chondroitin sulfate balances the activity and localization of these two growth factors [44, 45].

Fibroblast growth factor and BMP signaling have opposing functions in the growth plate. They interact through mutual antagonism. FGF ligands and FGF receptors (FGFR) are both expressed in developing skeletal and cartilage anlage. Several human craniosynostosis disorders have been linked to activating mutations in FGF receptors. Disruption of FGFR2 signaling in skeletal tissues results in skeletal dwarfism and lower bone-mineral density (BMD). Lower proliferation of osteoprogenitor cells is combined with reduced anabolic function of mature osteoblasts and diminished osteoblast differentiation [46, 47]. FGF-2, a prototypical member of the FGF family that is involved in tissue morphogenesis and neurogenesis, binds to two kinds of cell-surface receptors: high affinity FGF receptors (FGFRs) and low-affinity receptors (composed of HS proteoglycans) that act as extracellular FGF2 reservoirs and co-receptors. Formation of the FGF-2-FGFR-HSPG complex is necessary for mitogenesis and optimal biologic response to FGF-2 [48]. Dermatan sulfate (DS) also binds and activates FGF-2. The interaction between DS and FGF-2 has been studied only with respect to cellular proliferation: in its capacity to stimulate cell growth *in vitro*, DS exceeded HS [49].

Three studies have suggested that high concentrations of small, abnormally sulfated HS chains (such as those present in Hurler syndrome) can have a detrimental effect on orderly hematopoietic stem-cell growth and differentiation [50-52].

TEETH

Teeth, too, are bony structures. Their shaft consists of dentin and the crown protruding in the oral cavity is covered with enamel. The inner part of teeth, the dental pulp, is composed of loose connective tissue. Odontoblasts are the cells that form the organic matrix of the shaft (dentin) (fig. 6), which consists of collagen type I, phosphoproteins, phospholipids and proteoglycans. Newly formed, not yet calcified dentin is called pre-dentin and has its equivalent in osteoid, uncalcified young bone [16]. During tooth development, ameloblasts are aligned across the cap of the primitive tooth and produce a layer of enamel, also a type of bone, which forms the crown. The root is covered with a layer of cementum produced by the cementoblasts which is connected to the bony socket of the jaw by the periodontal ligament, an array of collagen fibers that also hold the teeth in position [53].

Figure 6 Embryonic tooth formation

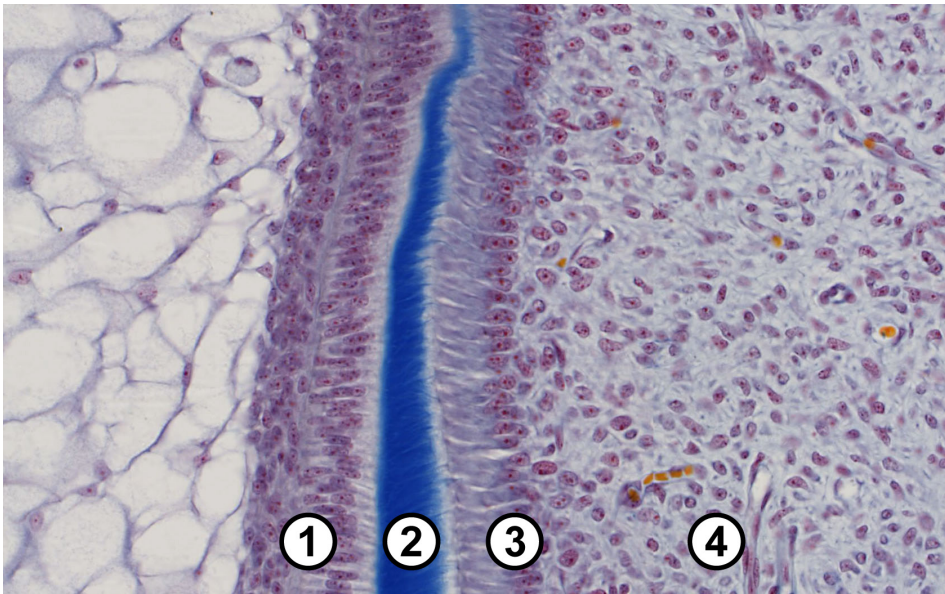


Fig. 6. Embryonic tooth formation in rabbit. 1) ameloblast; 2) dentin; 3) odontoblast; 4) mesenchyme

Development of the teeth

The mandible and maxilla grow to accommodate the developing teeth. The enamel on the crown of the teeth is derived from ectoderm; all other parts differentiate from the surrounding mesenchyme. Tooth buds of the primary dentition appear around the tenth week of embryonic development; the buds for the second dentition start to develop four years after birth [53].

BMPs and FGFs and their role in tooth development

GAGs can affect BMP activity as described above. BMP4 plays an important role in tooth development from the moment the initial epithelial lamina is formed until the late bell stage [54]. During postnatal tooth development, it is highly expressed in both the odontoblasts and in ameloblasts. Initial tooth development appears to require a BMP signal. Deletion of the BMP4 gene in odontoblasts and surrounding osteoblasts leads to permanent defects in tooth cytodifferentiation and also in the supporting periodontal tissue (decreasing the rate of formation from pre-dentin, decreasing odontoblast maturation, affecting proper dentinal tubule formation and reducing the expression of collagen type I and osteocalcin). In mice, dysmorphogenic odontoblasts were seen that failed to properly elongate and differentiate, thereby producing permanently thinner dentin, enlarged pulp chambers in the molars and less bone tissue to support the teeth. Indirectly, deletion of the BMP4 gene also disturbed the process of enamel formation. Postnatally, odontoblast-derived BMP4 plays a key paracrine or endocrine role in amelogenesis [54].

The BMP2 gene appears to be involved in BMP4 activation. Its deletion in odontoblasts leads to disorganization of morphologically altered odontoblasts at the dentinal tubule stage and failure to mature in later stages of tooth development [54].

Fibroblast growth factors (FGFs) are involved in epithelial-mesenchymal tissue interaction. FGF signaling via FGFR2 in the epithelium is crucial for cell proliferation during tooth and palate development [55]. Interference of abnormal HS and DS (as seen in MPS) with the FGF pathway may cause abnormal growth and differentiation of teeth in MPS [48, 52].

BONE, JOINT AND TEETH PROBLEMS IN MUCOPOLYSACCHARIDOSES

Although the severity of bone disease varies by the type of MPS, most of the skeletal anomalies in MPS patients are likely to originate from aberrant cartilage and bone development. For instance, the complex skeletal pathology observed in six-week-old MPS I mice suggests that very early changes predispose for the dysostosis that becomes apparent later in life [56]. Growth in length relies on the perfectly orchestrated proliferation and differentiation of chondrocytes in the growth plate, a process which is irreversibly disturbed in MPS by the lack of GAG turnover.

Various bone problems in MPS patients can be explained by abnormal endochondral ossification. These include thoracolumbar kyphosis/scoliosis, odontoid hypoplasia, wide oar-shaped ribs, shortened long bones, coxa valga, dysplastic femoral heads, genu valgum and bullet-shaped phalanges. Additionally, histological abnormalities have been reported in each of the 5 zones of the growth plate as described below. The main causes of osteopenia in MPS patients are probably abnormal bone remodeling (osteoblast/osteoclast dysfunction) and abnormalities in the growth plate, exacerbated by immobility in an advanced stage of the disease. Developmental deformities of the vertebral bodies and the femoral heads accelerate the normal degeneration of the joints caused by weight-bearing forces and also induce inflammation.

Macrocephaly with thickened skull and short wide clavicles can be explained by abnormal intramembranous ossification and abnormal bone remodeling. Reports of MPS cases with craniosynostosis in the literature have speculated that GAGs may interact with the FGF receptor [46, 47].

Dental complications in Mucopolysaccharidoses (MPS I, IV and VI) can be severe. They include hypoplastic peg-shaped teeth with retarded eruption or unerupted dentition; thin enamel (often 'greyish'); a pitted surface; dentigerous, cyst like follicles, malocclusions; short mandibular rami with abnormal condyles (condylar defects); and gingival hyperplasia [57-59]. Affected MPS patients easily develop dental caries and need regular, conservative dental therapy [60]. Secondary cellular responses involving interactions of GAGs with BMP and FGF may play a role in all bone, joint and tooth problems seen in MPS patients.

Endochondral ossification and the epiphyseal growth plate in MPS patients and animals

Resting zone

Chondrocytes in the resting zone of the growth plates of patients with MPS I, II and IV are unusually large and contain granular material. They are named “foam” cells because they contain numerous, large cytoplasmic vacuoles filled with undegraded GAGs. Foci of loose connective tissue interrupt the architecture of the growth plate, creating irregularly shaped metaphyses. The remaining parts of the growth plate are fairly regular, with well-organized endochondral ossification [61]. In a MPS VI feline model, the resting zone of the tibia occupies a larger than usual space in which the chondrocytes are rather tightly packed (hyperplasticity) [62].

Clonal expansion of the chondrocytes in the resting zone, which is seen in MPS VI felines, can be explained by a response to GAG accumulation. GAGs are negatively charged and able to mobilize and bind mitotic growth factors. Compared with the proliferative and hypertrophic chondrocytes, the articular chondrocytes and the chondrocytes in the resting zone have a long half-life. Pathology is therefore more likely to develop in the slowly dividing cells in the resting zone.

Proliferative and hypertrophic zones

In the MPS VII mice, the number of chondrocytes in the proliferative zone is markedly decreased (60%); the proliferative capacity is only 55%. The ECM directly surrounding the chondrocytes is very rich in chondroitin-4-sulfate (C4S). On the basis of these findings it has been hypothesized that C4S might interact with a cell membrane receptor and thereby reduce chondrocyte proliferation and bone growth [63]. In six-week-old MPS I mice the growth plate is abnormally broad with distended resting, proliferative and hypertrophic zones and the chondrocytes are hypertrophic. In contrast to the decreased proliferation in the MPS VII mice, the proliferative zone in six-week-old MPS I mice occupies a relatively high number of chondrocytes and the columnar organization is relatively well preserved. In older mice, the columnar organization of the growth plate is disrupted and the bone trabeculae begin to thin [56].

Similar defects in the process of endochondral ossification have been observed in MPS I patients, in felines with MPS I and MPS VI and in mice with MPS VI [64]. For instance, chondrocyte maturation in distinct regions of the hypertrophic zone was disorganized in the iliac crest growth plate of MPS I patients and in the growth plates in the femoral head and tibia of MPS VI felines [64]. The lower rate of bone growth in MPS patients and animal models may be attributable to delayed turnover of hypertrophic cells [62]. The lower number of hypertrophic cells in MPS VI rats has been ascribed to enhanced expres-

sion of TGF- β that inhibits the terminal differentiation of immature chondrocytes [38]. A decrease in the number of hypertrophic chondrocytes that are subsequently replaced by bone can explain the osteopenia in MPS VI rats.

The ossification zone

The accumulation of GAGs in MPS VII mice and dogs has been demonstrated in osteoclasts and osteoblasts located in the ossification zone [65]. In the iliac growth plate of humans with MPS I there were fewer longitudinal septa upon which cartilage mineralization and metaphyseal osteoblastic activity could occur. The primary spongiosum was irregular with poor speculation [64]. In the femoral growth plate of MPS VI felines, calcifying cartilage was disorganized by irregularities in the chondro-osseous junction and there were osteoclast deficits [66]. Abnormalities in the cortical bone structure supporting the growth plate have been reported in a murine MPS I model [56]: at six weeks of age, the zone of provisional calcification and primary spongiosa was abnormally wide, indicating either that more matrix was produced or that it was less degraded than normal. Islands of un-ossified cartilage persisted amidst the newly formed bone, resulting in the loss of well-defined narrow trabeculae. Some of these findings could be explained by the lack of osteoclast activity, which normally degrade GAGs from the cartilage matrix, leaving a well ordered scaffold consisting mainly of type II collagen fibers to which the osteoblasts can adhere.

The GAG storage in MPS I appears to compromise this process. Ossification starts before the GAGs have been removed from the matrix and remnants of the cartilage anlage are retained within the newly formed bone. This leads to abnormalities in the composition and architecture of the growth plate and thus to growth retardation. The abnormalities persist, which suggests that the lack of GAG degradation also affects the process of bone remodeling [56].

In a MPS VI cat model the abnormalities are not restricted to the cartilage of the growth plate but also pertain to osteoblast function, suggesting that bone formation is deficient [62]. Osteonectin, a glycoprotein secreted by osteoblasts, with affinity for collagen and promoting bone mineralization, has been mentioned in this context. It is a substrate for MMP-2 and 9 that are both elevated in MPS bones and joints [38]. Like the osteoblasts, but to an even greater extent, the osteoclasts in MPS VII mice contain large foamy vacuoles [20]. The osteoclasts fail to form ruffled border membranes and seem to detach easily from the bone surface. These defects are intrinsic to the MPS VII osteoclasts and not the result of an abnormal bone matrix. They are corrected during bone marrow transplantation, when the osteoclasts are replaced. Osteoclast function may also be impaired by an excess of GAGs in the extracellular matrix, which inhibits cathepsin K activity and thereby cartilage resorption [35].

The role of signal transducers and activator of transcription (STAT)

Several studies have indicated the role of STAT in the process of endochondral ossification and MPS-related change. STAT stands for a family of transcription factors. The phosphorylation and activation of STAT1 by activated FGFR3 increases the expression of the cell-cycle inhibitor p21, reducing chondrocyte proliferation [46]. Metcalf et al. have shown that mRNAs that encode several of the STAT transcription factors known to be selectively altered by inflammation were abnormally expressed in the growth plates of MPS VII mice [63].

Osteopenia and osteoporosis in MPS

The abnormal cartilaginous structures in the epiphyseal growth plate are an important cause of osteopenia in most MPS patients, but not in MPS III patients. Heparan sulfate accumulation causes neurological complications (psychomotor retardation) and only minor skeletal abnormalities including coarse facies and joint stiffness [67].

The psychomotor retardation in MPS I, II and III might also contribute to osteopenia or osteoporosis. The secondary inducers include immobilization, too little exposure to the sun, poor nutritional status, vitamin D deficiencies and treatment with anti-epileptics [68]. In MPS IV and VI patients, severe bone deformities (immobilization) and vitamin D deficiencies are also described [69].

The role of weight-bearing forces on abnormally shaped bones and joints

In MPS patients, abnormal bone structures (dysostosis multiplex) are seen very early in life. The acetabula of the hips in MPS I, II, IV and VI patients are short and steep and form an abnormal acetabular cup. The morphology of the femoral head and neck can be changed not only by accumulation of GAGs in the growth plate and bone cells, but also by abnormal weight-bearing forces. The latter is shown in figure 7, which demonstrates hallux valgus in a patient with MPS II. Hallux valgus is an abnormal angulation of the big toe involving the joint between the metatarsal bone and the proximal phalanx. It also occurs in the unaffected population (fig. 8). Mis-directed pressure on the bones can cause joint inflammation, affect the GAG content of the articular cartilage and induce secondary alterations in the underlying bone. It also has a long-range effect on the cartilage structure of the joint between the proximal and distal phalanges. The proximal site of the joint between the metatarsal bone and the proximal phalanx has fully disappeared due to the inflammation. The distal site of this joint has a very low GAG content, although the gross structure is still preserved. In response to the primary pathologic changes, new bone is formed at the periphery of the joint (osteophyte) and immature cartilage and bone are formed just under the zone of articular cartilage. BMPs and other growth factors are likely involved in these processes. Although not directly involved, the cartilage of the joint

between the proximal and distal phalange of this toe also has a very low GAG content; therefore, in this pathology, mixed aspects of osteoarthritis and rheumatoid arthritis (OA and RA) are seen, which also occur in MPS. Recently, Baldo et al. described this phenomenon in a knee joint of an MPS I murine model [70] showing inflammatory infiltration and pannus formation with hypertrophy of synovial cells. Although the primary causes of hallux valgus in the general population and in MPS patients are totally different, the cascade of pathologic events and the consequences are partly similar.

Figure 7 Hallux valgus MPS II patient



Fig. 7. Hallux valgus of the left foot of a 12 years old MPS II patient. Notice the redness of the skin over the joint between the metatarsal bone and the proximal phalanx, which is caused by inflammation (arrow).

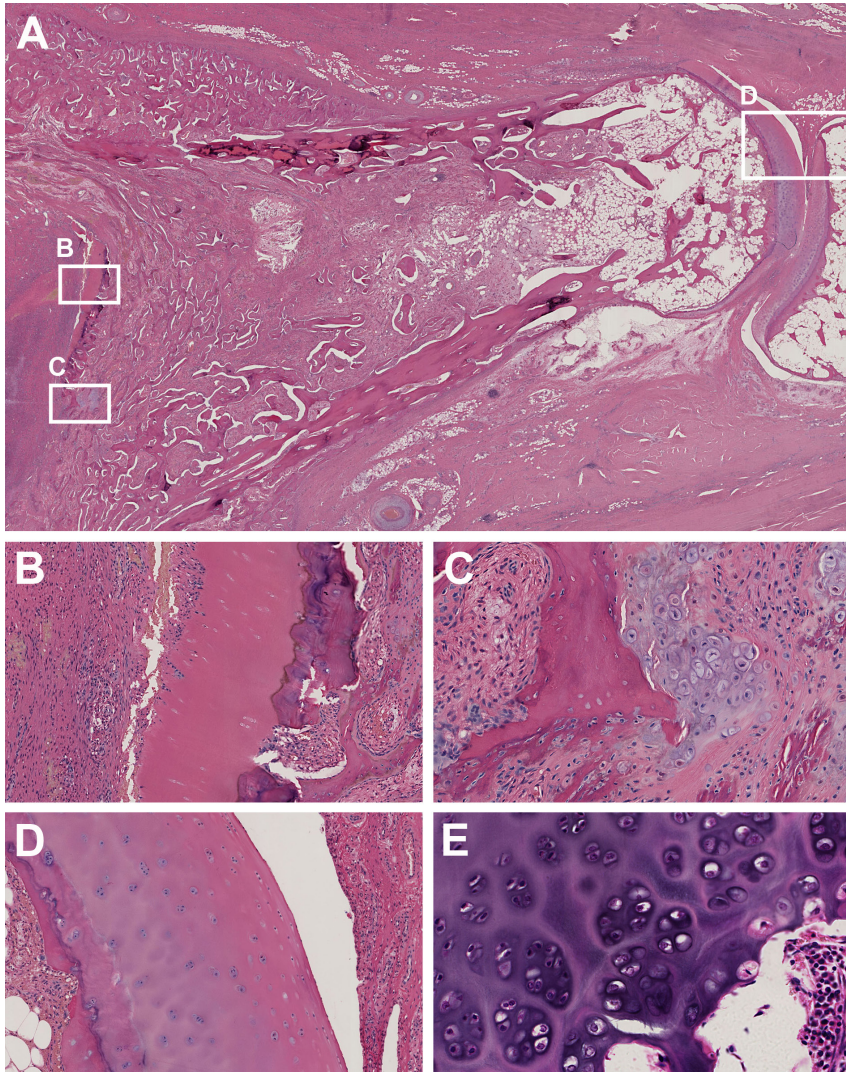
Figure 8 Amputated great toe

Fig. 8. Microscopic image of an amputated great toe of a 52 year old women not affected by MPS (hallux valgus).

A) Overview. **B)** and **C)** show details of the joint between the metatarsal bone and the proximal phalanx and **D)** shows a detail of the joint between the proximal phalanx and the distal phalanx. The joint between the metatarsal bone and the proximal phalanx has been destroyed by inflammation due to the abnormal pressure and the GAG content in the cartilage has diminished (asterisk) (B). Secondary alterations in the underlying bone are also visible in this joint specifically, abnormal cartilage formation (arrows) (C). Although the gross architecture is still preserved, the cartilage of the joint between the proximal phalanx and the distal phalanx has a very low GAG content (asterisks) (D). Image **E)** shows healthy cartilage with normal GAG content (asterisk).

Joints and inflammation

Simonaro et al. hypothesized that lysosomal and/or extracellular GAG storage in MPS disorders induce inflammation and affect the growth of connective tissue cells and other cell types by activating the toll-like receptor 4 (TLR4) signaling pathway [71]. Activation of this pathway can be induced either by 1) GAG fragments interacting with CD44, a hyaluronan-binding cell surface glycoprotein receptor (55 kDa) and myeloid differentiation factor-88 (MyD88), or 2) through lipopolysaccharide (LPS), which requires MyD88, lipopolysaccharide binding protein LBP and CD14 [72-76]. Simonaro et al. have shown that the expression of MyD88, LBP and CD14 is up-regulated in MPS connective tissue cells [71]. Large fragments of hyaluronic acid and oligosaccharides released by the breakdown of the extracellular matrix also signal through TLR4 via MyD88 and CD44, providing further support for the concept that this pathway is activated by GAG storage in the MPS disorders [73]. TLR4 activation in MPS animals resulted in the production of ceramide, a proapoptotic lipid and the release of numerous inflammatory cytokines and proteases [77]. Among the cytokines, TNF- α was markedly elevated both in the circulation and within the joint tissue of MPS animals [71].

There is great similarity in the secretion of pro-inflammatory cytokines like TNF- α , IL-1 β and nitric oxide in the extracellular matrix of cartilage and bone of animals and humans with primary MPS syndromes, compared with primary degenerative and inflammatory process like osteo- or rheumatoid arthritis. The cytokines are produced by MPS chondrocytes, synoviocytes and macrophages [38].

Stimulation of MPS connective tissue cells by the inflammatory cytokines cause enhanced secretion of several of the matrix metalloproteinases (MMPs). Dramatically elevated expression of MMP-2 and MMP-9 and abnormally high expression of TIMP-1 accompany joint disease in MPS [38]. The imbalance of MMPs over tissue inhibitors of metalloproteinase, the TIMPs, precipitate features of both osteoarthritis as well as rheumatoid arthritis in joints of MPS patients. Patients without MPS but with osteoarthritis (OA) and cartilage degeneration have changes in the structure and composition of the extracellular matrix, characterized by lower proteoglycan content and enhanced collagen degradation [78]. To compensate for the loss of matrix substance, the rate of synthesis of both matrix components is increased [79, 80].

Dental problems

Güven et al. have investigated the ultrastructural and chemical properties of MPS I (Hurler) teeth. The dentin of the primary teeth was characterized by extremely narrow dentinal tubules with an irregular wave-like pattern. The enamel-dentin junction was poorly shaped, micro gaps occurred and the enamel displayed an irregular arrangement of prisms. Both the enamel and the dentin had an abnormal protein structure and the dentin protein content was low [57].

SECONDARY CELLULAR EFFECTS AND RESPONSES IN MPS

Interaction of GAGs with BMPs and FGFs

Impaired BMP-4 signaling by GAGs in multipotent adult progenitor cells (MAPCs) in human Hurler syndrome identifies a mechanism that might contribute to the progressive skeletal abnormalities. The same mechanisms may be involved in the development of neurological problems [43]. It has been demonstrated that cell and matrix associated GAGs promote proliferation and block BMP-4-mediated differentiation of several types of human malignant cells. The storage of GAGs in Hurler cells may have the same effect. GAGs impair the BMP-4 activity but do not change the expression of various BMPs or their receptors. The activity of BMP-4 can be restored by clearing the lysosomal GAG storage with exogenously supplied enzyme as demonstrated in cultured cells. Both heparan sulfate (HS) and dermatan sulfate (DS) accumulate in Hurler syndrome and are cleared by treatment with α -L-iduronidase. The role of DS cannot be ruled out as a contributor to impaired BMP-4 signaling [43] as observed in Hurler MAPCs. HS in Hurler syndrome is structurally and functionally abnormal and has impaired ability to bind to and mediate the effects of fibroblast growth factor-2 (FGF-2) signaling [48]. This results in FGF-2-induced proliferation and survival of Hurler multipotent progenitor cells. Both the mitogenic and survival-promoting activities of FGF-2 were restored by substitution of Hurler HS with normal HS. Chondroitin 4-sulfate (C4S), one of the GAGs that store in MPS VII, can activate FGF signaling, as well through some of the FGFRs [81].

Autophagy, polyubiquitination and mitochondrial function

The molecular pathways underlying pathology in lysosomal storage diseases (LSDs) are largely unknown [82]. Recycling of the building blocks of cells, organelles, (glycol)proteins, (glycol)lipids, carbohydrates and other kind of macromolecular compounds is required for cellular homeostasis [83]. The ubiquitin-proteasome proteolytic system and the autophagosome to lysosome pathways are both used for large scale degradation of cellular components. The ubiquitin-proteasome system degrades short lived regulatory proteins that are for instance important for processes like cell-cycle progression, regulation of gene transcription and signal transduction [84]. The long-lived structures are mainly targeted to the lysosomes by autophagosomes [85]. Lysosomal storage leads to reduced functionality of the lysosomal compartment and consequently leads to build-up in the autophagocytic and endocytic pathways [86-88]. Dysfunction of autophagy as secondary event seems to play an important role in the pathophysiology of LSDs. It has been shown that lysosomal storage induces impaired autophagy. A recent study also showed mitochondrial dysfunction and inflammation to occur as secondary event in MPS VI [83]. Similar anomalies in association with DS storage have been observed in the visceral

organs but not in the central nervous system of MPS VI rats accompanied by inflammation and cell death. Prevention of dermatan sulfate storage in these rats by gene therapy resulted in restoration of autophagy, as well as regression of inflammation and apoptosis.

Compromised lysosome membrane integrity

Compromised lysosomal membrane integrity is another problem resulting from the accumulation of undegraded or partially degraded substrates in the lysosomes of LSD patients [89, 90]. By leading to leakage of ions and metabolites from the lysosomes to the cytosol, it causes alterations in cellular homeostasis. Pereira et al. have shown that secondary alterations, such as changes in the Ca^{2+} and H^{+} homeostasis caused by lysosomal membrane permeability, can contribute to cell death and to the pathophysiology of MPS I mice [90]. For example, too high a calcium concentration in the cytosol compromises the fusion between endosomes and lysosomes. Similarly, endosomal and lysosomal pH that is too high also has a detrimental effect [91] as has been demonstrated in mucopolipidosis type IV [92]. Large changes in lysosomal membrane integrity causes leakage of lysosomal enzymes and other macro-molecules from the lysosomes in the cytosol, where the presence of lysosomal proteases, such as cathepsins, may contribute to apoptotic cell death [89, 93-96].

RELEVANCE TO THERAPEUTIC OPTIONS

The following section describes the existing and potential therapeutic options for preventing or correcting short stature, osteopenia, joint stiffness and contractures in MPS patients.

Enzyme replacement therapy

Enzyme replacement therapy (ERT) is currently available for MPS I, II and VI [97]. So far, although ERT ameliorates bone and/or joint problems in MPS animal models if started very early, it has achieved little improvement of bone disease in humans [77]. In a cat with MPS VI, Auclair et al. injected the enzyme directly into the joint rather than administer it intravenously [98] to improve the therapeutic efficacy in joints. This significantly reduced storage material in the articular chondrocytes and the synovial membrane; however, within two months of treatment, GAG accumulation recurred [98]. Monthly injections produced more positive effects than injections every three months and this method of intra-articular therapy is currently being tested in two MPS VI patients [99].

It should be noted that the correction of MPS storage in the articular cartilage and the growth plate remains challenging because the accessibility of the chondrocytes is mechanically restricted by slow diffusion of the relatively large therapeutic enzymes through the molecular structure of the matrix.

With regard to age-related effects, McGill et al. reported a sibling study in which one sibling with MPS VI started ERT in the eighth week after birth and the other at 3.6 years. Therapeutic efficacy was assessed by comparing the two siblings' bone and joint problems. Although the child who had been treated very young preserved joint movement, did not develop scoliosis and had no facial dysmorphism [100], the growth rate of both siblings was similarly decreased and macrocephaly was not prevented in the period between birth and 3.6 years. In both siblings, radiological changes of the skeleton progressed and degenerative changes took place in the joints [100]. Likewise, in the MPS VI cat model, the best response occurred when therapy was started directly after birth and if antibody development was prevented [101]. It appears that bones and joints respond better to ERT when the treatment is started early, therefore, neonatal screening for MPS enzyme deficiencies might be an option for diagnosing MPS in children as early as possible [102].

Bone marrow and hematopoietic stem cell transplantation

Although bone marrow transplantation (BMT) or hematopoietic stem cell transplantation (HSCT) in MPS I (ideally before 18 months of age) leads to several positive changes, it does not greatly reduce the skeletal abnormalities [103]. If no matched donor is available, cord blood from unrelated individuals can be used for transplantation [104]. However, despite early transplantation, transplant recipients often require major orthopedic surgery for genu valgum, acetabular hip dysplasia and kyphoscoliosis later in life [103, 105, 106]. In MPS animal models, osteoblast and osteoclast function was restored by bone marrow transplantation [20].

Gene therapy in MPS animals

Mango et al. examined the effect of liver-targeted retroviral gene therapy in β -glucuronidase (GUSB) deficient MPS VII mice and dogs. In mice, full correction of femur length was not attained despite high level enzyme expression from the liver. This was even not achieved when gene therapy was used in very young animals and was explained by the poor accessibility of the growth plate [65]. As an alternative to ERT and BMT/HSCT, Byers et al. examined the effect of direct transduction of the synovial membrane of rats with a GUSB containing lentiviral vector [107]. The transduction was only partially successful. Enzyme expression was obtained in the synovia for 8 weeks, but the chondrocytes and the fibroblasts of the ligament were not transduced. This was probably due to steric exclusion of viral particles by cartilage ECM. In theory, the treatment can only work if enough enzyme is produced by the synovial cells, which can then leak into the synovial fluid and reach the chondrocytes by diffusion through the ECM.

Short stature and growth hormone (GH)

Even though they did not have a growth-hormone deficiency, a number of MPS IV patients have been given growth hormone. There was no evidence that this improved their growth [60]. Eight children with MPS I Hurler syndrome who had previously undergone HSCT also received GH treatment [108,109]. Some of them had HSCT induced GH deficiency, others did not, but all had growth failure. After one year of treatment with GH their growth failure was partially corrected. Potential complications of GH are Legg-Calvé-Perthes disease, scoliosis and carpal tunnel syndrome [110, 111]. Although none of the transplanted patients had to discontinue GH treatment due to progressive scoliosis, one had a slipped capital femoral epiphysis, which can be caused by the GH therapy. The orthopedic complications characteristic of MPS I (Hurler) can be exacerbated by GH treatment, though opinions differ with regard to the prevalence and progression of scoliosis or kyphosis during GH treatment. Some studies have indicated that the percentage and rate of progression of the scoliosis curve is generally higher than expected during GH therapy, while others have reported little to no progression [112-115].

Hip abnormalities with a Perthes-like disease aspect (femoral head dysplasia, see fig. 1A) are common in untreated MPS patients and in patients treated with ERT [116]. It is not known whether GH aggravates this problem, but it can be envisaged that the growth plate becomes disorganized when chondroblast proliferation is randomly stimulated by GH.

The occurrence of pubertal delay in MPS VI patients and precocious puberty in MPS III patients may both be related to primary abnormalities of the hypothalamic-pituitary gonadal/thyroid hormone axes and may potentially affect growth. However, gonadal and thyroid hormonal dysfunctions have seldom been demonstrated in MPS patients and argue against the existence of any substantial abnormalities of the hypothalamic pituitary-gonadal/thyroid hormone axes [117, 118].

Osteopenia and the use of growth hormone

Throughout human life, GH and Insulin-like growth factor-I (IGF-I) play important roles in the homeostasis of bone. GH acts directly on the target tissues, e.g., bone, skeletal muscle and many others tissues. Many of the effects of GH are indirectly mediated by circulating (liver-derived) or locally produced IGF-I. Although GH treatment improves osteopenia in pediatric patients with growth hormone deficiency [119], the question is whether it also improves the osteopenia in MPS patients [120]. In a GH deficient rat model, it was demonstrated that GH administration increases periosteal and endocortical bone formation. GH also mitigates trabecular bone loss by increasing bone formation [119]. Since trabecular bone loss has been demonstrated in most MPS animal models, there is good reason to investigate the effect of GH dosing in MPS patients, particularly in younger ones whose bone abnormalities and growth retardation are still limited.

Osteopenia and the use of parathyroid hormone

Parathyroid hormone (PTH) is best known for releasing calcium from bone; primary hyperparathyroidism causes bone resorption. Parathyroid hormone also has anabolic activity [121]. The anabolic properties of PTH manifest at a low, intermittent dose. Under this regimen, PTH positively affects bone volume and microarchitecture by stimulating bone formation. This effect was seen in postmenopausal women with osteoporosis as well as in young women with growth disturbances [121, 122]. In the GH-deficient rat model (created by hypophysectomy), PTH increases bone formation mainly by reducing the osteoclast density per bone area, but has almost no effect on growth in length [119]. Given that PTH lowers osteoclast density, it would be unlikely to have a positive effect on osteopenia in MPS patients since the number of osteoclasts can be low (MPS VI cats) and their function defective (MPS VII mice) [66].

Osteopenia and the use of bisphosphonates

Patients with Gaucher disease (GD), a lysosomal glycolipidosis, may have severe osteopenia even when treated with ERT. In Gaucher disease this has been attributed to “chronic macrophage activation”, inflammation and induction of accelerated bone turnover [103]. Bone-mineral density was improved by the administration of bisphosphonates, whose effect is attributed to the inhibition of osteoclast function [123]. Another lysosomal storage disorder characterized by substantial bone abnormalities is Mucopolipidosis. Patients with Mucopolipidosis type III (ML III, pseudo-Hurler polydystrophy), have skeletal manifestations resembling those of MPS patients. They have a distinctively high turnover of bone [124] caused by vigorous, osteoclast driven, subperiosteal bone resorption pertaining to virtually the entire periosteal surface. ML III patients treated with bisphosphonates have a clinical response, with a decrease in pain and improved mobility. Their bone density also increased, particularly in the metaphyseal regions.

Due to immobilization, children with psychomotor retardation related to causes other than MPS may have severe osteoporosis. In our clinic, such patients are treated successfully with bisphosphonates. If we take these facts into consideration, it could be that MPS patients will also benefit from bisphosphonates. On the other hand, bisphosphonates inhibit osteoclast function, which seems to be already compromised in MPS [66].

Osteopenia and the use of BMPs

It has been demonstrated that BMP-2 can be used to treat osteoporosis [41]. BMP-2 can accelerate bone healing in animal models [125] and in humans it promotes intervertebral and lumbar posterolateral fusions [126]. It has also been shown to induce new dentine formation, have a potential application in root canal surgery and to be an effective bone inducer around dental implants for periodontal reconstruction [127]. Because of the stimulating effect of BMPs on osteoblast differentiation, their potential application in MPS deserves attention (this review).

Osteopenia and exercise

The bone and joint problems in hips and knees causes pain and restricted mobility, which indirectly leads to osteopenia. Physical exercise improves bone mass in growing children. Although the precise mechanism whereby it influences bone metabolism is not known, a response to greater mechanical stress and to changes in endocrine parameters are both likely contributors [32]. Physiotherapy and exercise might therefore improve osteopenia in MPS patients.

Intervention at the level of secondary cellular events

As stated above, various secondary effects occur in the pathophysiology of MPS, including disturbed autophagy and polyubiquitination, mitochondrial dysfunction, inflammation, apoptosis and loss of lysosomal membrane integrity. These secondary events can be prevented or resolved by reducing the lysosomal storage of GAGs. While this can be achieved by ERT or gene therapy [20, 35, 83, 128], the lysosomal GAG load can also be limited by reducing GAG synthesis. Such substrate reduction is used in Gaucher disease and Niemann Pick disease type C [97]. Used as a substrate inhibitor in MPS III animal models, Rhodamine B has had a beneficial affect on CNS function [97]. However, the effect of substrate inhibition on bone problems in this and other MPSs has not yet been demonstrated.

Inflammation

Research has been done on preventing the damage of bones and cartilage caused by inflammation. Simonaro et al showed the important role of TLR4 signaling in MPS bone and joint disease and suggested that targeting TNF- α may have positive therapeutic effects [77].

CONCLUDING REMARKS

Growth retardation, dysostosis multiplex, osteopenia/osteoporosis, stiff joints and abnormal teeth in MPS patients are the final result of lysosomal GAG accumulation in connective-tissue-forming cells such as mesenchymal cells, fibroblasts, chondrocytes, osteoblasts and osteocytes, osteoclasts, odontoblasts, ameloblasts and cementoblasts. The primary cause of cellular dysfunction is intralysosomal GAG storage, which directly affects the composition and metabolism of the extra-cellular matrix. These primary events evoke a cascade of pathological processes that have local effects on tissue and organ function and distant effects on systemic functions. As the MPS degrading enzyme deficiencies are determined genetically, the GAG storage starts in utero, eliciting a long-term effect on body structure and function. Skeletal malformations, dental dysplasia and hypoplasia are all pre-eminent examples of this process. To conclude this review, figure 9 summarizes the cascade of pathologic events, starting with primary GAG storage.

Primary and secondary cellular events

GAGs, one of the major components of the ECM, are synthesized and recycled by connective tissue cells. They enter the cell by endocytosis and are degraded in the lysosomes. If one of the lysosomal enzymes involved in their degradation is missing or malfunctioning because of a genetic defect, GAGs accumulate in lysosomes. Intralysosomal GAG storage not only expands the volume of the lysosomal system, but also the functioning of the lysosomes as end-stations of the endocytic and autophagocytic transport pathways. The lysosomal membrane integrity is compromised, which has several consequences such as dysfunction of the lysosomal membrane ATPase proton pump and leakage of proteases (cathepsins) into the cytosol. The high intralysosomal pH prohibits optimal functioning of lysosomal hydrolases, thereby contributing to secondary lysosomal storage. The release of lysosomal cathepsins and other lysosomal proteases into the cytoplasm has been associated with apoptosis. Dysfunction of autophagy leads to a series of cellular disturbances, including mitochondrial dysfunction. Abnormal vesicular traffic also affects endocytosis and thereby remodeling of the extra-cellular matrix. Such remodeling is also affected by the excess of proteoglycan, which can inhibit or stimulate cathepsin K activity. Most of the secondary cellular events are not unique for MPS, but occur in several of the lysosomal storage disorders. A review of the pathological cascade in neuropathic lysosomal storage disorders has recently been published and it shows several similarities with the model presented here for the MPS [129].

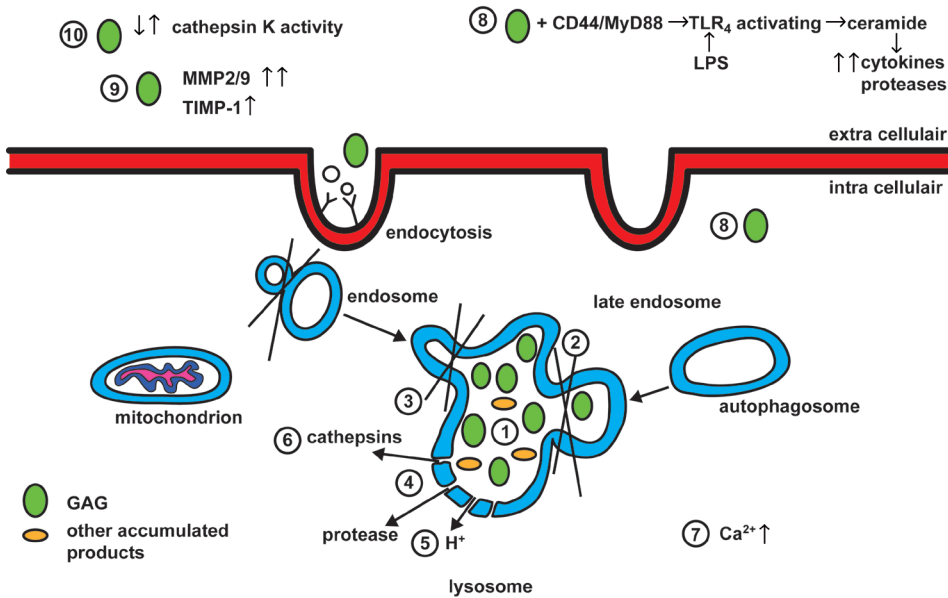
Figure 9 Pathologic cascade in Mucopolysaccharidoses

Fig.9 1) Lysosomal GAG storage due to deficiencies of MPS-degrading enzyme. 2) Impairment of autophagosome-lysosome fusion. 3) Impairment of endosome-lysosome fusion, affecting remodeling of the extra-cellular matrix. 4) Compromised lysosomal membrane integrity and disturbances of ion homeostasis. 5) Leakage of lysosomal hydrolases and H^+ out of the lysosome elevates the lysosomal pH and diminishes lysosomal function. 6) Leakage of cathepsins and other proteases into the cytosol may contribute to apoptosis. 7) Elevated Ca^{2+} levels in the cytosol, compromises the fusion of endosomes and lysosomes. 8) Activation of the TLR4 pathway by GAGs leads to the production of ceramide, which in turn leads to the release of cytokines and proteases, further elevating the TNF α level. 9) GAG-induced imbalance of MMP-2/9 and TIMP-1 causes degradation of the ECM. 10) Certain GAG's can modulate the cathepsin K activity, which might affect ECM remodeling.

Cell-type-specific and tissue-specific events

Lysosomal GAG storage in chondrocytes directly affects the growth and maintenance of cartilage. In early life, long bones grow by endochondral ossification. A disturbance of this process by chondrocyte malfunction leads to poor growth, skeletal malformations and also osteopenia, whereby fewer trabeculae are formed and less calcification takes place. Articular cartilage of the joints persists throughout life. The GAG storage in this tissue culminates in a pathology resembling osteoarthritis, as well as rheumatoid arthritis. GAG storage in osteoblasts, osteocytes and osteoclasts hampers adequate bone formation and bone remodeling. Early anatomical abnormalities of bones can induce and enhance osteoarthritis and inflammation such as that caused by abnormal weight-bearing forces. Inflammation itself is detrimental to chondrocyte function as it leads to loss of ECM components (as in hallux valgus).

Lysosomal storage of GAGs in teeth-forming cells such as the odontoblasts, ameloblasts and cementoblasts seems to be the greatest cause of abnormally shaped and irregularly positioned dental elements. The formation of teeth also requires interplay between teeth and bony elements of the mandibula and maxilla and it is likely that GAG storage in the osteocytes contributes to the problem.

Secondary responses

Partially degraded and undegraded GAGs interact with several growth factors, such as BMPs, FGFs and the FGF receptor. Activation of the TLR4 signaling pathway has been demonstrated in osteoblasts, osteocytes, osteoclasts, chondrocytes and odontoblasts and in the ECM in association with inflammation. Elevated expression of metalloproteinases and unbalanced elevation of metalloproteinase inhibitors cause osteoarthritis and rheumatoid arthritis, leading to articular cartilage degeneration. The proteoglycan content of the ECM is low and collagen is degraded abnormally fast.

Primary and secondary intervention

Therapeutic interventions reducing the lysosomal GAG storage are also expected to resolve some of the secondary pathophysiological events. While enzyme-replacement therapy seems the first logical option, its effect on bone, joint and teeth pathology is limited by the texture of these tissues. Cartilage is avascular and large molecules can barely diffuse through the matrix. Bone cells are nourished by short connections with the blood vessels, but bone has a very slow turnover. In addition, the bone, joint and teeth problems are the result of long-term aberrant formation and maintenance of these tissues, which makes the abnormalities largely irreversible. Therefore, very early intervention is mandatory. Surgical intervention can correct or minimize some of the joint, bone and dental problems at a later age. Standard approaches can help to resolve inflammation related morbidity. Growing insight in the cascade of pathophysiological events is slowly but steadily opening the doors that will enable us to improve the lives of MPS patients by manipulating the disease process at the primary or secondary levels.

REFERENCES

- [1] McKusick VA editor. Heritable Disorders of Connective Tissue. St. Louis: Mosby, C.V.; 1972.
- [2] Spranger J. The systemic mucopolysaccharidoses. *Ergeb Inn Med Kinderheilkd* 1972;32:165-265.
- [3] Sly WS. The mucopolysaccharidoses. In: Bondy PD, Rosenberg LE, editors. *Metabolic Control and Disease* Philadelphia: Saunders; 1980. p. 545.
- [4] McKusick VA, Neufeld EF. The Mucopolysaccharide storage diseases. In: Stanbury JB, Wyngaarden JB, Frederickson DS, Goldstein JL, Brown MS, editors. *The Metabolic Basis of Inherited Disease*. 5th ed. New York: McGraw-Hill; 1983. p. 751.
- [5] Muenzer J. Mucopolysaccharidoses. *Adv Pediatr* 1986;33:269-302.
- [6] Whitley CB. The mucopolysaccharidoses. In: Beighton P, editor. *McKusick's Heritable Disorders of Connective Tissue*. 5th ed. St. Louis: Mosby, C.V.; 1992.
- [7] McKusick VA. The William Allan Memorial Award Lecture: Genetic nosology: three approaches. *Am J Hum Genet* 1978 Mar;30(2):105-122.
- [8] Neufeld EF. Lessons from genetic disorders of lysosomes. *Harvey Lect* 1979 -1980;75:41-60.
- [9] Neufeld EF, Muenzer J. The mucopolysaccharidoses. In: Scriver CR, Beaudet AL, Sly WS, Valle D, editors. *The Metabolic and Molecular Bases of Inherited Disease*. 7th ed. New York: McGraw-Hill; 1995. p. 2465.
- [10] Trowbridge JM, Gallo RL. Dermatan sulfate: new functions from an old glycosaminoglycan. *Glycobiology* 2002 Sep;12(9):117R-25R.
- [11] Rostand KS, Esko JD. Microbial adherence to and invasion through proteoglycans. *Infect Immun* 1997 Jan;65(1):1-8.
- [12] Schmidtchen A, Frick IM, Bjorck L. Dermatan sulphate is released by proteinases of common pathogenic bacteria and inactivates antibacterial alpha-defensin. *Mol Microbiol* 2001 Feb;39(3):708-713.
- [13] Aldenhoven M, Sakkers RJ, Boelens J, de Koning TJ, Wulffraat NM. Musculoskeletal manifestations of lysosomal storage disorders. *Ann Rheum Dis* 2009 Nov;68(11):1659-1665.
- [14] Keller C, Briner J, Schneider J, Spycher M, Rampini S, Gitzelmann R. Mucopolysaccharidosis 6-A (Maroteaux-Lamy disease): comparison of clinical and pathologico-anatomic findings in a 27-year-old patient. *Helv Paediatr Acta* 1987;42(4):317-333.
- [15] Manolagas SC, Parfitt AM. What old means to bone. *Trends Endocrinol Metab* 2010 Mar 9.
- [16] Mescher AL. *Junqueira's Basic Histology*. 12th ed. New York: McGraw-Hill Medical Publishing Division; 2010.
- [17] Netter, Frank H. *Musculoskeletal system: anatomy, physiology, and metabolic disorders*. New Jersey: Ciba-Geigy Corporation; 1987. p. 169.
- [18] Lakkakorpi P, Tuukkanen J, Hentunen T, Jarvelin K, Vaananen K. Organization of osteoclast microfilaments during the attachment to bone surface in vitro. *J Bone Miner Res* 1989 Dec;4(6):817-825.
- [19] Blair HC, Teitelbaum SL, Ghiselli R, Gluck S. Osteoclastic bone resorption by a polarized vacuolar proton pump. *Science* 1989 Aug 25;245(4920):855-857.
- [20] Monroy MA, Ross FP, Teitelbaum SL, Sands MS. Abnormal osteoclast morphology and bone remodeling in a murine model of a lysosomal storage disease. *Bone* 2002 Feb;30(2):352-359.
- [21] Teitelbaum SL, Abu-Amer Y, Ross FP. Molecular mechanisms of bone resorption. *J Cell Biochem* 1995 Sep;59(1):1-10.
- [22] Nesbitt SA, Horton MA. Trafficking of matrix collagens through bone-resorbing osteoclasts. *Science* 1997 Apr 11;276(5310):266-269.

- [23] Salo J, Lehenkari P, Mulari M, Metsikko K, Vaananen HK. Removal of osteoclast bone resorption products by transcytosis. *Science* 1997 Apr 11;276(5310):270-273.
- [24] Brighton CT, Sugioka Y, Hunt RM. Cytoplasmic structures of epiphyseal plate chondrocytes. Quantitative evaluation using electron micrographs of rat costochondral junctions with special reference to the fate of hypertrophic cells. *J Bone Joint Surg Am* 1973 Jun;55(4):771-784.
- [25] Hall BK. The embryonic development of bone. 1988;76:174-181.
- [26] van der Eerden BC, Karperien M, Wit JM. Systemic and local regulation of the growth plate. *Endocr Rev* 2003 Dec;24(6):782-801.
- [27] Li Z, Yasuda Y, Li W, Bogyo M, Katz N, Gordon RE, et al. Regulation of collagenase activities of human cathepsins by glycosaminoglycans. *J Biol Chem* 2004 Feb 13;279(7):5470-5479.
- [28] Eyre DR. Collagens and cartilage matrix homeostasis. *Clin Orthop Relat Res* 2004 Oct;(427 Suppl):S18-22.
- [29] Eyre DR. The collagens of articular cartilage. *Semin Arthritis Rheum* 1991 Dec;21(3 Suppl 2):2-11.
- [30] Kiani C, Chen L, Wu YJ, Yee AJ, Yang BB. Structure and function of aggrecan. *Cell Res* 2002 Mar;12(1):19-32.
- [31] Bastiaansen-Jenniskens YM, Koevoet W, Jansen KM, Verhaar JA, De Groot J, Van Osch GJ. Inhibition of glycosaminoglycan incorporation influences collagen network formation during cartilage matrix production. *Biochem Biophys Res Commun* 2009 Feb 6;379(2):222-226.
- [32] Maimoun L, Sultan C. Effects of physical activity on bone remodeling. *Metabolism* 2010 Mar 30.
- [33] Yasuda Y, Kaleta J, Bromme D. The role of cathepsins in osteoporosis and arthritis: rationale for the design of new therapeutics. *Adv Drug Deliv Rev* 2005 May 25;57(7):973-993.
- [34] Ballock RT, O'Keefe RJ. The biology of the growth plate. *J Bone Joint Surg Am* 2003 Apr;85 A(4):715-726.
- [35] Wilson S, Hashamiyan S, Clarke L, Saftig P, Mort J, Dejica VM, et al. Glycosaminoglycan-mediated loss of cathepsin K collagenolytic activity in MPS I contributes to osteoclast and growth plate abnormalities. *Am J Pathol* 2009 Nov;175(5):2053-2062.
- [36] Wilson S, Bromme D. Potential role of cathepsin K in the pathophysiology of mucopolysaccharidoses. *J Pediatr Rehabil Med* 2010;3(2):139-146.
- [37] Ortega N, Behonick D, Stickens D, Werb Z. How proteases regulate bone morphogenesis. *Ann N Y Acad Sci* 2003 May;995:109-116.
- [38] Simonaro CM, D'Angelo M, Haskins ME, Schuchman EH. Joint and bone disease in mucopolysaccharidoses VI and VII: identification of new therapeutic targets and biomarkers using animal models. *Pediatr Res* 2005 May;57(5 Pt 1):701-707.
- [39] Tetlow LC, Adlam DJ, Woolley DE. Matrix metalloproteinase and proinflammatory cytokine production by chondrocytes of human osteoarthritic cartilage: associations with degenerative changes. *Arthritis Rheum* 2001 Mar;44(3):585-594.
- [40] Visse R, Nagase H. Matrix metalloproteinases and tissue inhibitors of metalloproteinases: structure, function, and biochemistry. *Circ Res* 2003 May 2;92(8):827-839.
- [41] Chen D, Zhao M, Mundy GR. Bone morphogenetic proteins. *Growth Factors* 2004 Dec;22(4):233-241.
- [42] Alliston T, Piek E, Derynck R. TGF- β family signaling in skeletal development, maintenance, and disease. In: Derynck R, Miyazono K, editors. *The TGF- β Family* Woodbury, NY: Cold Spring Harbor Press; 2008. p. 667-723.
- [43] Khan SA, Nelson MS, Pan C, Gaffney PM, Gupta P. Endogenous heparan sulfate and heparin modulate bone morphogenetic protein-4 signaling and activity. *Am J Physiol Cell Physiol* 2008 Jun;294(6):C1387-97.
- [44] Kluppel M, Wight TN, Chan C, Hinek A, Wrana JL. Maintenance of chondroitin sulfation balance by chondroitin-4-sulfotransferase 1 is required for chondrocyte development and growth factor signaling during cartilage morphogenesis. *Development* 2005 Sep;132(17):3989-4003.

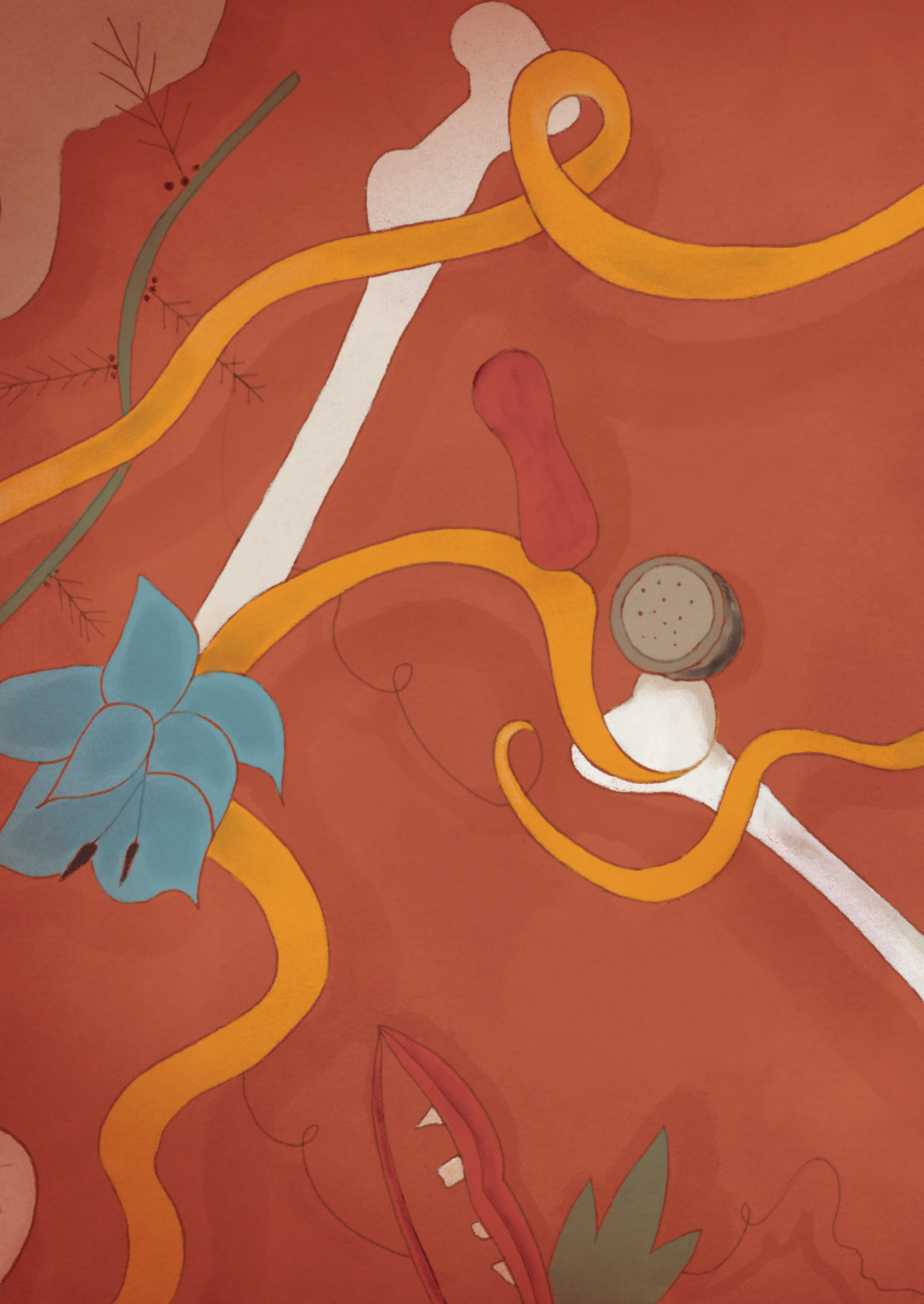
- [45] Alliston T. Chondroitin sulfate and growth factor signaling in the skeleton: Possible links to MPS VI. *J Pediatr Rehabil Med* 2010;3(2):129-138.
- [46] Karsenty G, Wagner EF. Reaching a genetic and molecular understanding of skeletal development. *Dev Cell* 2002 Apr;2(4):389-406.
- [47] Yang Y. *Skeletal Morphogenesis and Embryonic Development. Primer on the Metabolic Diseases and Disorders of Mineral Metabolism*; 2008.
- [48] Pan C, Nelson MS, Reyes M, Koodie L, Brazil JJ, Stephenson EJ, et al. Functional abnormalities of heparan sulfate in mucopolysaccharidosis-I are associated with defective biologic activity of FGF-2 on human multipotent progenitor cells. *Blood* 2005 Sep 15;106(6):1956-1964.
- [49] Penc SF, Pomahac B, Winkler T, Dorschner RA, Eriksson E, Herndon M, et al. Dermatan sulfate released after injury is a potent promoter of fibroblast growth factor-2 function. *J Biol Chem* 1998 Oct 23;273(43):28116-28121.
- [50] Gupta P, McCarthy JB, Verfaillie CM. Stromal fibroblast heparan sulfate is required for cytokine-mediated ex vivo maintenance of human long-term culture-initiating cells. *Blood* 1996 Apr 15;87(8):3229-3236.
- [51] Gupta P, Oegema TR, Jr, Brazil JJ, Dudek AZ, Slungaard A, Verfaillie CM. Structurally specific heparan sulfates support primitive human hematopoiesis by formation of a multimolecular stem cell niche. *Blood* 1998 Dec 15;92(12):4641-4651.
- [52] Gupta P, Oegema TR, Jr, Brazil JJ, Dudek AZ, Slungaard A, Verfaillie CM. Human LTC-IC can be maintained for at least 5 weeks in vitro when interleukin-3 and a single chemokine are combined with O-sulfated heparan sulfates: requirement for optimal binding interactions of heparan sulfate with early-acting cytokines and matrix proteins. *Blood* 2000 Jan 1;95(1):147-155.
- [53] Moore KLaP, TV.N. *The integumentary system. The Developing Human. Clinically Oriented Embryology*. 5th edition ed. Philadelphia: W.B. Saunders Company; 1993. p. 443.
- [54] Gluhak-Heinrich J, Guo D, Yang W, Harris MA, Lichtler A, Kream B, et al. New roles and mechanism of action of BMP4 in postnatal tooth cytodifferentiation. *Bone* 2010 Mar 3.
- [55] Hosokawa R, Deng X, Takamori K, Xu X, Urata M, Bringas P, Jr, et al. Epithelial-specific requirement of FGFR2 signaling during tooth and palate development. *J Exp Zool B Mol Dev Evol* 2009 Jun 15;312B(4):343-350.
- [56] Russell C, Henderson G, Jevon G, Matlock T, Yu J, Aklujkar M, et al. Murine MPS I: insights into the pathogenesis of Hurler syndrome. *Clin Genet* 1998 May;53(5):349-361.
- [57] Guven G, Cehreli ZC, Altun C, Sencimen M, Ide S, Bayari SH, et al. Mucopolysaccharidosis type I (Hurler syndrome): oral and radiographic findings and ultrastructural/chemical features of enamel and dentin. *Oral Surg Oral Med Oral Pathol Oral Radiol Endod* 2008 Jan;105(1):72-78.
- [58] Alpoz AR, Coker M, Celen E, Ersin NK, Gokcen D, van Diggelenc OP, et al. The oral manifestations of Maroteaux-Lamy syndrome (mucopolysaccharidosis VI): a case report. *Oral Surg Oral Med Oral Pathol Oral Radiol Endod* 2006 May;101(5):632-637.
- [59] Kuratani T, Miyawaki S, Murakami T, Takano-Yamamoto T. Early orthodontic treatment and long-term observation in a patient with Morquio syndrome. *Angle Orthod* 2005 Sep;75(5):881-887.
- [60] Northover H, Cowie RA, Wraith JE. Mucopolysaccharidosis type IVA (Morquio syndrome): a clinical review. *J Inherit Metab Dis* 1996;19(3):357-365.
- [61] Rimoin DL, Silberberg R, Hollister DW. Chondro-osseous pathology in the chondrodystrophies. *Clin Orthop Relat Res* 1976 Jan-Feb;(114):137-152.
- [62] Nuttall JD, Brumfield LK, Fazzalari NL, Hopwood JJ, Byers S. Histomorphometric analysis of the tibial growth plate in a feline model of mucopolysaccharidosis type VI. *Calcif Tissue Int* 1999 Jul;65(1):47-52.
- [63] Metcalf JA, Zhang Y, Hilton MJ, Long F, Ponder KP. Mechanism of shortened bones in mucopolysaccharidosis VII. *Mol Genet Metab* 2009 Jul;97(3):202-211.

- [64] Silveri CP, Kaplan FS, Fallon MD, Bayever E, August CS. Hurler syndrome with special reference to histologic abnormalities of the growth plate. *Clin Orthop Relat Res* 1991 Aug;(269):305-311.
- [65] Mango RL, Xu L, Sands MS, Vogler C, Seiler G, Schwarz T, et al. Neonatal retroviral vector-mediated hepatic gene therapy reduces bone, joint, and cartilage disease in mucopolysaccharidosis VII mice and dogs. *Mol Genet Metab* 2004 May;82(1):4-19.
- [66] Abreu S, Hayden J, Berthold P, Shapiro IM, Decker S, Patterson D, et al. Growth plate pathology in feline mucopolysaccharidosis VI. *Calcif Tissue Int* 1995 Sep;57(3):185-190.
- [67] Ruijter GJ, Valstar MJ, van de Kamp JM, van der Helm RM, Durand S, van Diggelen OP, et al. Clinical and genetic spectrum of Sanfilippo type C (MPS IIIC) disease in The Netherlands. *Mol Genet Metab* 2008 Feb;93(2):104-111.
- [68] Rigante D, Caradonna P. Secondary skeletal involvement in Sanfilippo syndrome. *QJM* 2004 Apr;97(4):205-209.
- [69] Fung EB, Johnson J, Madden J, Kim T, Harmatz P. Bone density assessment in patients with mucopolysaccharidosis: A preliminary report from patients with MPS II and VI. 2010;Volume 3(Number 1):1-82.
- [70] Baldo G, Oliveira P, Mayer FQ, Meurer L, Xavier RM, Matte U, et al. Joint disease progression in the murine model of mucopolysaccharidosis. 2010:97, 11th International Symposium on Mucopolysaccharide and Related Diseases, Adelaide, Australia.
- [71] Simonaro CM, D'Angelo M, He X, Eliyahu E, Shtraizent N, Haskins ME, et al. Mechanism of glycosaminoglycan-mediated bone and joint disease: implications for the mucopolysaccharidoses and other connective tissue diseases. *Am J Pathol* 2008 Jan;172(1):112-122.
- [72] Hoshino K, Tsutsui H, Kawai T, Takeda K, Nakanishi K, Takeda Y, et al. Cutting edge: generation of IL-18 receptor deficient mice: evidence for IL-1 receptor-related protein as an essential IL-18 binding receptor. *J Immunol* 1999 May 1;162(9):5041-5044.
- [73] Taylor KR, Yamasaki K, Radek KA, Di Nardo A, Goodarzi H, Golenbock D, et al. Recognition of hyaluronan released in sterile injury involves a unique receptor complex dependent on Toll-like receptor 4, CD44, and MD-2. *J Biol Chem* 2007 Jun 22;282(25):18265-18275.
- [74] Xia Y, Yamagata K, Krukoff TL. Differential expression of the CD14/TLR4 complex and inflammatory signaling molecules following i.c.v. administration of LPS. *Brain Res* 2006 Jun 20;1095(1):85-95.
- [75] Boettger MK, Hensellek S, Richter F, Gajda M, Stockigt R, von Banchet GS, et al. Antinociceptive effects of tumor necrosis factor alpha neutralization in a rat model of antigen-induced arthritis: evidence of a neuronal target. *Arthritis Rheum* 2008 Aug;58(8):2368-2378.
- [76] Nagasawa H, Kameda H, Sekiguchi N, Amano K, Takeuchi T. Improvement of the HAQ score by infliximab treatment in patients with RA: its association with disease activity and joint destruction. *Mod Rheumatol* 2009;19(2):166-172.
- [77] Simonaro CM, Ge Y, Eliyahu E, He X, Jepsen KJ, Schuchman EH. Involvement of the Toll-like receptor 4 pathway and use of TNF- α antagonists for treatment of the mucopolysaccharidoses. *Proc Natl Acad Sci U S A* 2010 Jan 5;107(1):222-227.
- [78] Billingham RC, Dahlberg L, Ionescu M, Reiner A, Bourne R, Rorabeck C, et al. Enhanced cleavage of type II collagen by collagenases in osteoarthritic articular cartilage. *J Clin Invest* 1997 Apr 1;99(7):1534-1545.
- [79] Aigner T, Gluckert K, von der Mark K. Activation of fibrillar collagen synthesis and phenotypic modulation of chondrocytes in early human osteoarthritic cartilage lesions. *Osteoarthritis Cartilage* 1997 May;5(3):183-189.
- [80] Nelson F, Dahlberg L, Laverty S, Reiner A, Pidoux I, Ionescu M, et al. Evidence for altered synthesis of type II collagen in patients with osteoarthritis. *J Clin Invest* 1998 Dec 15;102(12):2115-2125.

- [81] McDowell LM, Frazier BA, Studelska DR, Giljum K, Chen J, Liu J, et al. Inhibition or activation of Apert syndrome FGFR2 (S252W) signaling by specific glycosaminoglycans. *J Biol Chem* 2006 Mar 17;281(11):6924-6930.
- [82] Klionsky DJ, Emr SD. Autophagy as a regulated pathway of cellular degradation. *Science* 2000 Dec 1;290(5497):1717-1721.
- [83] Tessitore A, Pirozzi M, Auricchio A. Abnormal autophagy, ubiquitination, inflammation and apoptosis are dependent upon lysosomal storage and are useful biomarkers of mucopolysaccharidosis VI. *Pathogenetics* 2009 Jun 16;2(1):4.
- [84] Hershko A, Ciechanover A. The ubiquitin system. *Annu Rev Biochem* 1998;67:425-479.
- [85] Klionsky DJ, Cuervo AM, Seglen PO. Methods for monitoring autophagy from yeast to human. *Autophagy* 2007 May-Jun;3(3):181-206.
- [86] Settembre C, Fraldi A, Rubinsztein DC, Ballabio A. Lysosomal storage diseases as disorders of autophagy. *Autophagy* 2008 Jan 1;4(1):113-114.
- [87] Settembre C, Fraldi A, Jahreiss L, Spanpanato C, Venturi C, Medina D, et al. A block of autophagy in lysosomal storage disorders. *Hum Mol Genet* 2008 Jan 1;17(1):119-129.
- [88] Takamura A, Higaki K, Kajimaki K, Otsuka S, Ninomiya H, Matsuda J, et al. Enhanced autophagy and mitochondrial aberrations in murine G(M1)-gangliosidosis. *Biochem Biophys Res Commun* 2008 Mar 14;367(3):616-622.
- [89] Futerman AH, van Meer G. The cell biology of lysosomal storage disorders. *Nat Rev Mol Cell Biol* 2004 Jul;5(7):554-565.
- [90] Pereira VG, Gazarini ML, Rodrigues LC, da Silva FH, Han SW, Martins AM, et al. Evidence of lysosomal membrane permeabilization in mucopolysaccharidosis type I: Rupture of calcium and proton homeostasis. *J Cell Physiol* 2010 Jan 15.
- [91] Pryor PR, Mullock BM, Bright NA, Gray SR, Luzio JP. The role of intraorganellar Ca(2+) in late endosome-lysosome heterotypic fusion and in the reformation of lysosomes from hybrid organelles. *J Cell Biol* 2000 May 29;149(5):1053-1062.
- [92] Bach G, Chen CS, Pagano RE. Elevated lysosomal pH in Mucopolipidosis type IV cells. *Clin Chim Acta* 1999 Feb;280(1-2):173-179.
- [93] Turk B, Stoka V. Protease signalling in cell death: caspases versus cysteine cathepsins. *FEBS Lett* 2007 Jun 19;581(15):2761-2767.
- [94] Turk B, Turk D, Salvesen GS. Regulating cysteine protease activity: essential role of protease inhibitors as guardians and regulators. *Curr Pharm Des* 2002;8(18):1623-1637.
- [95] Boya P, Kroemer G. Lysosomal membrane permeabilization in cell death. *Oncogene* 2008 Oct 27;27(50):6434-6451.
- [96] Ferri KF, Kroemer G. Organelle-specific initiation of cell death pathways. *Nat Cell Biol* 2001 Nov;3(11):E255-63.
- [97] Beck M. Therapy for lysosomal storage disorders. *IUBMB Life* 2010 Jan;62(1):33-40.
- [98] Auclair D, Hein LK, Hopwood JJ, Byers S. Intra-articular enzyme administration for joint disease in feline mucopolysaccharidosis VI: enzyme dose and interval. *Pediatr Res* 2006 Apr;59(4 Pt 1):538-543.
- [99] Auclair D. An overview of intra-articular therapy for mucopolysaccharidosis VI. *Journal of pediatric rehabilitation medicine* 2010;3(1):3.
- [100] McGill JJ, Inwood AC, Coman DJ, Lipke ML, de Lore D, Swiedler SJ, et al. Enzyme replacement therapy for mucopolysaccharidosis VI from 8 weeks of age - a sibling control study. *Clin Genet* 2009 Nov 23.
- [101] Crawley AC, Niedzielski KH, Isaac EL, Davey RC, Byers S, Hopwood JJ. Enzyme replacement therapy from birth in a feline model of mucopolysaccharidosis type VI. *J Clin Invest* 1997 Feb 15;99(4):651-662.

- [102] Alonso-Fernandez JR, Fidalgo J, Colon C. Neonatal screening for mucopolysaccharidoses by determination of glycosaminoglycans in the eluate of urine-impregnated paper: preliminary results of an improved DMB-based procedure. *J Clin Lab Anal* 2010;24(3):149-153.
- [103] Pastores GM, Meere PA. Musculoskeletal complications associated with lysosomal storage disorders: Gaucher disease and Hurler-Scheie syndrome (mucopolysaccharidosis type I). *Curr Opin Rheumatol* 2005 Jan;17(1):70-78.
- [104] Staba SL, Escolar ML, Poe M, Kim Y, Martin PL, Szabolcs P, et al. Cord-blood transplants from unrelated donors in patients with Hurler's syndrome. *N Engl J Med* 2004 May 6;350(19):1960-1969.
- [105] Weisstein JS, Delgado E, Steinbach LS, Hart K, Packman S. Musculoskeletal manifestations of Hurler syndrome: longterm follow-up after bone marrow transplantation. *J Pediatr Orthop* 2004 Jan-Feb;24(1):97-101.
- [106] Masterson EL, Murphy PG, O'Meara A, Moore DP, Dowling FE, Fogarty EE. Hip dysplasia in Hurler's syndrome: orthopaedic management after bone marrow transplantation. *J Pediatr Orthop* 1996 Nov-Dec;16(6):731-733.
- [107] Byers S, Rothe M, Lalic J, Koldej R, Anson DS. Lentiviral-mediated correction of MPS VI cells and gene transfer to joint tissues. *Mol Genet Metab* 2009 Jun;97(2):102-108.
- [108] Polgreen LE, Tolar J, Plog M, Himes JH, Orchard PJ, Whitley CB, et al. Growth and endocrine function in patients with Hurler syndrome after hematopoietic stem cell transplantation. *Bone Marrow Transplant* 2008 Jun;41(12):1005-1011.
- [109] Polgreen LE, Plog M, Schwender JD, Tolar J, Thomas W, Orchard PJ, et al. Short-term growth hormone treatment in children with Hurler syndrome after hematopoietic cell transplantation. *Bone Marrow Transplant* 2009 Sep;44(5):279-285.
- [110] Docquier PL, Mousny M, Jouret M, Bastin C, Rombouts JJ. Orthopaedic concerns in children with growth hormone therapy. *Acta Orthop Belg* 2004 Aug;70(4):299-305.
- [111] Wang SY, Tung YC, Tsai WY, Chien YH, Lee JS, Hwu WL. Slipped capital femoral epiphysis as a complication of growth hormone therapy. *J Formos Med Assoc* 2007 Feb;106(2 Suppl):S46-50.
- [112] Wang ED, Drummond DS, Dormans JP, Moshang T, Davidson RS, Gruccio D. Scoliosis in patients treated with growth hormone. *J Pediatr Orthop* 1997 Nov-Dec;17(6):708-711.
- [113] Day GA, McPhee IB, Batch J, Tomlinson FH. Growth rates and the prevalence and progression of scoliosis in short statured children on Australian growth hormone treatment programmes. *Scoliosis* 2007 Feb 22;2:3.
- [114] Quigley CA, Gill AM, Crowe BJ, Robling K, Chipman JJ, Rose SR, et al. Safety of growth hormone treatment in pediatric patients with idiopathic short stature. *J Clin Endocrinol Metab* 2005 Sep;90(9):5188-5196.
- [115] Vidil A, Journeau P, Soulie A, Padovani JP, Pouliquen JC. Evolution of scoliosis in six children treated with growth hormone. *J Pediatr Orthop B* 2001 Jul;10(3):197-200.
- [116] Kanazawa T, Yasunaga Y, Ikuta Y, Harada A, Kusaka O, Sukegawa K. Femoral head dysplasia in Morquio disease type A: bilateral varus osteotomy of the femur. *Acta Orthop Scand* 2001 Feb;72(1):18-21.
- [117] Decker C, Yu ZF, Giugliani R, Schwartz IV, Guffon N, Teles EL, et al. Enzyme replacement therapy for mucopolysaccharidosis VI: Growth and pubertal development in patients treated with recombinant human N-acetylgalactosamine 4-sulfatase. *J Pediatr Rehabil Med* 2010;3(2):89-100.
- [118] Concolino D, Muzzi G, Pisaturo L, Piccirillo A, Di Natale P, Strisciunglio P. Precocious puberty in Sanfilippo IIIA disease: diagnosis and follow-up of two new cases. *Eur J Med Genet* 2008 Sep-Oct;51(5):466-471.

- [119] Guevarra MS, Yeh JK, Castro Magana M, Aloia JF. Synergistic effect of parathyroid hormone and growth hormone on trabecular and cortical bone formation in hypophysectomized rats. *Horm Res Paediatr* 2010;73(4):248-257.
- [120] Toledo SP, Costa VH, Fukui RR, Abelin N. Serum growth hormone levels in Hunter's syndrome. *Rev Hosp Clin Fac Med Sao Paulo* 1991 Jan-Feb;46(1):9-13.
- [121] Pleiner-Duxneuner J, Zwettler E, Paschalis E, Roschger P, Nell-Duxneuner V, Klaushofer K. Treatment of osteoporosis with parathyroid hormone and teriparatide. *Calcif Tissue Int* 2009 Mar;84(3):159-170.
- [122] Finkelstein JS, Klibanski A, Schaefer EH, Hornstein MD, Schiff I, Neer RM. Parathyroid hormone for the prevention of bone loss induced by estrogen deficiency. *N Engl J Med* 1994 Dec 15;331(24):1618-1623.
- [123] Wenstrup RJ, Bailey L, Grabowski GA, Moskovitz J, Oestreich AE, Wu W, et al. Gaucher disease: alendronate disodium improves bone mineral density in adults receiving enzyme therapy. *Blood* 2004 Sep 1;104(5):1253-1257.
- [124] Robinson C, Baker N, Noble J, King A, David G, Sillence D, et al. The osteodystrophy of mucopolidosis type III and the effects of intravenous pamidronate treatment. *J Inherit Metab Dis* 2002 Dec;25(8):681-693.
- [125] Li RH, Boussein ML, Blake CA, D'Augusta D, Kim H, Li XJ, et al. rhBMP-2 injected in a calcium phosphate paste (alpha-BSM) accelerates healing in the rabbit ulnar osteotomy model. *J Orthop Res* 2003 Nov;21(6):997-1004.
- [126] Boden SD, Kang J, Sandhu H, Heller JG. Use of recombinant human bone morphogenetic protein-2 to achieve posterolateral lumbar spine fusion in humans: a prospective, randomized clinical pilot trial: 2002 Volvo Award in clinical studies. *Spine (Phila Pa 1976)* 2002 Dec 1;27(23):2662-2673.
- [127] Cochran DL, Schenk R, Buser D, Wozney JM, Jones AA. Recombinant human bone morphogenetic protein-2 stimulation of bone formation around endosseous dental implants. *J Periodontol* 1999 Feb;70(2):139-150.
- [128] Tessitore A, Faella A, O'Malley T, Cotugno G, Doria M, Kunieda T, et al. Biochemical, pathological, and skeletal improvement of mucopolysaccharidosis VI after gene transfer to liver but not to muscle. *Mol Ther* 2008 Jan;16(1):30-37.
- [129] Bellettato CM, Scarpa M. Pathophysiology of neuropathic lysosomal storage disorders. *J Inherit Metab Dis* 2010 Aug;33(4):347-362.





CHAPTER 3

A SIMPLE PROCEDURE
TO DIFFERENTIATE RESIDUAL
 α -L-IDURONIDASE ACTIVITY
IN MILD AND SEVERE
MPS I PATIENTS

E. Oussoren, J. Keulemans, O. P. van Diggelen, L. F. Oemardien,
R. G. Timmermans, A. T. van der Ploeg, G.J.G. Ruijter

Molecular Genetics and Metabolism 2013 **109**:377–381

ABSTRACT

Introduction: Three major clinical subgroups are usually distinguished for Mucopolysaccharidosis type I, Hurler (MPS IH, severe presentation), Hurler/Scheie (MPS IH/S, intermediate) and Scheie (MPS IS, mild). For MPS IH patients, early diagnosis is important to facilitate treatment with hematopoietic stem cell transplantation. Newborn screening of MPS I would enable detection at a young age; however, prediction of the phenotype on the basis of the genotype in these young children may be difficult.

Methods: We developed a relatively easy method to measure residual α -L-iduronidase (IDUA) activity in MPS I fibroblasts using the commonly employed substrate 4-methylumbelliferyl- α -L-iduronide. Enzyme incubation was performed with high protein concentrations at different time points up to 8 h. IDUA activity was analyzed in fibroblasts from 5 MPS IH, 3 MPS I H/S and 5 MPS IS patients.

Results: Mean residual IDUA activity was 0.18% (range 0-0.6) of the control value in MPS IH fibroblasts, 0.27% (range 0.2-0.3) in MPS IH/S cells and 0.79% (range 0.3-1.8) in MPS IS fibroblasts. These results suggest a correlation of residual IDUA activity to severity of the MPS I phenotype. Two MPS IS patients with rare (E276K/E276K) or indefinite (A327P/unknown) IDUA genotypes had residual IDUA activity in the MPS IS range demonstrating the potential of our method to predict phenotypes. IDUA^{E276K} was very unstable at 37 °C, but more stable at 23 °C suggestive for thermal instability.

Conclusion: We report a procedure to determine residual IDUA activity in fibroblasts of MPS I patients which may be useful to predict MPS I phenotype.

INTRODUCTION

Mucopolysaccharidosis type I (MPS I, OMIM #252800) is an autosomal recessively inherited lysosomal storage disorder caused by deficiency of α -L-iduronidase (IDUA, E.C. 3.2.1.76), a glycosidase involved in the degradation of the glycosaminoglycans (GAG) dermatan- and heparan sulfate [1, 2]. The partially degraded GAG, which accumulate in the lysosomes, cause a wide range of clinical manifestations in MPS I patients. Three major clinical subgroups are commonly distinguished, Hurler syndrome (MPS IH, OMIM #607014; severe presentation), Hurler-Scheie syndrome (MPS IH/S, OMIM #607015; intermediate) and Scheie syndrome (MPS IS, OMIM #607016; mild). This classification in subgroups is, however, not precisely delineated clinically or biochemically [1]. MPS IH is characterised by early onset of clinical signs and symptoms including organomegaly, dysmorphic cardiac valves, restrictive pulmonary and obstructive airway disease, skeletal deformities, growth retardation, neurological complications and severe mental retardation. Their life expectancy is short, with death usually occurring in childhood. In MPS IS clinical problems develop later in life and are relatively mild (compared to MPS IH) and patients have normal intelligence. The phenotype of the MPS IH/S patients is intermediate [1] with variable neurological involvement. Later in life (early to mid-teens), these patients develop the clinical symptoms described for MPS IH patients. It may be difficult to distinguish MPS IH/S patients from the severe or the mild forms of MPS I.

The clinical diagnosis MPS I is confirmed by elevated levels of dermatan and heparan sulfate in urine and a deficiency of IDUA enzyme activity in leukocytes or fibroblasts [1]. The gene encoding IDUA is located on chromosome 4 (locus 4p16.3) and spans 19 kb including 14 exons [3]. More than 100 different mutations in the IDUA gene have been reported (Human Gene Mutation Database, <http://www.hgmd.org>). Prediction of the clinical phenotype of MPS I patients by analysis of the *IDUA* gene is not straightforward due to the large number of disease causing mutations, attenuating polymorphisms, rare sequence variants present in the *IDUA* gene and variation in genetic backgrounds [4].

Nowadays the two main therapies for MPS I patients are hematopoietic stem cell transplantation (HSCT) for MPS IH patients and enzyme replacement therapy (ERT) for the less severely affected MPS I patients (MPS IH/S and S). HSCT is ideally performed before 18 months of age (maximum age of 2 ½ years) and may prevent disease progression in the central nervous system to a large extent if performed in time [5, 6]. ERT cannot access sites of brain pathology due to protection of the brain by the blood-brain barrier therefore, ERT does not affect or prevent mental retardation although it effectively reduces the storage in other tissues such as liver and spleen [7, 8]. Early recognition/prediction of the phenotype of MPS I patients is essential in order to ensure that the most appropri-

ate, therapeutic strategy is initiated in a timely manner [9]. Newborn screening for MPS I might be an option to detect patients at a very young age before clinical features have become evident [10]. In such an event, determination of IDUA activity in leukocytes and mutation analysis of the *IDUA* gene would be the next steps to confirm the diagnosis. However, if novel mutations are found with unknown effects on IDUA function, the phenotype cannot be predicted precluding selection of the right therapy.

In this article an attempt is made to correlate residual IDUA activity in MPS I patients with phenotype and genotype. To this end, we have adapted the commonly used IDUA assay described by Stirling et al. in such a way that it allows discrimination between MPS IH and MPS IS [11]. Residual activity was measured in fibroblasts of MPS I patients with different mutations in the *IDUA* gene. Such enzymatic investigations in cells of young patients with previously undetected mutations can be helpful to predict clinical outcome, therefore aiding decision making with respect to the most optimal therapeutic strategy for individual patients.

MATERIALS AND METHODS

Sample preparation

Fibroblast cultures of MPS I patients, along with cultures from healthy controls, were provided by the European Cell Bank, Rotterdam, the Netherlands. Fibroblasts were cultured under standard conditions in Ham's F10 medium supplemented with 10% fetal calf serum, harvested by trypsinisation and stored as cell pellets at -80°C . One cell pellet was prepared from one 75 cm^2 flask. This study was approved by the Erasmus MC Institutional Review Board.

Enzyme assays

Fibroblast homogenates were prepared by resuspending one cell pellet in $100\ \mu\text{L}$ water followed by sonication for 10 sec at 130 W. Ten μL of homogenate was taken to determine protein concentration using the Pierce BCA Protein Assay kit (Thermo Scientific) in accordance with manufacturer's instructions. Protein concentration in homogenates from MPS I cells was adjusted to 2 mg/mL , while homogenates from control cells were diluted with 0.2% BSA to 0.02 mg/mL homogenate protein. α -L-Iduronidase activity was measured essentially as described by Stirling et al. [11] using $10\ \mu\text{L}$ fibroblast homogenate with $20\ \mu\text{L}$ substrate solution containing 2 mmol/L 4MU- α -L-iduronide (Glycosynth), 0.1 mol/L sodiumformate (pH 3.5) and 37.5 mmol/L NaCl. In some experiments, the protease inhibitor Pefabloc (Sigma) was added to the homogenate (final concentration 0.45 mg/mL). The reaction was terminated after different incubation times (0 to 8 h) by adding $200\ \mu\text{L}$ 0.5 mol/L sodium carbonate (pH 10.7) containing 0.25% (w/v) Triton-X-100. Substrate blanks were prepared at each time point and contained $10\ \mu\text{L}$ water instead of fibroblast homogenate. The fluorescence intensity was measured with a fluorimeter (Varioskan, Thermo Electron Corporation / Thermo Fisher Scientific Inc, Waltham, MA, US) using an excitation wavelength of 365 nm and an emission wavelength of 448 nm. A standard was prepared containing 750 nmol/L 4-methylumbelliferone (4MU). α -L-Iduronidase activities were calculated by subtraction of corresponding substrate blanks and conversion of fluorescence readings to nmol product released per mg protein. The limit of detection (signal-to-noise ratio 3) was 3.5 pmol 4MU, which is equivalent to an activity of 0.2 nmol/mg protein for MPS I cell homogenates. Typical fluorescence readings after 8 h of incubation corresponded to $20\text{--}30\text{ pmol}$ for substrate blanks, $30\text{--}40\text{ pmol}$ for MPS IH cell lines, $100\text{--}200\text{ pmol}$ for MPS IS cell lines and 400 pmol for controls. Half-life of IDUA activity was defined as the incubation time resulting in a 50% decrease of activity compared to the value at the start of the incubation. Total β -hexosaminidase was used as a control enzyme and was measured according to O'Brien et al. using 4MU-2-acetamido-2-deoxy- β -D-glucopyranoside (Melford) [12].

Statistical analysis

Statistical analysis was performed with SPSS, software version 17. A Mann-Whitney U test was used to test differences in IDUA activity between MPS IH and MPS IS for significance. Statistical significance was defined as $P < 0.05$ (two-tailed).

RESULTS

The residual activity of IDUA was measured in fibroblast cell lines of 5 MPS IH patients, three MPS IH/S patients and seven MPS IS patients (table 1, fig. 1). For three of the MPS IH patients, homozygous for Q70X, W402X and 134del12, barely detectable activities of maximal 0.2 nmol/mg protein/h at 37 °C were found. The very low activities (0.1 to 0.2% of the controls) were in accordance with the fact that the aforementioned mutations are essentially null alleles. The MPS IH fibroblast cell line homozygous for A327P consistently showed a residual activity of about 0.5 nmol/mg protein/h in the first 30 min of the incubation, but then decreased to an activity comparable to Q70X and W402X (fig. 1B). In the MPS IH cell line homozygous for L218P the residual IDUA activity was initially higher, with a maximal activity of 1.6 nmol/mg protein/h (0.6% of the controls) after one hour of incubation. However, the enzyme appeared to be unstable during longer incubation, with half-life activity of 2-4 h (fig. 1B). MPS IH cell lines carrying L218P in combination with other MPS IH alleles, W402X/L218P and A327P/L218P, had intermediate IDUA activities of 1.0 and 0.6 nmol/mg protein/h respectively (0.2 - 0.4% of the controls).

Two MPS IH/S cell lines analyzed were homozygous for P533R and L490P (table 1, fig. 1C). The activity of IDUA in these cell lines was 0.8 and 0.9 nmol/mg protein/h respectively, corresponding to 0.3% of the controls. In a third MPS IH/S cell line, genotype Q70X/R383H, IDUA activity was 0.5 nmol/mg protein/h (0.2% of the controls). IDUA activities in these three MPS IH/S cell lines were slightly higher than observed for the Q70X and W402X MPS IH cell lines.

Seven MPS IS cell lines with five different genotypes were analyzed. A cell line homozygous for R383H had a residual IDUA activity of 1.9 nmol/mg protein/h (0.7% of the controls; table 1, fig. 1C). The activity of IDUA of an MPS IS cell lines with genotype A327P/R383H was lower than the activity observed in the cell line homozygous for R383H as was expected on the basis of the combination of a milder Scheie mutation (R383H) with a severe Hurler mutation (A327P). An MPS IS cell line with genotype R621X/974ins12 had a residual activity of 2.5 nmol/mg protein/h (0.9% relative to the controls) with maximal activity up to 2 hours of incubation at 37 °C (fig. 1C). In this cell line the IDUA half-life was approximately 4-6 h. The fourth MPS IS cell line carried A327P on one allele, while the second mutation was not found. This cell line had an activity of 1.6 nmol/mg protein/h (0.6% residual activity).

Table 1 Residual IDUA activity in control and MPS I fibroblast cell lines at 37 °C

Phenotype	Genotype	Activity IDUA at 37 °C (nmol/mg/h) ^a	Residual activity at 37 °C (%) ^b
Control 1	Wt/Wt	197 ± 4	73
Control 2	Wt/Wt	313 ± 24	116
Control 3	Wt/Wt	247	92
Control 4	Wt/Wt	318	118
Hurler	Q70X/Q70X	0.2 ± 0.1	0.1
Hurler	W402X/W402X	0.2 ± 0.1	0.1
Hurler	A327P/A327P	0.5 ± 0.1	0.2
Hurler	L218P/L218P	1.6 ± 0.2	0.6
Hurler	134del12/134del12	<0.1	0.1
Hurler/Scheie	P533R/P533R	0.8 ± 0.3	0.3
Hurler/Scheie	L490P/L490P	0.9 ± 0.1	0.3
Hurler/Scheie	Q70X/R383H	0.5 ± 0.1	0.2
Scheie	R383H/R383H	1.9 ± 0.7	0.7
Scheie	A327P/R383H	0.8 ± 0.1	0.3
Scheie	A327P/unknown	1.6 ± 0.1	0.6
Scheie	R621X/974ins12	2.5 ± 0.2	0.9
Scheie	E276K/E276K ^c	3.0 ± 0.4	1.1
Scheie	E276K/E276K ^c	3.3 ± 1.1	1.2
Scheie	E276K/E276K ^c	4.9 ± 1.5	1.8

^a Activity was determined in the initial linear part of the trace (see also Fig. 1). Average values with standard deviation of at least two independent determinations are given. For controls 3 and 4 no duplicate values were available.

^b IDUA activity relative to the mean value of 4 different controls (269 nmol/mg/h). ^c Sibship.

Three siblings in one Turkish family with MPS IS were homozygous for a recently described, novel *IDUA* mutation, E276K [13]. IDUA activity in these fibroblasts was very unstable; almost all activity was lost after 30 minutes of incubation at 37 °C (fig. 1C), while IDUA activity was 3-4.9 nmol/mg protein/h (1.1 to 1.8% compared to controls) during the first 30 minutes of incubation. The IDUA activity did not stabilize with the addition of the protease inhibitor Pefabloc (data not shown). The next step was to investigate thermal stability by measuring IDUA activity of the E276K fibroblasts at 23 and 30 °C in addition to 37 °C (the incubation temperature normally used). By lowering the incubation temperature, the activity of IDUA in control fibroblast decreased to 57% at 30 °C and 26% at 23 °C of the activity measured at 37 °C (fig. 2A).

Figure 1 Residual IDUA activity in control and MPS I fibroblast cell lines at 37 °C

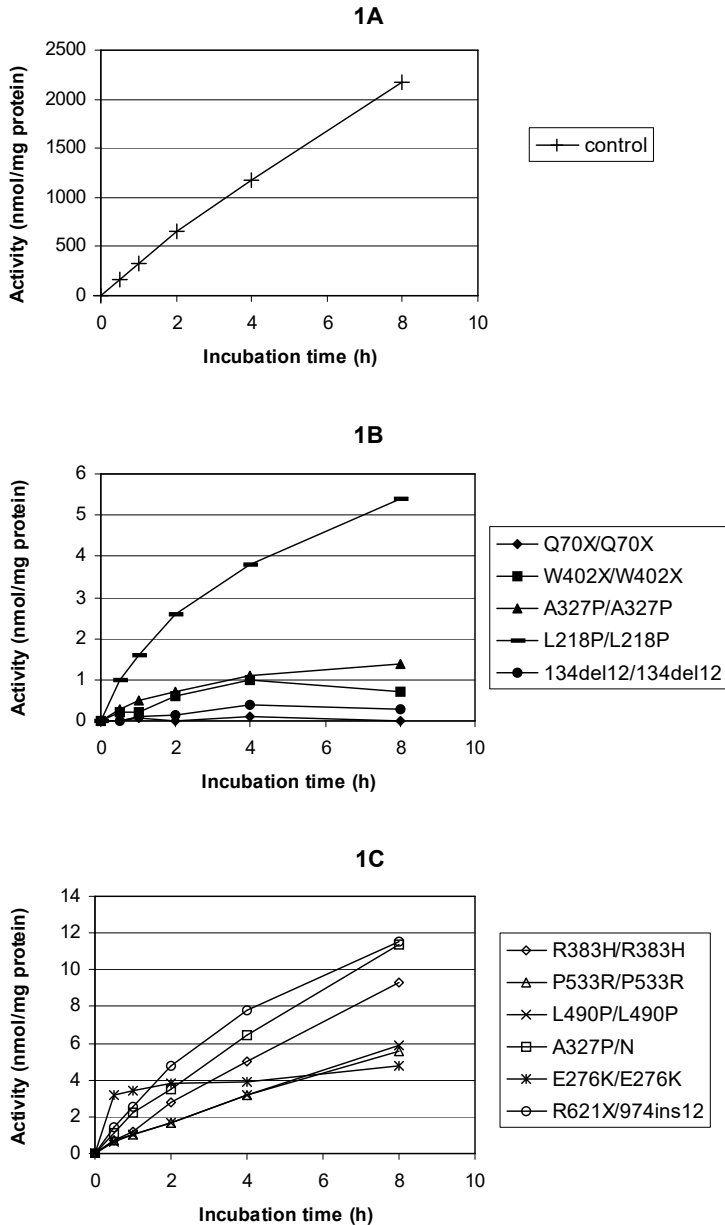


Fig. 1. IDUA activity in normal control and MPS I fibroblast cell lines. Activity was determined at 37 °C as described in the Materials and methods.

A, normal control; **B**, MPS IH cell lines (homozygous for Q70X, W402X, A327P, L218P and 134del12); **C**, MPS IH/S cell lines (homozygous for P533R and L490P) and MPS IS cell lines (R383H/R383H, E276K/ E276K, R621X/974ins12 and A327P/unknown).

The IDUA activity in the E276K fibroblasts showed comparable results at 30 °C and 37 °C during the first 30 minutes of incubation (fig. 2B), while a longer incubation time suggested a slightly more stable activity at 30 °C compared to 37 °C. At 23 °C the activity was approximately 50% of the value measured at 37 °C after 30 minutes, but at this lower temperature, activity levels were maintained much longer. These results suggest that the mutant E276K enzyme is thermo labile.

Mean residual IDUA activity was 0.18% (range 0-0.6) of the control value in MPS IH fibroblasts, 0.27% (range 0.2-0.3) in MPS IH/S cells and 0.79% (range 0.3-1.8) in MPS IS fibroblasts. IDUA activity was significantly different ($p = 0.02$) between MPS IH and MPS IS fibroblasts. The IDUA activity in MPS IH/S cells did not differ significantly from MPS IH and MPS IS cells ($p = 0.39$ and 0.1 respectively).

Figure 2 IDUA activity of the homozygous E276K fibroblast cell line

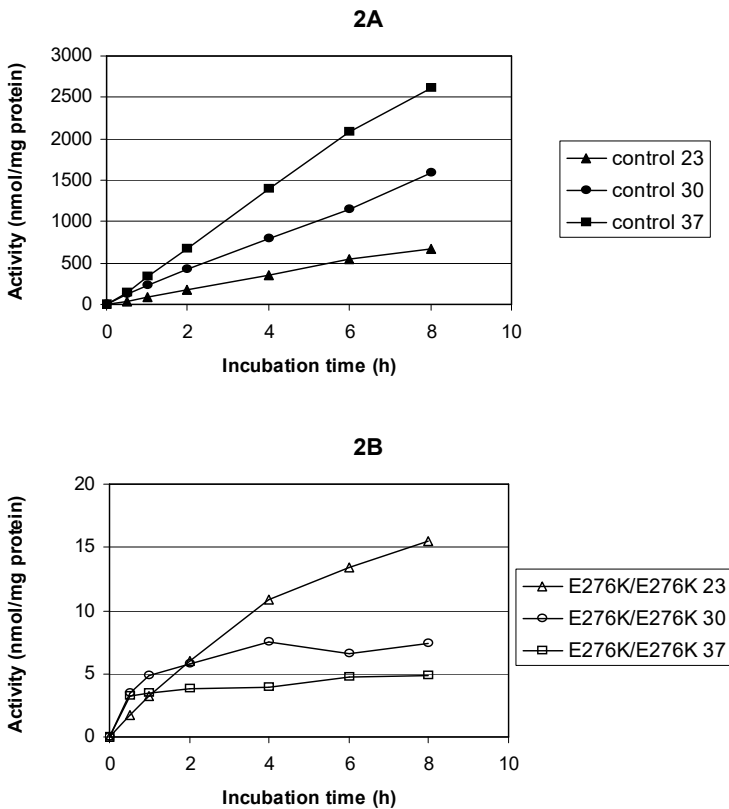


Fig. 2. IDUA activity in a normal control (A) and in an MPS IS fibroblast cell line homozygous for E276K (B) at 23, 30 and 37 °C.

DISCUSSION

The two main therapeutic options for MPS I are hematopoietic stem cell transplantation (HSCT) for MPS IH patients and enzyme replacement therapy (ERT) for the less severe MPS I phenotypes (MPS I H/S and S). Currently, the determination of the clinical phenotype is mainly based on clinical judgement which then determines the therapeutic strategy to be implemented. Since the age of symptom onset and the severity of symptoms clearly differ between the MPS IH and MPS IS patients, this may not pose a problem in most cases. However, with the growing awareness that particularly the mental development in MPS IH patients is much better when HSCT is performed at young age, interest in newborn screening programs increase. Newborn screening may enable detection of MPS IH patients at an early and potentially pre-symptomatic age. However, while the choice of therapy is relatively straightforward after a clinical diagnosis, it may not be as easy to determine with pre-symptomatic diagnosis through newborn screening. Prediction of the phenotype in these very young MPS I patients based on IDUA deficiency in bloodspots/leukocytes and genotype may be difficult and only reliably performed when patients have two known truncating IDUA mutations; therefore, additional diagnostic tools are required. Assuming that different MPS I phenotypes result from differences in residual IDUA activity, one such tool could be accurate determination of residual enzyme activity as presented in our study.

We showed that fibroblasts of MPS IH patients generally have very low or no residual IDUA activity, with an average of 0.18% of the control. Fibroblasts of the severely affected MPS IH patient homozygous for L218P had an unexpected, relatively high activity corresponding to 0.6% of the control. The highest residual activity, on average 0.79% of the control value, was found in fibroblasts of MPS IS patients, while MPS IH/S fibroblasts had an intermediate residual activity of 0.27%. Previously, Bunge et al. and Yogalingam et al. have measured residual IDUA activity in fibroblasts of patients with different MPS I phenotypes [14, 15]. Using the substrates K-L-iduronosyl anhydro-[1-3H]mannitol 6-sulfate (IMS) and tritiated α -L-iduronosyl(1-4)anhydromannitol-6-sulfate, they showed that there were differences in residual IDUA activity in fibroblasts of MPS IH and MPS IS patients. Our results are in line with those reported in the study of Bunge et al [14]. They measured less than 0.13% residual IDUA activity in cells of severely affected Hurler patients, whereas the residual activity in cells from Scheie patients ranged from 0.4-7% [14]. In MPS IH/S patients, residual IDUA activity has been reported in several studies to range from 0.03-1.8% [14, 16-18]. The potential advantage of the method used in our study is that we have used the widely employed substrate 4-methylumbelliferyl- α -L-iduronide, an assay that is easy to perform, with reliable results. The differences compared to the routine IDUA assay are a higher protein concentration, being 2 mg/mL instead of 1 mg/mL and longer

incubation times. Instead of 1 hour of incubation at 37 °C, we prolonged the incubation time up to 8 hours and measured the activity at different time points during this period. These modifications enabled a better determination of residual IDUA activity and provided information on IDUA stability.

The mean residual IDUA activity in MPS IH cells (0.18% of the control value) was significantly lower ($p = 0.02$) than the value measured in MPS IS cells (0.79%), suggesting a correlation between IDUA activity and the severity of the phenotype. The utility of our method is demonstrated for several patients with MPS IS phenotype: a sibship with the rare E276K mutation and a patient carrying A327P in combination with an unknown mutation. Both had clear residual IDUA activity (0.6-1.8% of the control) consistent with their MPS IS phenotype.

For 12 out of 13 cell lines (92%) with different MPS I genotypes (4 MPS IH, 3 MPS IH/S and 5 MPS IS), residual IDUA activity correlated to MPS I phenotype. An exception was the severely affected MPS IH patient homozygous for mutation L218P, which had a higher residual IDUA activity compared to the other homozygous Hurler mutations. IDUA^{L218P} activity resembled residual activity observed in MPS IS patients. On the basis of the observed residual IDUA^{L218P} activity, our method did not predict the severe MPS IH phenotype documented for this mutation [9, 17, 19]; however, IDUA^{L218P} activity was unstable (fig. 1B). In a structural study of mutant IDUA, Sugawara et al. suggested that L218P (as well as A327P) probably causes serious conformation changes in the IDUA enzyme, leading to decreased stability of the enzyme [9]. Alternately, the higher than expected activity of IDUA^{L218P} could perhaps be explained by a relatively high activity with the artificial 4MU substrate compared to the natural substrate. This has been described by Harzer et al. in Niemann–Pick A/B patients who exhibited pseudo-normal sphingomyelinase activity with the artificial substrate HMU-phosphorylcholine [20].

An interesting finding was the detection of the novel E276K mutation in a sibship of Scheie patients from Turkish ancestry. This mutation was recently reported in one Thai patient [13]. The E276K mutation resulted in a very unstable IDUA enzyme leading to an almost complete loss of enzyme activity within 30 minutes after start of incubation at 37 °C. Subsequent determination of IDUA activity at incubation temperatures of 23 °C and 30 °C showed a much better stability, particularly at 23 °C, suggesting that the rapid decrease in IDUA^{E276K} activity at 37 °C was due to thermal instability.

CONCLUSION

We report a simple procedure to determine residual IDUA activity in cultured fibroblasts of MPS I patients. This method may offer a potential tool for early prediction of the MPS I phenotype of patients. This may be particularly informative when the genotype is uninformative (e.g., when a novel mutation with unknown effect is detected), which becomes highly important in the event that neonatal screening would be introduced for MPS I (see proposed diagnostic algorithm; fig. 3). In such an event, our new method may be helpful as was shown for a sibship with the recently reported novel E276K mutation and for a patient carrying A327P in combination with an unknown mutation. Both had clear residual IDUA activity which correlated to their MPS IS phenotype. Additionally, incubation during longer periods and at different temperatures appeared helpful in detecting (thermal) instable IDUA species.

Figure 3 Flowchart MPS I newbornscreening

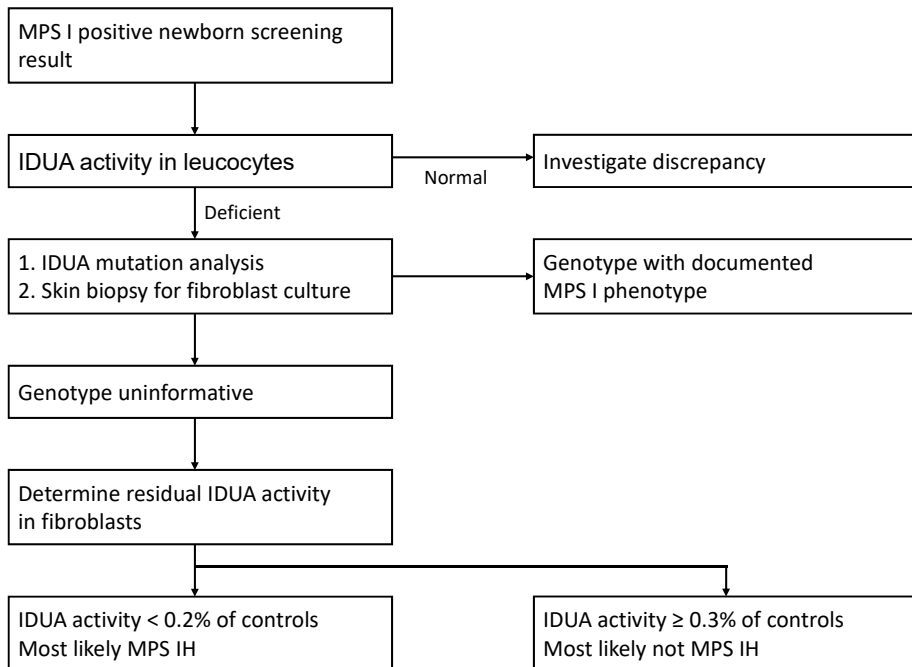
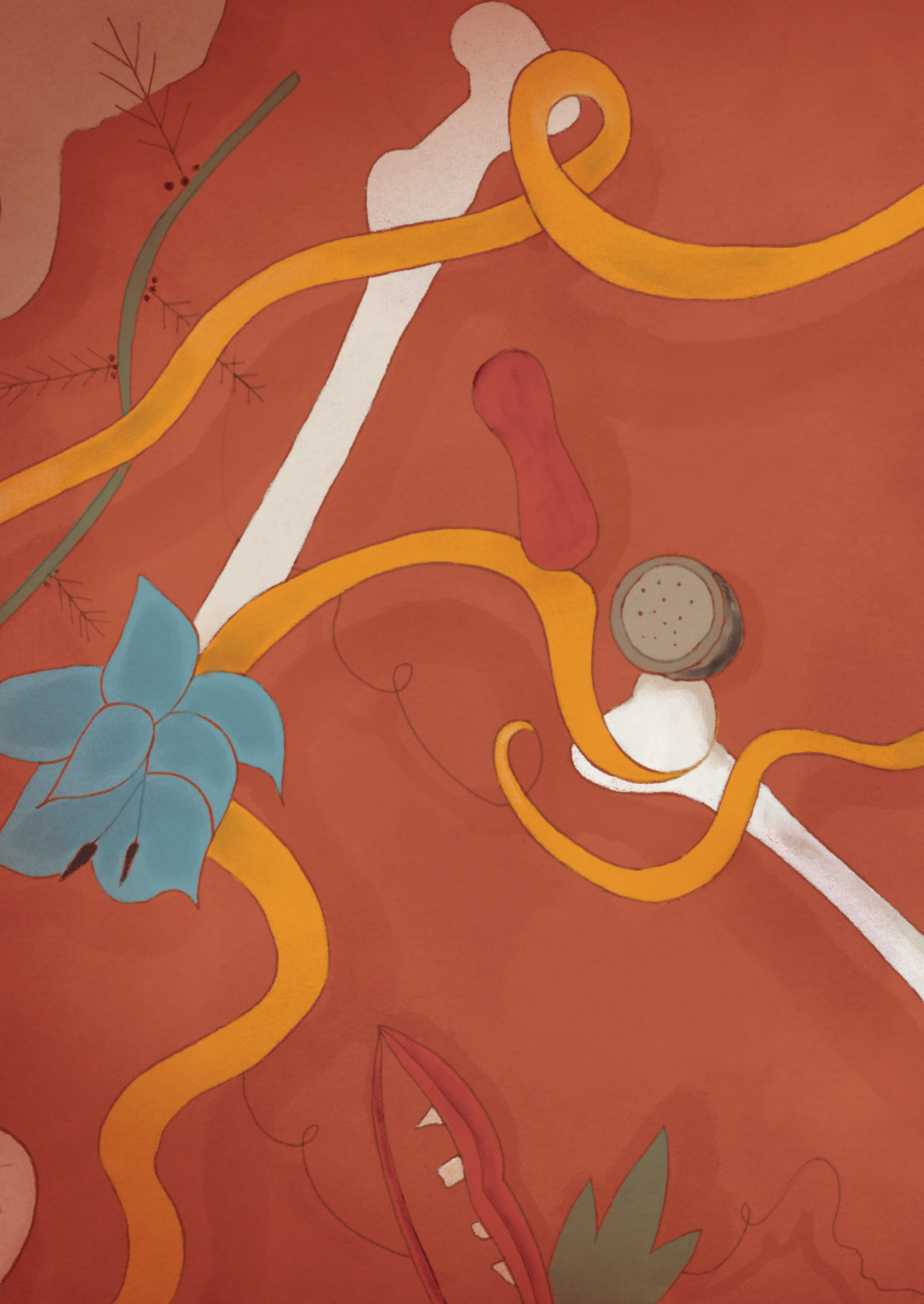


Fig.3. Proposed flowchart for diagnostic follow-up after a positive MPS I newborn screening result.

REFERENCES

- [1] E.F. Neufeld, J. Muenzer, "The Metabolic Bases of Inherited Disease," McGraw-Hill, New York, 2001.
- [2] J.J. Hopwood, C.P. Morris, The mucopolysaccharidoses. Diagnosis, molecular genetics and treatment, *Mol Biol Med*, 7 (1990) 381-404.
- [3] A.E. Schaffer, V.R. Eggens, A.O. Caglayan, M.S. Reuter, E. Scott, N.G. Coufal, J.L. Silhavy, Y. Xue, H. Kayserili, K. Yasuno, R.O. Rosti, M. Abdellateef, C. Caglar, P.R. Kasher, J.L. Cazemier, M.A. Weterman, V. Cantagrel, N. Cai, C. Zweier, U. Altunoglu, N.B. Satkin, F. Aktar, B. Tuysuz, C. Yalcinkaya, H. Caksen, K. Bilguvar, X.D. Fu, C.R. Trotta, S. Gabriel, A. Reis, M. Gunel, F. Baas, J.G. Gleeson, CLP1 founder mutation links tRNA splicing and maturation to cerebellar development and neurodegeneration, *Cell*, 157 (2014) 651-663.
- [4] H.S. Scott, S. Bunge, A. Gal, L.A. Clarke, C.P. Morris, J.J. Hopwood, Molecular genetics of mucopolysaccharidosis type I: diagnostic, clinical, and biological implications, *Hum Mutat*, 6 (1995) 288-302.
- [5] J.J. Boelens, R.F. Wynn, A. O'Meara, P. Veys, Y. Bertrand, G. Souillet, J.E. Wraith, A. Fischer, M. Cavazzana-Calvo, K.W. Sykora, P. Sedlacek, A. Rovelli, C.S. Uiterwaal, N. Wulffraat, Outcomes of hematopoietic stem cell transplantation for Hurler's syndrome in Europe: a risk factor analysis for graft failure, *Bone Marrow Transplant*, 40 (2007) 225-233.
- [6] M.H. de Ru, J.J. Boelens, A.M. Das, S.A. Jones, J.H. van der Lee, N. Mahlaoui, E. Mengel, M. Offringa, A. O'Meara, R. Parini, A. Rovelli, K.W. Sykora, V. Valayannopoulos, A. Vellodi, R.F. Wynn, F.A. Wijburg, Enzyme replacement therapy and/or hematopoietic stem cell transplantation at diagnosis in patients with mucopolysaccharidosis type I: results of a European consensus procedure, *Orphanet J Rare Dis*, 6 (2011) 55.
- [7] M. Beck, Therapy for lysosomal storage disorders, *IUBMB Life*, 62 (2010) 33-40.
- [8] E.D. Kakkis, J. Muenzer, G.E. Tiller, L. Waber, J. Belmont, M. Passage, B. Izykowski, J. Phillips, R. Doroshov, I. Walot, R. Hoft, E.F. Neufeld, Enzyme-replacement therapy in mucopolysaccharidosis I, *N Engl J Med*, 344 (2001) 182-188.
- [9] K. Sugawara, S. Saito, K. Ohno, T. Okuyama, H. Sakuraba, Structural study on mutant alpha-L-iduronidases: insight into mucopolysaccharidosis type I, *J Hum Genet*, 53 (2008) 467-474.
- [10] S. Blanchard, M. Sadilek, C.R. Scott, F. Turecek, M.H. Gelb, Tandem mass spectrometry for the direct assay of lysosomal enzymes in dried blood spots: application to screening newborns for mucopolysaccharidosis I, *Clin Chem*, 54 (2008) 2067-2070.
- [11] J.L. Stirling, D. Robinson, A.H. Fensom, P.F. Benson, J.E. Baker, Fluorimetric assay for prenatal detection of Hurler and Scheie homozygotes or heterozygotes, *Lancet*, 1 (1978) 147.
- [12] J.S. O'Brien, S. Okada, A. Chen, D.L. Fillerup, Tay-sachs disease. Detection of heterozygotes and homozygotes by serum hexosaminidase assay, *N Engl J Med*, 283 (1970) 15-20.
- [13] K. Prommajan, S. Ausavarat, C. Srichomthong, V. Puangrichareon, K. Suphapeetiporn, V. Shotelersuk, A novel pE276K IDUA mutation decreasing alpha-L-iduronidase activity causes mucopolysaccharidosis type I, *Mol Vis*, 17 (2011) 456-460.
- [14] S. Bunge, P.R. Clements, S. Byers, W.J. Kleijer, D.A. Brooks, J.J. Hopwood, Genotype-phenotype correlations in mucopolysaccharidosis type I using enzyme kinetics, immunoquantification and in vitro turnover studies, *Biochim Biophys Acta*, 1407 (1998) 249-256.
- [15] G. Yogalingam, X.H. Guo, V.J. Muller, D.A. Brooks, P.R. Clements, E.D. Kakkis, J.J. Hopwood, Identification and molecular characterization of alpha-L-iduronidase mutations present in mucopolysaccharidosis type I patients undergoing enzyme replacement therapy, *Hum Mutat*, 24 (2004) 199-207.

- [16] S. Laradi, T. Tukel, M. Erazo, J. Shabbeer, L. Chkioua, S. Khedhiri, S. Ferchichi, M. Chaabouni, A. Miled, R.J. Desnick, Mucopolysaccharidosis I: Alpha-L-Iduronidase mutations in three Tunisian families, *J Inherit Metab Dis*, 28 (2005) 1019-1026.
- [17] N.J. Terlato, G.F. Cox, Can mucopolysaccharidosis type I disease severity be predicted based on a patient's genotype? A comprehensive review of the literature, *Genet Med*, 5 (2003) 286-294.
- [18] Y.N. Teng, T.R. Wang, W.L. Hwu, S.P. Lin, G.J. Lee-Chen, Identification and characterization of -3c-g acceptor splice site mutation in human alpha-L-iduronidase associated with mucopolysaccharidosis type IH/S, *Clin Genet*, 57 (2000) 131-136.
- [19] S. Bunge, W.J. Kleijer, C. Steglich, M. Beck, C. Zuther, C.P. Morris, E. Schwinger, J.J. Hopwood, H.S. Scott, A. Gal, Mucopolysaccharidosis type I: identification of 8 novel mutations and determination of the frequency of the two common alpha-L-iduronidase mutations (W402X and Q70X) among European patients, *Hum Mol Genet*, 3 (1994) 861-866.
- [20] K. Harzer, A. Rolfs, P. Bauer, M. Zschesche, E. Mengel, J. Backes, B. Kustermann-Kuhn, G. Bruchelt, O.P. van Diggelen, H. Mayrhofer, I. Krageloh-Mann, Niemann-Pick disease type A and B are clinically but also enzymatically heterogeneous: pitfall in the laboratory diagnosis of sphingomyelinase deficiency associated with the mutation Q292 K, *Neuropediatrics*, 34 (2003) 301-306.





CHAPTER 4

A LONG TERM
FOLLOW-UPSTUDY OF
THE DEVELOPMENT OF HIP DISEASE
IN MUCOPOLYSACCHARIDOSIS
TYPE VI

E. Oussoren, J.H.J.M. Bessems, V. Pollet, J. C. van der Meijden, I. Plug,
A. S. Devos, G.J.G. Ruijter, A.T. van der Ploeg, Mirjam Langeveld

Mol Genet Metab 2017, **121**(3):241-251.

ABSTRACT

Introduction: Hip problems in Mucopolysaccharidosis type VI (MPS VI) lead to severe disability. Lack of data on the course of hip disease in MPS VI make decisions regarding the necessity, timing and type of surgical intervention difficult. Therefore, we studied the development of hip pathology in MPS VI patients over time.

Methods: Data was collected as part of a prospective follow-up study. Standardized supine AP pelvis and frog leg lateral radiographs of both hips were performed yearly or every 2 years. Image assessment was performed quantitatively (angle measurements) as well as qualitatively (hip morphology). Clinical burden of hip disease was evaluated by physical examination, a six-minute walking test (6MWT) and a questionnaire assessing pain, wheelchair dependency and walking distance.

Results: A total of 157 pelvic radiographs of 14 ERT treated MPS VI patients were evaluated. Age at first image ranged from 2.0 to 21.1 years. Median follow up duration was 6.8 years. In all patients, even in the youngest, the acetabulum and os ilium were dysplastic. Coverage of the femoral head by the acetabulum improved over time, but remained insufficient. While the femoral head appeared normal in the radiographs at a young age, over time, the ossification pattern became abnormal in all patients. A decrease in the distance covered in the 6MWT was also observed in all patients, as well as in the BRUCE treadmill test (median Z scores -3.3). Twelve patients had a waddling gait, four patients were partially wheelchairdependent and ten patients had limitations in their maximum walking distance.

Conclusion: Clinically significant hip abnormalities develop in all MPS VI patients very early in life, starting with deformities of the os ilium and acetabulum. Femoral head abnormalities occur later, most likely due to altered mechanical forces in combination with epiphyseal abnormalities due to glycosaminoglycan storage. The final shape and angle of the femoral head differs significantly between individual MPS VI patients and is difficult to predict.

INTRODUCTION

The lysosomal enzyme N-acetyl galactosamine 4-sulfatase (arylsulfatase B, coding gene ARSB, EC 3.1.6.12) is deficient in patients with Mucopolysaccharidosis type VI (MPS VI) or Maroteaux–Lamy syndrome (OMIM#253200). This deficiency causes intra-lysosomal accumulation of the glycosaminoglycans (GAGs) dermatan sulfate and chondroitin 4-sulfate in various connective tissues and organs, including cartilage and bone [1]. The birth prevalence of this autosomal recessive disorder in the Netherlands is 1 in 667,000 [2], whereas estimations worldwide range from 1:238,095 to 1:1,505,160 [3].

Patients in whom the disease progresses rapidly have high levels of GAG excretion in urine (above 22.7 mg/mmol creatinine) [4], early onset of symptoms and a shorter life expectancy compared to those in whom the disease progresses more slowly. However, even in patients with slow disease progression, invalidating manifestations of the disease develop [5]. Until enzyme replacement therapy (ERT) became available in 2007, allogeneic or hematopoietic stem-cell transplantation (HSCT) was the only treatment option for MPS VI patients. ERT has positive effects on visceral manifestations of the disease, range of motion of the shoulders, endurance capacity and some aspects of quality of life [6-8]. However, both HSCT and ERT seem ineffective in preventing the progression of skeletal complications such as kyphosis, scoliosis and hip disease [9-12]. Hip problems have a great impact on quality of life in all MPS VI patients, including those with milder forms of the disease [13-19]. Symptoms include pain in hips and legs, decreased movement and difficulty in walking caused by joint contractures. Some patients become partly or completely wheelchair dependent at a young age and orthopedic surgery is often deemed necessary [20]. In this prospective follow-up study, we focused in particular on the developmental pattern of hip disease in MPS VI in order to better understand clinical needs and direct future research.

MATERIAL AND METHODS

Patients

We included all patients with a diagnosis of Mucopolysaccharidosis type VI followed at the Center for Lysosomal and Metabolic diseases at the Erasmus MC University Medical Center in Rotterdam, the Netherlands, who had available hip radiographs. The protocol was approved by the Medical Ethical Committee at Erasmus University Medical Center in 2007. The diagnosis was established by measuring deficient arylsulfatase B activity in leucocytes and fibroblasts, as well as performing DNA analysis of the *ARSB* gene. All patients were treated with 1mg/kg of recombinant human arylsulfatase B (galsulfase, Naglazyme®, BioMarin Corporation) weekly.

Assessment of the AP pelvis and frog leg lateral radiographs

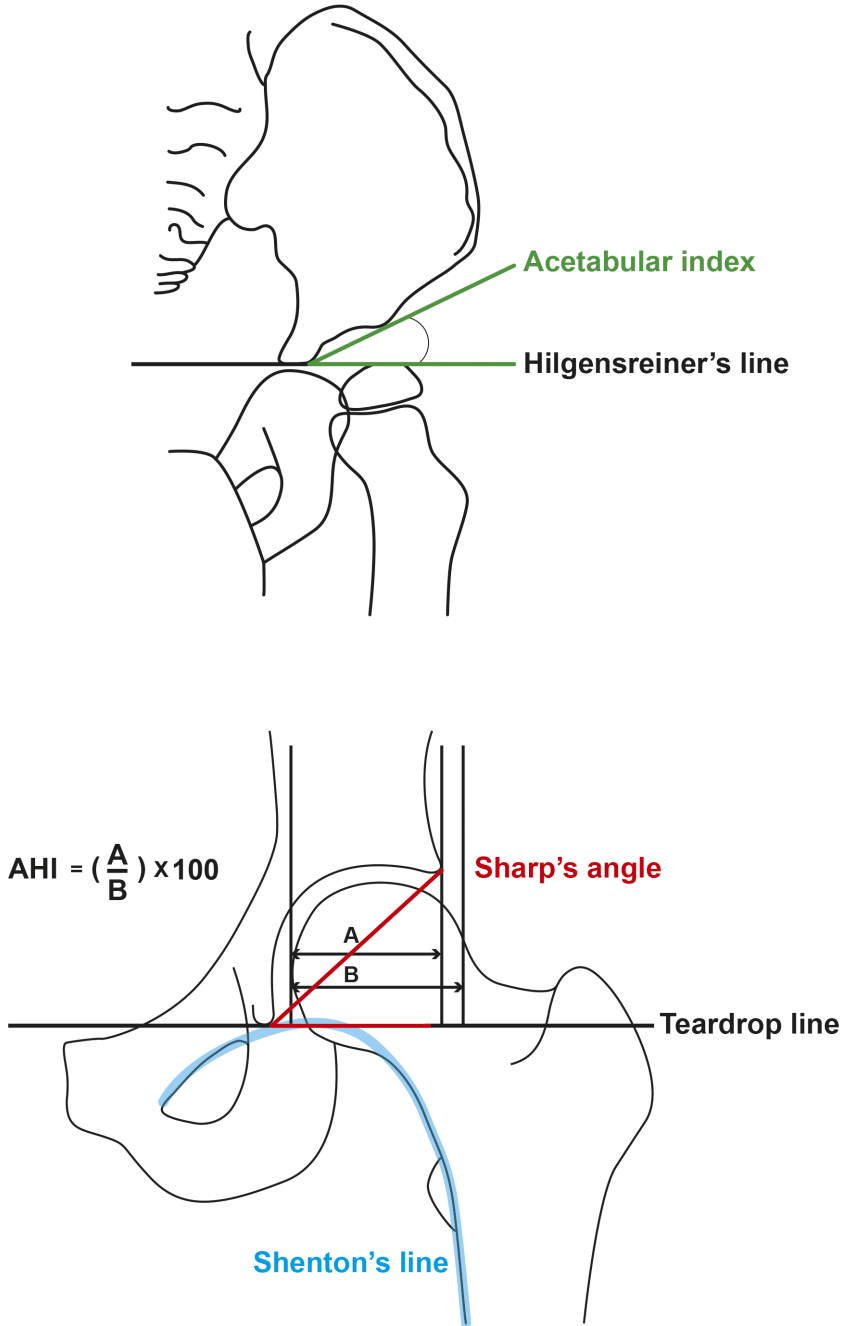
Yearly supine hip radiographs (Anteroposterior (AP) and frog leg lateral (Lauenstein)) radiographs were obtained as part of the standardized clinical follow-up protocol from 2007 onwards. We also included a small number of radiographs available before this date. One patient underwent hip reconstruction and two patients underwent guided growth of the knees, postoperative images were excluded from the analysis.

Quantitative assessment

To evaluate hip morphology in a standardized manner, we evaluated the following parameters (appendix fig. 1A). Acetabular index: The acetabular index (AI) (the inclination angle of the acetabulum) [21] was used to evaluate acetabular dysplasia. The AI values were compared with normal values as described by Schmid [22]. Sharp's angle: After closure of the triradiate epiphysis (around twelve years of age in girls and fourteen years in boys), the Sharp's angle (i.e., the angle between the inter-teardrop-line and the line connecting the inferior tip of the teardrop to the lateral acetabular rim) was measured [23]. A Sharp's angle value greater than 42.5 degrees is indicative of a dysplastic acetabulum [24]. Acetabular head index: The acetabular head index was used to quantify the femoral head coverage [25].

Shenton's line: The continuity of Shenton's line (drawn along the inferior border of the superior pubic ramus and along the inferomedial border of the neck of the femur) was assessed. This line is normally continuous and smooth, so interruption of this line is an indication of loss of containment. Neck shaft angle (NSA): The neck shaft angle of the femoral neck was measured to determine abnormalities of the position of the proximal femur. Coxa vara refers to a decreased neck-shaft angle and an increased neck-shaft angle is named coxa valga [26]. The NSA values were compared with normal values as described by Schmid [22].

Appendix figure 1A Measurements of different angles of the pelvis



Appendix fig. 1A. AI=acetabular index, SA=Sharp's angle, AHI=acetabular head index.

Statistical analysis

At group level, the change in the estimated mean of the left and right acetabular index (both as degrees and standard deviations) from birth up to age 12 were reported. The framework of linear mixed effects models was used to account for the correlations between the repeated measurements in individual patients. To account for potential non-linear profiles we used natural cubic splines in the fixed-effects and random-effects parts of the model with a maximum of 3 degrees of freedom. For the random-effects part of the model, an unstructured covariance matrix was used. The nlme package of R (version 3.2.1) was used to generate these models [27]. Trajectories of the NSA of individual patients were plotted over age for each patient.

Qualitative assessment

In all patients, the morphology and development of the hip joint over time were assessed and compared to normal hip development. The following aspects were assessed: Pelvis: Pelvic shape and congruency of the hip joint. Epiphyseal ossification: Shape and irregularities of the femoral head and femur epiphyseal. Metaphyseal ossification: The shape of the femoral metaphysis and angularity of the femoral neck.

Clinical assessment

Cardiac and pulmonary functions were assessed to evaluate the potential influence of heart or lung disease on mobility. For this assessment, shortening fraction and left-ventricular posterior wall thickness in diastole (LVPWd) were measured by echocardiography and forced vital capacity (FVC) by spirometry using a Lilly-type pneumograph (Viasys Healthcare, Wurzburg, Germany). The maximum value of three reproducible tests was used. Overnight polysomnography was conducted as described previously [7].

The six minute walking test (6MWT) was executed according to guidelines of the American Thoracic Society [28], reported as meters walked in 6 minutes. Z scores were calculated using age specific reference values [29]. Extension of the knees and hips were assessed using standardized goniometry measurements. During the 6MWT, two experienced physicians (a metabolic pediatrician and a physiotherapist) observed whether a waddling gait was present. Neurological examination was performed by a pediatric neurologist to detect neurological causes of limited mobility (e.g., spinal cord compression). On indication, an MRI of the craniocervical junction or complete spinal cord was made. When abnormal, spinal cord and spinal root function was assessed via somatosensory evoked potentials (SSEP). Clinical burden of hip disease in daily life was evaluated by a questionnaire assessing pain, wheelchair dependency and walking distance. These questionnaires were filled out once, at the time of the last outpatient clinic visit or by telephone interview, most often by the parent or caretaker of the patient.

RESULTS

Patient characteristics

Patient characteristics of the 14 included MPS VI patients are shown in table 1. Among them were three pairs of siblings. Seven of the fourteen patients had a rapidly progressive phenotype defined by disease presentation before the age of 5 years and urinary GAG levels above 22.7 mg/mmol creatinine [4]. The remaining seven patients had a slowly progressive phenotype. In our study urinary GAG levels of the rapidly progressive patients ranged from 59 to 88 mg/mmol creatinine (median 77 μ g/mg creatinine). The age of the patients at diagnosis ranged from 0.7 to 10.3 years (median 2.2 years in the rapidly progressive and 6.4 years in the slowly progressive patients).

The mutations of patients 1 to 11 have been described in an earlier study [7]. The mutations of patient 13 are not yet known. The sibs 12 and 14 are homozygous for the c.937C>G, p.Pro313Ala (*ARSB*, exon 05) mutation, which has been described in a heterozygous state previously [30]. All patients received enzyme replacement therapy. The duration of treatment at the last outpatient visit ranged from 1.9 to 9.8 years, median of 8.1 years. Age at the time of the first radiographs ranged from 2 to 16.6 years and for the last radiographs from 3.6 to 21.1 years. Time between first and last radiograph ranged from 0.5 to 11.9 years (median 6.8 years) (Table 1).

Assessment of the AP pelvis and frog leg lateral radiographs

A total of 88 AP pelvis and 69 frog leg lateral radiographs were available for analysis.

Quantitative assessment

Acetabular index: fig. 1A shows the average trend of the acetabular index (AI) of 13 MPS VI patients over time. On an individual level, 4 patients had an increase of the AI, 5 remained stable and 4 decreased over time. All patients AIs were above +2 SD during their entire follow-up. On a group level, the AI remained stable high over time in contrast to fast (normal) decline in healthy children. At the age of 12 years, the AI value is +6SD on group level (fig. 1B). This indicates severe acetabular dysplasia. Sharp's angle: all but two hips were dysplastic as defined by Sharp's angle of >42.5 degrees.

Acetabular head index: over time, the acetabular head index increased (9 patients) or remained unchanged (2 patients), indicating an improvement in coverage of the femoral head due to ossification of cartilage at the lateral side of the acetabulum and the formation of a neoacetabulum (examples fig.3 B-F). In two patients (patient 9 and 13), the acetabular index decreased, but both patients were still young.

Table 1 Patients characteristics

Pt nr.	Age at diagnosis (years)	First GAG (mg/mmol creatinine)	Type of disease (progression)	ARSB gene Allele 1	Allele 2
1*	7	12	Slowly	454C>T, (p.R152W), exon 2	454C>T, (p.R152W), exon 2
2	7.5	21.4	Slowly	454C>T, (p.R152W), exon 2	454C>T, (p.R152W), exon 2
3	2.9	67.5	Rapidly	1142+2T>C, exon 5	1142+2T>C, exon 5
4	10.3	22	Slowly	629A>G, (p.Y210C), exon 3	937C>G, (p.P313A), exon 5
5*	0.7	26.3	Slowly	454C>T, (p.R152W), exon 2	454C>T, (p.R152W), exon 2
6#	6.4	22.6	Slowly	629A>G, (p.Y210C), exon 3	979C>T, (p.R327X), exon 5
7	5	17.2	Slowly	629A>G, (p.Y210C), exon 3	979C>T, (p.R327X), exon 5
8#	5.9	21.7	Slowly	629A>G, (p.Y210C), exon 3	979C>T, (p.R327X), exon 5
9	2.7	86	Rapidly	995 T>G, (p.V332G), exon 2	995 T>G, (p.V332G), exon 2
10	1.9	88	Rapidly	903C>G, (p.N301K), exon 5 1151G>A, (p.S384N), exon 6 (neutral)	903C>G, (p.N301K), exon 5 1151G>A, (p.S384N), exon 6 (neutral)
11	1.4	84	Rapidly	971G>T, (p.G324V), exon 5	971G>T, (p.G324V), exon 5
12+	4.6	59	Rapidly	937C>G, (p.P313A), exon 5	937C>G, (p.P313A), exon 5
13	3.1	86.4	Rapidly	Unknown	Unknown
14+	2.2	71	Rapidly	937C>G, (p.P313A), exon 5	937C>G, (p.P313A), exon 5

Pt patient; *, #, + siblings; GAG glycosaminoglycans; ERT enzyme replacement therapy. Patient 1 underwent hip surgery at age 21, after which his radiographs were excluded from analysis.

Shenton's line: in eight patients, Shenton's line was continuous at all ages (patients 1, 2, 4, 5, 8, 10, 12 and 14). In patients 3 and 6, Shenton's line was interrupted up to ages 12 and 14, after which it became continuous again. In patient 7, the line was discontinuous in both hips up to age 7, after which the right side was continuous, but the left remained discontinuous. In patient 9, the left hip showed interruption of Shenton's line in all radiographs evaluated. In patients 11 and 13, the line was discontinuous at all ages.

Neck shaft angle (NSA): individual trends of the mean of the right and left NSA until age 21 are shown in fig. 1C. There is great variance between the individual patients. The oldest (slowly progressive) patient had serious varus position of the neck shaft angle. He received an intertrochanteric valgus osteotomy of his left hip.

Qualitative assessments

Pelvis

The os ilium was abnormally shaped in all patients at all ages. Characteristic features were flaring of the iliac wings and hypoplasia of the basilar portions of the ilium (fig. 2). The acetabulum was abnormally shaped, being steep, shallow and small (current study)

Ethnicity	Age at start ERT (years)	Duration ERT (years)	Age first radiograph of pelvis/hips	Age last radiograph of pelvis/hips
Turkish	18.3	3.5	16.6	21.1
Turkish	8.2	8.8	7.6	16.8
Indian	6.8	9.8	3.9	15.8
Dutch	10.6	5.8	10	15.6
Turkish	7.6	8.6	7.6	15.1
Dutch	7.8	8.2	7.3	13.4
Dutch	5.9	9.5	5.3	13.4
Dutch	6.1	8.2	5.8	14.2
Morocco	3.0	8.7	2.9	10.5
Turkish	2.0	7.9	2	9.8
Guinea	2.3	7.1	2.2	8.2
Dutch	5.1	1.9	4.6	6.6
Dutch/ Zimbabwe	3.2	1.9	3.1	3.6
Dutch	2.7	1.9	2.4	4.4

[13-19]. The dysplasia of the acetabulum increases over time without loss of congruency as the shape of the acetabulum adjusts to the enlargement of the femoral head over time (formation of a neoacetabulum) (fig. 3B-F).

Epiphyseal ossification

Since patients with slowly progressive MPS VI are diagnosed at an older age compared to those with rapidly progressive disease, radiographs of the hips under the age of five were only available for patients with the rapidly progressive phenotype. Epiphyseal ossification appeared normal in the radiographs taken, up to the age of 3 years (patients 9, 10, 11, 13, 14 at age 3, 2, 2, 3.6 and 2 years old) (examples fig. 2 and 3E and F). In radiographs of all patients with both phenotypes, from age 3 onwards, ossification shows progressive abnormalities, altering the shape of the femoral head over time. The abnormal ossification was specifically noted in the central and medial part of the femoral head epiphysis. Only in one patient (patient 3) the medial part was altered. The final shape of the femoral head (at last available radiograph) differed between patients.

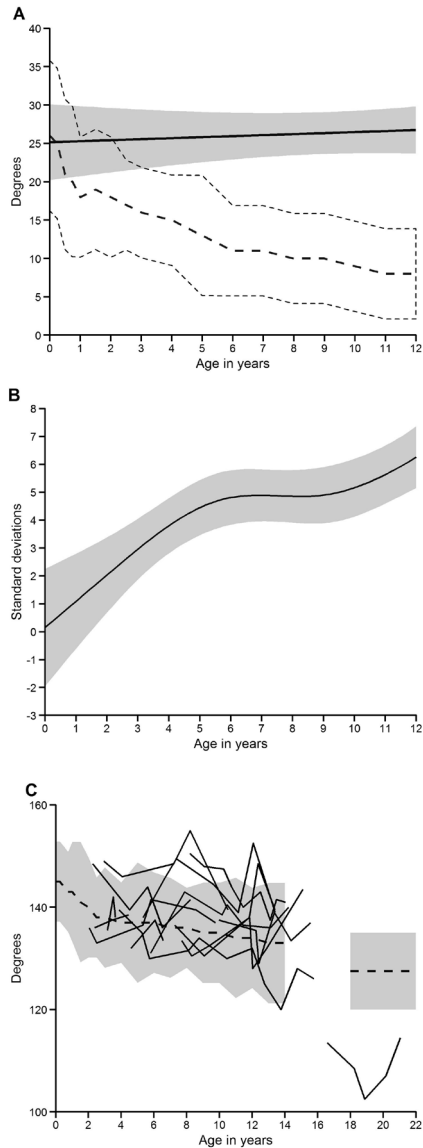
Figure 1 Quantitative assessment of pelvic radiographs

Fig.1. 1A: Modeled trend of the mean of the left and right acetabular index (AI) (solid line) and 95% prediction interval (PI) (grey area) based on radiographs of 13 MPS VI patients 0-12 years of age (delta 1.58, $p=0.57$). The reference mean (male and female) is indicated by the dotted black line, while the area between the grey dotted lines represents \pm 95% confidence interval.

1B: AI Z-score of the modeled trend shown in fig. 1A (solid line) with \pm 95% prediction interval (PI) (grey area) (delta 6.1, $p<0.0001$).

C: Individual trends of the mean of the left and right neck shaft angle of 14 MPS VI patients aged 0 to 21 y (solid lines). Dotted line indicates the reference values (mean of female and male) with \pm 95% confidence interval (grey area).

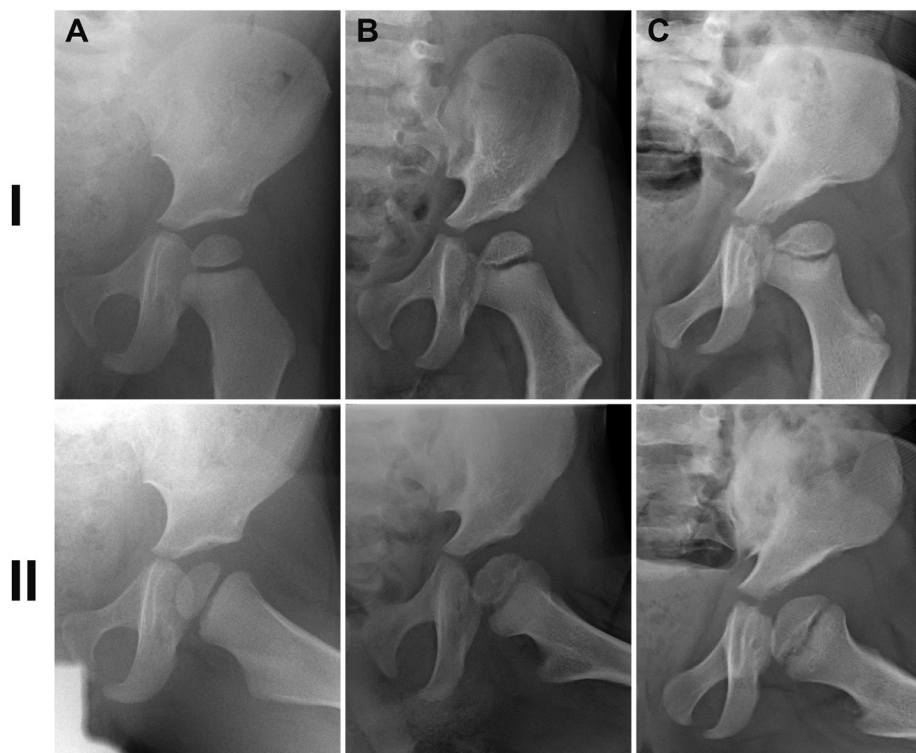
Figure 2 Hips of young MPS type VI patients

Fig. 2. Examples of two left hips of young, rapidly progressive MPS type VI patients compared to normal left hip aged 2 years. I: AP=anteroposterior radiograph, II: Frog leg lateral radiograph. Left part of the pelvis and femoral head of a normal control at the age of 2 years (**A**); abnormal shaped pelvis, with dysplasia of the os ilium and steep, shallow, small acetabulum and normal femoral head in patient 14 at the age of 2 years (**B**); and in patient 13 at the age of 3.6 y (**C**).

A number of patients (1, 2 and 5) had a broad and flat femoral head (also named coxa magna) (example fig. 3B and appendix fig. B 1,2 and 3). In others (patients 4, 6, 7, 8, 9, 11 and 13) the femoral head was extremely flat, while patients 4, 6, 7 and 8 showed irregularities of the epiphysis (appendix fig. B4-8) (examples fig. 3C and E). In patients 10, 12 and 14, less flattening of the femoral head occurred, but irregularities of the central part of the epiphysis were observed (example fig. 3F). Patient 3 was the only patient with an ovoid shape of the femoral head (example fig. 3 D).

Metaphyseal ossification (femoral neck)

Development of the femoral metaphysis was abnormal in all patients, resulting in abnormal shape or angularity of the femoral neck. For example, the femoral neck in patient 2 was broad from the beginning and the neck shaft angle (NSA) was decreased (coxa breva

and vara) (fig. 3B). The femoral neck in patients 7, 9 and 10 developed normally over time, but the NSA was increased (coxa valga) in patients 7 and 9 and decreased in patient 10 (coxa vara) (fig. 3C, E and F). In patient 3, the femoral neck narrows centrally over time resulting in an hour glass shape deformity (fig. 3D).

Figure 3 Hip development in MPS VI patients

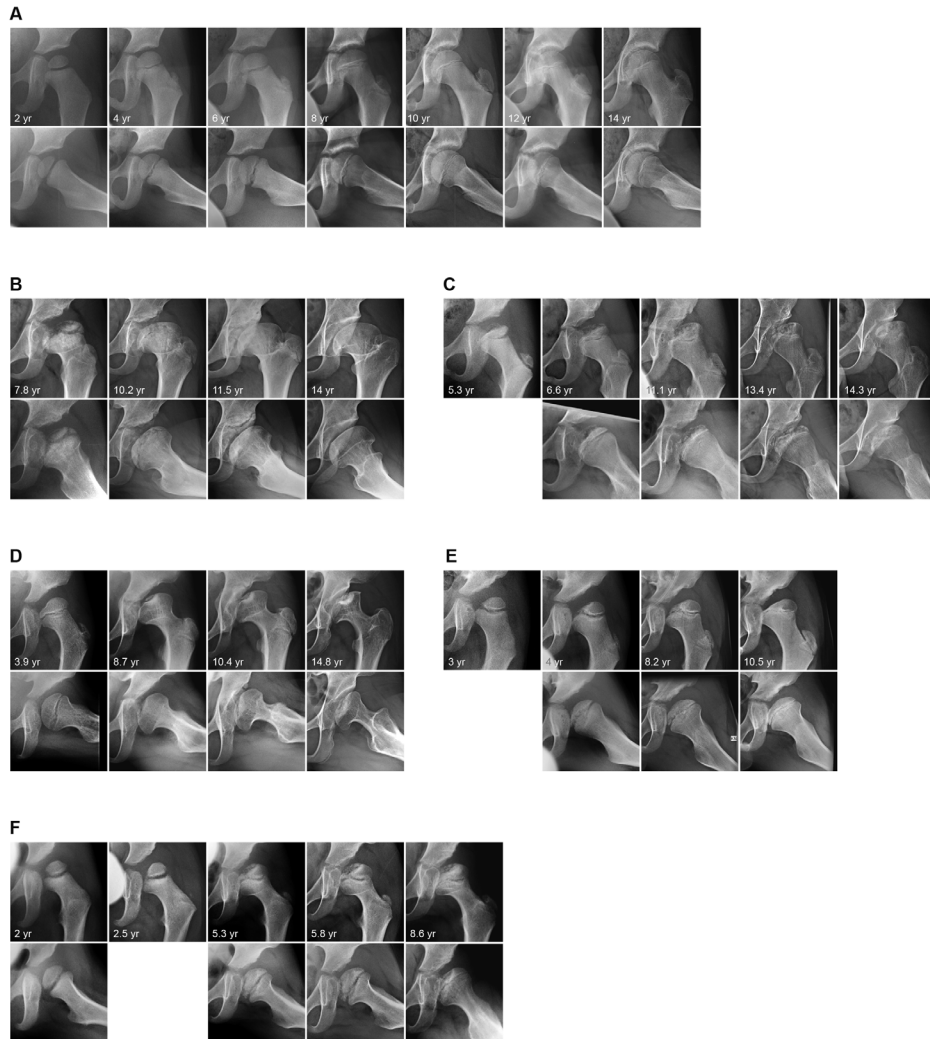
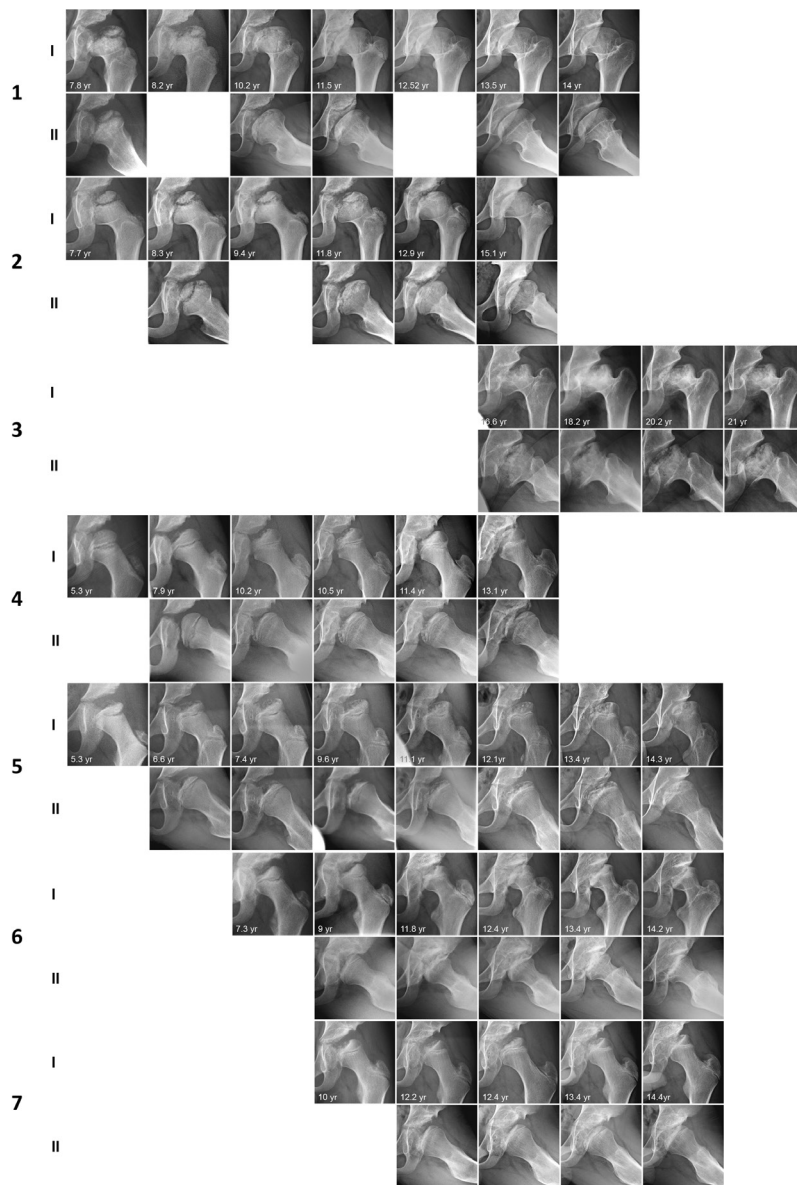


Fig.3. Examples of developmental patterns of the acetabulum, proximal femoral epiphysis and metaphysis in males aged 2-14 years: **A** with normal development (radiographs from different individuals) and of 5 MPS VI patients: **B**, patient 2; **C**, patient 7; **D**, patient 3; **E**, patient 9; **F**, patient 10.

Appendix figure B Examples of developmental patterns of the acetabulum, proximal femoral epiphysis and metaphysis according to mutation


Appendix fig. B. In patients homozygous for R152W (**1**, patient 2; **2**, patient 5; **3**, patient 1) the final shape of the femoral head is broad (coxa magna) and flat (coxa plana), with a decreased neck shaft angle (NSA) (coxa vara).

In patients with Y210C/R327X (**4**, patient 8; **5**, patient 7; **6**, patient 6) and one patient with Y210C/P313A (**7**, patient 4), the final shape of the femoral head is extremely flat with irregularities of the epiphysis, a normally shaped metaphysis with increased neck shaft angle (coxa valga).

I: AP=anteroposterior radiograph, II: Frog leg lateral radiograph

Table 2 Clinical assessments

Pt nr	SF% Z score age	LVPWd cm Z score age	FVC% Z score age	Polysomnography age	Goniometry Knee degrees flexion right/left age	Goniometry Hip degrees flexion right/left age	Waddling gait (y/n)
1	44.8 2.4 21.2 yr.	0.72 -2.1 21.2 yr.	82 -1.3 25 yr.	Mild signs of obstructive hyperpnea 24.6 yr.	162/160 21 yr.	165/166 21 yr.	y
2	38 0.8 15.7	0.92 0.74 15.7	94 -0.45 15.7	Normal 14.5 yr.	165/165 16.2 yr.	160/155 16.2 yr.	y
3	21.5 -5.1 15.4 yr.	0.8 1.9 15.4 yr.	63 -2.96 15.3 yr.	No obstructive hypopnea 15.2 yr.	170/170 15.8 yr.	165/165 15.8 yr.	y
4	36.4 0.34 14.6 yr.	0.79 -0.1 14.6 yr.	89 -1.3 15.1 yr.	No obstructive hypopnea 13.7 yr.	175/175 15.6 yr.	170/175 15.6 yr.	y
5	32.1 -0.96 14.6	1.2 * 2.5 14.6	110 1.17 15.1	Normal 13.4 yr.	175/170 15.6 yr.	170/170 15.6 yr.	y
6	33 -0.65 14.8	0.77 -0.3 14.8	132.6 2.7 14.8	Normal 12.6 yr.	185/185 15.3 yr.	160/160 15.3 yr.	y
7	31.6 -1.1 14 yr.	0.87 0.75 14 yr.	98.8 -0.2 14	Normal 12.6 yr.	160/167 12.9 yr.	170/171 12.9 yr.	y
8	38.1 0.8 12.9 yr.	0.8 -0.2 12.9 yr.	104.9 0.7 13.1 yr.	No obstructive hypopnea 12.9 yr.	170/175 13.6 yr.	160/160 13.6 yr.	y
9	37.3 0.54 10.5 yr.	0.48 -2 10.5 yr.	65 -4 10.5 yr.	Normal 10.4 yr.	170/170 11.1 yr.	165/165 11.1 yr.	y
10	37 0.41 8.1 yr.	0.48 -1.7 8.1 yr.	70 -2.56 8.6 yr.	Mild obstruction 7.7 yr.	165/167 9 yr.	160/165 9 yr.	y
11	40.4 1.4 7.8 yr.	0.68 0.2 7.8 yr.	65 -4 8.2 yr.	Normal 7.1 yr.	170/170 8.8 yr.	165/170 8.8 yr.	y
12	36.6 0.13 4.6 yr.	0.49 -0.94 4.6 yr.	106 0.48 5.8 yr.	Normal 4.7 yr.	170/175 6.3 yr.	165/170 6.3 yr.	n
13	41.4 1.5 3.8 yr.	0.6 0.56 3.8 yr.	NA NA NA	Normal 3.2 yr.	165/170 4.8 yr.	170/170 4.8 yr.	y
14	37 0.08 2.3 yr.	0.46 -0.86 2.3 yr.	NA NA NA	No obstructive hypopnea 2.4 yr.	170/175 4.2 yr.	175/170 4.2 yr.	n

SF shortening fraction; LVPWd left-ventricular posterior wall thickness in diastole in cm, *minor left ventricle hypertrophy, FVC forced vital capacity, neurological investigation included: clonus, Babinski and muscle tonus; SSEP somatosensory potentials yr year; ND not done, **This patient was unable to follow instructions.

6MWT meters Z score age	Neurological Examination Muscle strength legs right/left (MRC) age	MRI craniocervical junction MRI total spinal cord age	SSEP age
425 m -3.6 24.6 yr.	Normal 23.9 yr.	Craniocervical Co-C3 narrowing no spinal cord compression, ND 25.3 yr.	Normal 23.2 yr.
424 m -4.7 13.1 yr.	Normal 16.2 yr.	Craniocervical narrowing no spinal cord compression, ND 16 yr.	ND
264 m -7.8 14.8 yr.	Normal 15.8 yr.	Craniocervical narrowing no spinal cord compression, ND 15.4 yr.	Normal 9.9 yr.
512 m -2.5 15.2 yr.	Normal, hip flexors and abductors 4/4 15.6 yr.	Craniocervical narrowing no spinal cord compression/ lumbar, thoracic cord normal 14.4 yr.	Normal 11.2 yr.
466 m -3.1 12.0 yr.	Normal, hip abductors 4/4, 15.1 yr.	Total spinal cord no narrowing 7.9 yr., 15.2 yr.	ND
482m -3.2 11.8 yr.	Normal, hip abductors 4/4 15.3 yr.	Craniocervical (cannel) narrowing no spinal cord compression, ND 14.3 yr.	Normal 10.2 yr.
409 m -4.3 11.1 yr.	Normal, hip abductors 4/4 14.3 yr.	Craniocervical narrowing no spinal cord compression, ND 12.6 yr.	ND
505 m -2.7 10.2 yr.	Normal, hip abductors 4/4 13.6 yr.	Craniocervical narrowing no compression, ND 13.1 yr.	Normal 9.7 yr.
380 m -3.5 7.6yr.	Normal, hip abductors 4/4 11.1 yr.	Craniocervical narrowing, spinal cord compression/Th11/ Th12, Th12/ L1 discus herniation no compression 9.7 yr.	Normal 9.5 yr., 9.8 yr.
384 m -1.3 5.9 yr.	Normal 9.6 yr.	Craniocervical narrowing, no spinal cord compression, thoracic/lumbar spinal cord no narrowing 8.4 yr.	Normal 4.9 yr.
ND**	Seems normal** 8.8 yr.	Craniocervical narrowing no spinal cord compression/ thoracic, lumbar no narrowing 8.5 yr.	Normal 8.9 yr.
355 m -1.6 5.6 yr.	Normal 6.6 yr.	Craniocervical narrowing with spinal cord compression/ thoracic, lumbar no narrowing 6.4 yr.	Normal 6.4 yr.
ND	Normal 4.8 yr.	Craniocervical narrowing, no spinal cord compression, ND 4.4 yr.	ND
318 m -2.3 3.2 yr.	Normal 4.2 yr.	Craniocervical narrowing (also C3-C5) no spinal cord compression/thoracic, lumbar no narrowing 2.4 yr.	ND

Appendix table 1 Hip disease, clinical symptoms and physical limitations

Pt nr	Age at time questionnaire (years)	Pain in right hip (age onset)	Pain in left hip (age onset)	Abnormal gait (y/n)
1	24.8	-	-#	y
2	15.7	-	-	y
3	15.3	-	-	y
4	15.0	-	-	y
5	14.9	+ (7 yr.)	+ (7 yr.)	y
6	14.7	++ (13 yr.)	+ (13 yr.)	y
7	14.0	-	-	y
8	13.0	-	-	y
9	10.4	-	-	y
10	8.6	-##	-	y
11	8.1	NA	NA	y
12	5.6	-	-	y
13	3.8	-	-	y
14	3.3	-	-	n

Operation valgus and endorotation osteotomy proximal femur left at age 21 yr, NA not applicable. ## pain in knees. + mild, ++ moderate,+++ severe, y=yes, n=no, yrs= years, min=minutes, hrs= hours, m=meter, km=kilometer.

Clinical assessment

In three patients (3, 9 and 10), cardiac or pulmonary dysfunction could potentially explain the reduced mobility. Patient 3 underwent mitral and aortic valve replacement at age 8 and 14.5 years respectively (shortening fraction Z score -5 SD) and suffered from restrictive lung disease (FVC% -2.96 SD). Patients 9 and 10 had mild dilatation of the left ventricle with normal shortening fraction and restrictive lung disease (FVC% -4 and -2.6 SD). In three patients, a reliable measurement of pulmonary function was not possible because of either young age (patients 13 and 14), or because of inability to follow instructions (patient 11). In the remaining patients, systolic function of the heart and FVC% were within the normal range. Polysomnography showed mild, obstructive hypopneas in only two patients (patients 1 and 10).

The median distance covered in the 6MWT was 416.5 meters (range 264 to 512 m), median Z-score -3.15 (range -1.3 to -7.8). All patients had mild extension contractures of the knees and hips (table 2). Twelve of the fourteen patients had a waddling gait.

Waddling	Wheelchair Dependent (age onset)	Limited walking distance	Cause limited walking distance
y	No	y, 15-20 min	Pain left knee, muscle weakness left leg
y	No	y, 15-20 min	Exhausted, pain
y	Partial (always)	y, 10-15 min	Exhausted
y	Partial (10 yr.)	y, 1 km	Exhausted, stiffness legs
y	No	y, 2-3 hrs	Pain, upper leg or knees
y	No	No, very long distance	Exhausted
y	Partial (always)	y, 20-30 m	Exhausted, pain knees
y	No	No	Exhausted
y	Partial (always)	y, 50 m	Exhausted
y	No	y, 15-30 min/500 m	Exhausted
y	No	y, 30 min	Exhausted, stiffness hips
n	No	No	Exhausted
y	partial/buggy (always)	y, 1 km	Exhausted
n	Buggy	No	NA

Neurological examination showed a mild degree of muscle weakness of the hip abductors in 6 patients, further neurological examination was normal (table 2). The MRI of the craniocervical junction showed narrowing in almost all patients, but compression of the spinal cord in only one patient (patient 12). Neurological examination of this patient and the SEPP were normal (table 2).

Appendix table A summarizes the clinical findings related to hip pathology evaluated by a questionnaire (median age at assessment 13.7, range 3.5 to 21.8 years). Four patients were partially wheelchair dependent. The two youngest patients used a buggy for longer distances, which might also be explained by their young age (3.5 and 4 years old). In ten patients, the maximum walking distance was limited by exhaustion. The other four patients were able to walk long distances.

DISCUSSION

Our study shows that all patients with MPS VI develop progressive and debilitating hip disease. In contrast to other disease features (e.g. cardiac and pulmonary involvement [20]), no patients were spared and the hip abnormalities had an impact on mobility in all patients. In this cohort study, we did not detect differences in hip disease severity between patients with rapidly or slowly progressive MPS VI disease type. Even in those patients that started ERT very early in life (patients 9-11 and 13, 14, start of treatment before the age of 3.5 years), hip development was grossly abnormal and not significantly different from those patients that started ERT later in life (patients 3 and 12, started ERT at age 6.8 and 5.1 respectively).

Radiological abnormalities of the hip

The pelvic abnormalities already observed at very young age suggest that altered development already takes place early in life. An abnormal shape of the pelvis with a steep, shallow and small acetabulum and a dysplastic os ilium were observed in the earliest radiographs taken (our study age 2 and 3 years (fig. 2), published patients age 11 months and 1.1 years) [20]. The early presence of hip abnormalities in MPS VI suggests that they originate from altered fetal hip development [31, 32]. During normal fetal development, the ilium shows a defined pattern of internal organization. Specific architectural patterns occur in those regions known to be necessary to deal with forces caused by bipedal locomotion later in life [33]. GAGs have an important regulatory function in the endochondral ossification of growth plates. Studies in MPS animal models have shown that GAG accumulation during fetal life causes disorganization in different zones of the growth plates in long bones and the iliac crest [34]. This fetal developmental origin of the hip pathology in MPS VI could explain the limited effect of ERT, bone marrow, or hematopoietic stem cell transplantation on this disease characteristic [9-12].

The femoral head in very young MPS type VI patients appears to be normal (fig. 2 and 3B [20]). Over time, the femoral head became abnormally shaped in all patients. The abnormal pelvic shape probably induces different biomechanical forces on the femoral head once the patient starts walking, which is consistent with the finding that femoral head abnormalities occur from age three onwards. The fact that the growth plate of the femoral head itself is abnormally developed due to GAG accumulation could make the femoral head more vulnerable to these abnormal forces. This results in altered development of the femoral head and shape of the proximal femur.

It is important to note that the final shape of the femur head and neck differs largely between MPS VI patients (fig. 3). This is in contrast to MPS I Hurler, MPS II, III and IV in which the shape of the femoral head does not differ greatly between patients [10, 15, 19, 35-41]. In our study, though small, there seems to be a relation between the genotype and the type of femoral head deformity that occurs over time. For example, in teenagers and young adult patients homozygous for the 454 C>T (p.R152W) mutation (n=3), we found a coxa magna, whereas in patients of the same age with the relatively mild 629A>G (p.Y210C) mutation on one allele (n=4), a very flat, irregular femoral head in valgus position was found. For other genotypes, specific femoral head deformities were also found (appendix fig. B). To confirm this potential genotype-phenotype relationship, larger studies are needed. The differences could also be caused by other factors such as environmental (life style) factors or secondary genetic factors.

Clinical Burden and consideration for surgery

In this study we show that the clinical problem for the majority of MPS VI patients in the age range 2 to 17 years old is not hip pain. Walking distance in the majority of patients was primarily limited by exhaustion, likely caused by the high workload of walking with a waddling gait. This waddling gait is caused by the hip bone abnormalities and is not caused by primary knee problems or spinal stenosis (table 2 and appendix table A).

Planning hip surgery in MPS VI patients, both in terms of timing and type of intervention, is challenging. One can opt for early surgery, using the development over time to predict the most likely outcome of the shape and angulation of the femoral head in an individual patient. Changing the shape of the acetabulum (redirection or reshaping osteotomy), can be performed to improve coverage of the femoral head. However, in contrast to other forms of hip dysplasia, the cartilage of the femoral head is also grossly abnormal in MPS patients. This may limit a favorable outcome of improvement from this type of surgery. The other option is to wait until the patient develops significant complaints and then perform either a femoral or periacetabular osteotomy, or total hip replacement. Additional imaging techniques, including 3D and statistical shape modelling of the developing hip, may aid outcome prediction and surgery planning in the future [42, 43].

CONCLUSION

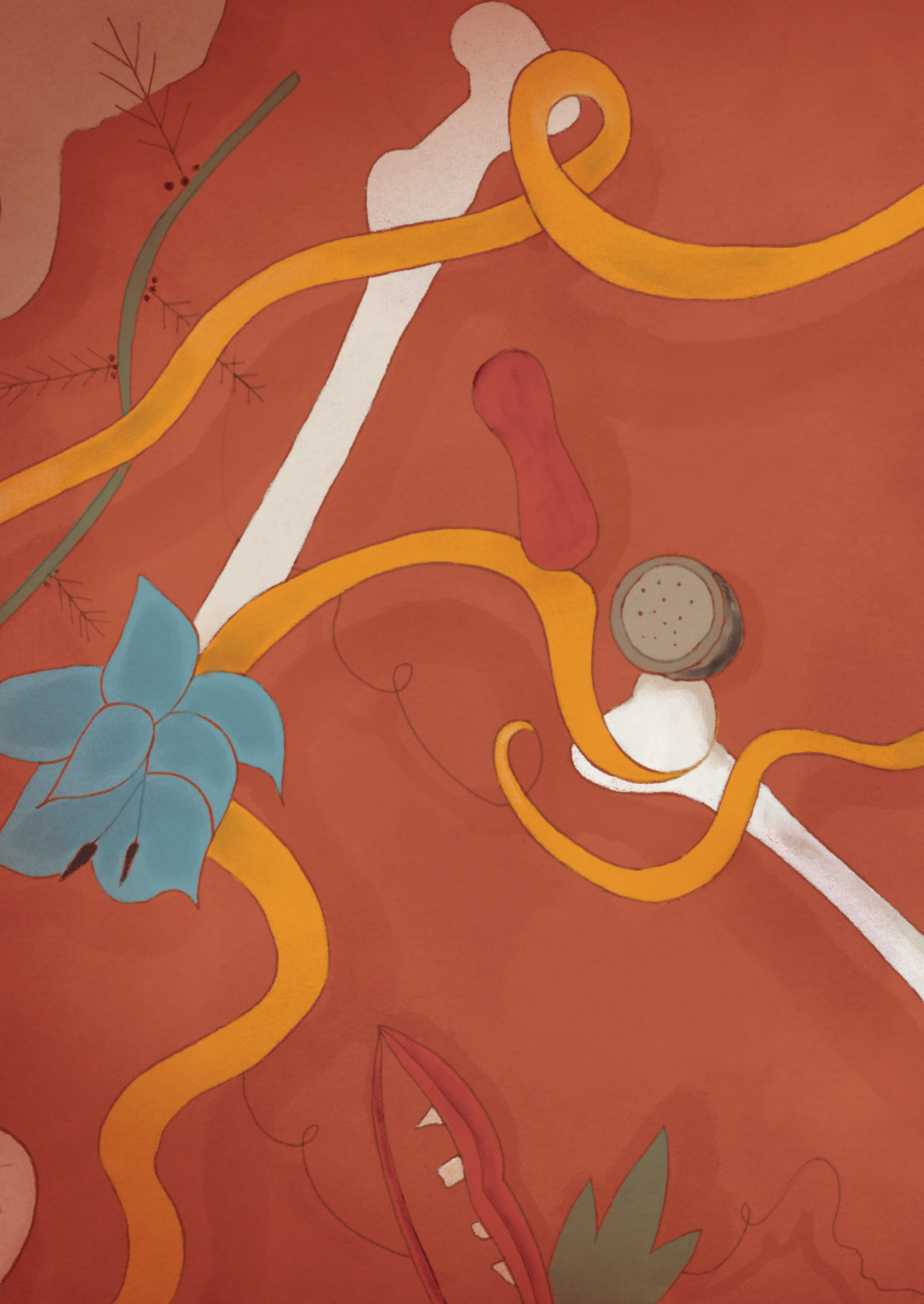
In all MPS VI patients, significant hip abnormalities develop very early in life starting with deformities of the os ilium and acetabulum. Femoral head abnormalities occur later, most likely due to altered mechanical forces in combination with epiphyseal abnormalities due to glycosaminoglycan storage. The final shape and angle of the femoral head differs significantly between individual MPS VI patients and is difficult to predict.

REFERENCES

- [1] E.F. Neufeld, J. Muenzer, "The Metabolic Bases of Inherited Disease," McGraw-Hill, Place Published, 2001.
- [2] B.J. Poorthuis, R.A. Wevers, W.J. Kleijer, J.E. Groener, J.G. de Jong, S. van Weely, K.E. Niezen-Koning, O.P. van Diggelen, The frequency of lysosomal storage diseases in The Netherlands, *Hum Genet*, 105 (1999) 151-156.
- [3] V. Valayannopoulos, H. Nicely, P. Harmatz, S. Turbeville, Mucopolysaccharidosis VI, *Orphanet J Rare Dis*, 5 (2010) 5.
- [4] S.J. Swiedler, M. Beck, M. Bajbouj, R. Giugliani, I. Schwartz, P. Harmatz, J.E. Wraith, J. Roberts, D. Ketteridge, J.J. Hopwood, N. Guffon, M.C. Sa Miranda, E.L. Teles, K.I. Berger, C. Piscia-Nichols, Threshold effect of urinary glycosaminoglycans and the walk test as indicators of disease progression in a survey of subjects with Mucopolysaccharidosis VI (Maroteaux-Lamy syndrome), *Am J Med Genet A*, 134A (2005) 144-150.
- [5] R. Giugliani, P. Harmatz, J.E. Wraith, Management guidelines for mucopolysaccharidosis VI, *Pediatrics*, 120 (2007) 405-418.
- [6] P. Harmatz, R. Giugliani, I.V. Schwartz, N. Guffon, E.L. Teles, M.C. Miranda, J.E. Wraith, M. Beck, L. Arash, M. Scarpa, D. Ketteridge, J.J. Hopwood, B. Plecko, R. Steiner, C.B. Whitley, P. Kaplan, Z.F. Yu, S.J. Swiedler, C. Decker, M.V.S. Group, Long-term follow-up of endurance and safety outcomes during enzyme replacement therapy for mucopolysaccharidosis VI: Final results of three clinical studies of recombinant human N-acetylgalactosamine 4-sulfatase, *Mol Genet Metab*, 94 (2008) 469-475.
- [7] M.M. Brands, E. Oussoren, G.J. Ruijter, A.A. Vollebregt, H.M. van den Hout, K.F. Joosten, W.C. Hop, I. Plug, A.T. van der Ploeg, Up to five years experience with 11 mucopolysaccharidosis type VI patients, *Mol Genet Metab*, 109 (2013) 70-76.
- [8] P. Harmatz, Z.F. Yu, R. Giugliani, I.V. Schwartz, N. Guffon, E.L. Teles, M.C. Miranda, J.E. Wraith, M. Beck, L. Arash, M. Scarpa, D. Ketteridge, J.J. Hopwood, B. Plecko, R. Steiner, C.B. Whitley, P. Kaplan, S.J. Swiedler, K. Hardy, K.I. Berger, C. Decker, Enzyme replacement therapy for mucopolysaccharidosis VI: evaluation of long-term pulmonary function in patients treated with recombinant human N-acetylgalactosamine 4-sulfatase, *J Inherit Metab Dis*, 33 (2010) 51-60.
- [9] M. Aldenhoven, R.F. Wynn, P.J. Orchard, A. O'Meara, P. Veys, A. Fischer, V. Valayannopoulos, B. Neven, A. Rovelli, V.K. Prasad, J. Tolar, H. Allewelt, S.A. Jones, R. Parini, M. Renard, V. Bordon, N.M. Wulfraat, T.J. de Koning, E.G. Shapiro, J. Kurtzberg, J.J. Boelens, Long-term outcome of Hurler syndrome patients after hematopoietic cell transplantation: an international multicenter study, *Blood*, 125 (2015) 2164-2172.
- [10] R.E. Field, J.A. Buchanan, M.G. Coppemans, P.M. Aichroth, Bone-marrow transplantation in Hurler's syndrome. Effect on skeletal development, *J Bone Joint Surg Br*, 76 (1994) 975-981.
- [11] E. Herskhovitz, E. Young, J. Rainer, C.M. Hall, V. Lidchi, K. Chong, A. Vellodi, Bone marrow transplantation for Maroteaux-Lamy syndrome (MPS VI): long-term follow-up, *J Inherit Metab Dis*, 22 (1999) 50-62.
- [12] S. Jester, J. Larsson, E.A. Eklund, D. Papadopoulou, J.E. Mansson, A.N. Bekassy, D. Turkiewicz, J. Toporski, I. Ora, Haploidentical stem cell transplantation in two children with mucopolysaccharidosis VI: clinical and biochemical outcome, *Orphanet J Rare Dis*, 8 (2013) 134.
- [13] T. Tonnesen, H.N. Gregersen, F. Guttler, Normal MPS excretion, but dermatan sulphaturia, combined with a mild Maroteaux-Lamy phenotype, *J Med Genet*, 28 (1991) 499-501.
- [14] J. Guiral, J.M. Sanchez, M.A. Gonzalez, Stress fracture of the femoral neck in a young adult with Maroteaux-Lamy syndrome, *Acta Orthop Belg*, 58 (1992) 91-92.

- [15] K.K. White, P. Harmatz, Orthopedic management of mucopolysaccharide disease, *J Pediatr Rehabil Med*, 3 (2010) 47-56.
- [16] I. Gottwald, J. Hughes, F. Stewart, K. Tylee, H. Church, S.A. Jones, Attenuated mucopolysaccharidosis type VI (Maroteaux-Lamy syndrome) due to homozygosity for the p.Y210C mutation in the ARSB gene, *Mol Genet Metab*, 103 (2011) 300-302.
- [17] A. Thumler, E. Miebach, C. Lampe, S. Pitz, W. Kamin, C. Kampmann, B. Link, E. Mengel, Clinical characteristics of adults with slowly progressing mucopolysaccharidosis VI: a case series, *J Inherit Metab Dis*, 35 (2012) 1071-1079.
- [18] N.J. Mendelsohn, T. Wood, R.A. Olson, R. Temme, S. Hale, H. Zhang, L. Read, K.K. White, Spondyloepiphyseal dysplasias and bilateral legg-calve-perthes disease: diagnostic considerations for mucopolysaccharidoses, *JIMD Rep*, 11 (2013) 125-132.
- [19] K.K. White, T. Sousa, Mucopolysaccharide disorders in orthopaedic surgery, *J Am Acad Orthop Surg*, 21 (2013) 12-22.
- [20] P. Garcia, S.B. Sousa, T.P. Ling, M. Conceicao, J. Seabra, K.K. White, L. Diogo, Skeletal complications in mucopolysaccharidosis VI patients: Case reports, *J Pediatr Rehabil Med*, 3 (2010) 63-69.
- [21] S. Kleinberg, H.S. Lieberman, The acetabular index in infants in relation to congenital dislocation of the hip, *Archives of Surgery*, 32 (1936) 1049-1054.
- [22] F. Schmid, *Pädiatrische Radiologie*, Springer, Place Published, 1973.
- [23] I.K. Sharp, ACETABULAR DYSPLASIA, *The Acetabular Angle*, 43-B (1961) 268-272.
- [24] B.D. Tönns D, Eine Abgrenzung normaler und pathologischer Hüftpfannendachwinkel zur Diagnose der Hüftdysplasie, *Arch Orthop Trauma Surg*, 64 (1968) 197-228.
- [25] D. Tonnis, Normal values of the hip joint for the evaluation of X-rays in children and adults, *Clin Orthop Relat Res*, (1976) 39-47.
- [26] M.B.Da.J.A. Morcuende, *Pediatric Orthopedics*, J.B. Lippincott Company, Place Published, 1986.
- [27] B.D. Pinheiro J, Debroy S, Sarkar D, [nlme]: Linear and Nonlinear Mixed Effects Models, (2015).
- [28] A.T.S.Co.P.S.f.C.P.F. Laboratories, ATS statement: guidelines for the six-minute walk test, *Am J Respir Crit Care Med*, 166 (2002) 111-117.
- [29] R. Geiger, A. Strasak, B. Treml, K. Gasser, A. Kleinsasser, V. Fischer, H. Geiger, A. Loeckinger, J.I. Stein, Six-minute walk test in children and adolescents, *J Pediatr*, 150 (2007) 395-399, 399 e391-392.
- [30] E. Garrido, A. Chabas, M.J. Coll, M. Blanco, C. Dominguez, D. Grinberg, L. Vilageliu, B. Cormand, Identification of the molecular defects in Spanish and Argentinian mucopolysaccharidosis VI (Maroteaux-Lamy syndrome) patients, including 9 novel mutations, *Mol Genet Metab*, 92 (2007) 122-130.
- [31] J.J. McGill, A.C. Inwood, D.J. Coman, M.L. Lipke, D. de Lore, S.J. Swiedler, J.J. Hopwood, Enzyme replacement therapy for mucopolysaccharidosis VI from 8 weeks of age--a sibling control study, *Clin Genet*, 77 (2010) 492-498.
- [32] M. Furujo, T. Kubo, M. Kosuga, T. Okuyama, Enzyme replacement therapy attenuates disease progression in two Japanese siblings with mucopolysaccharidosis type VI, *Mol Genet Metab*, 104 (2011) 597-602.
- [33] C.A. Cunningham, S.M. Black, Development of the fetal ilium--challenging concepts of bipedality, *J Anat*, 214 (2009) 91-99.
- [34] E. Oussoren, M.M. Brands, G.J. Ruijter, A.T. der Ploeg, A.J. Reuser, Bone, joint and tooth development in mucopolysaccharidoses: relevance to therapeutic options, *Biochim Biophys Acta*, 1812 (2011) 1542-1556.
- [35] E.L. Masterson, P.G. Murphy, A. O'Meara, D.P. Moore, F.E. Dowling, E.E. Fogarty, Hip dysplasia in Hurler's syndrome: orthopaedic management after bone marrow transplantation, *J Pediatr Orthop*, 16 (1996) 731-733.

- [36] J.S. Weisstein, E. Delgado, L.S. Steinbach, K. Hart, S. Packman, Musculoskeletal manifestations of Hurler syndrome: long-term follow-up after bone marrow transplantation, *J Pediatr Orthop*, 24 (2004) 97-101.
- [37] C. Taylor, P. Brady, A. O'Meara, D. Moore, F. Dowling, E. Fogarty, Mobility in Hurler syndrome, *J Pediatr Orthop*, 28 (2008) 163-168.
- [38] J. de Ruijter, M. Maas, A. Janssen, F.A. Wijburg, High prevalence of femoral head necrosis in Mucopolysaccharidosis type III (Sanfilippo disease): a national, observational, cross-sectional study, *Mol Genet Metab*, 109 (2013) 49-53.
- [39] E.J. Langereis, M.M. den Os, C. Breen, S.A. Jones, O.C. Knaven, J. Mercer, W.P. Miller, P.M. Kelly, J. Kennedy, T.G. Ketterl, A. O'Meara, P.J. Orchard, T.C. Lund, R.R. van Rijn, R.J. Sackers, K.K. White, F.A. Wijburg, Progression of Hip Dysplasia in Mucopolysaccharidosis Type I Hurler After Successful Hematopoietic Stem Cell Transplantation, *J Bone Joint Surg Am*, 98 (2016) 386-395.
- [40] K.K. White, A. Jester, C.E. Bache, P.R. Harmatz, R. Shediak, M.M. Thacker, W.G. Mackenzie, Orthopedic management of the extremities in patients with Morquio A syndrome, *J Child Orthop*, 8 (2014) 295-304.
- [41] E. Ashby, M. Baker, D.M. Eastwood, Characterization of Hip Morphology in Children With Mucopolysaccharidosis Types I and II, *J Pediatr Orthop*, (2015).
- [42] T. Tarhan, D. Froemel, A. Meurer, [EOS imaging acquisition system : 2D/3D diagnostics of the skeleton], *EOS-Imaging : 2-D/3-D-Diagnostik des Skeletts, Orthopade*, 44 (2015) 977-985; quiz 986-977.
- [43] M.T. Bah, J. Shi, M. Browne, Y. Suchier, F. Lefebvre, P. Young, L. King, D.G. Dunlop, M.O. Heller, Exploring inter-subject anatomic variability using a population of patient-specific femurs and a statistical shape and intensity model, *Med Eng Phys*, 37 (2015) 995-1007.





CHAPTER 5

MUCOLIPIDOSIS TYPE III, A SERIES OF ADULT PATIENTS

E. Oussoren, D. van Eerd, E. Murphy, R. Lachmann, J.C. van der Meijden,
L.H. Hoefsloot, R. Verdijk, G.J.G. Ruijter, M. Maas, C.E.M. Hollak,
J.G. Langendonk, A.T. van der Ploeg, M. Langeveld

J Inherit Metab Dis. 2018, **41**(5):839-848.

ABSTRACT

Introduction: Mucopolipidosis type III α/β or γ (ML III) are rare autosomal recessive diseases in which reduced activity of the enzyme UDP-*N*-acetyl glucosamine-1-phosphotransferase (GLcNAc-PTase) leads to intra-lysosomal accumulation of different substrates. Publications on the natural history of ML III, especially the milder forms, are scarce. This study provides a detailed description of the disease characteristics and its natural course in adult patients with ML III.

Methods: In this retrospective chart study, the clinical, biochemical and molecular findings in adult patients with a confirmed diagnosis of ML III from three treatment centers were collected.

Results: Thirteen patients with ML III were included in this study. Four patients (31%) were initially misdiagnosed with a type of MPS. Four patients (31%) had mild cognitive impairment. Six patients (46%) needed help with activities of daily living (ADL) or were wheelchair dependent. All patients had dysostosis multiplex and progressive secondary osteoarthritis, characterized by cartilage destruction and bone lesions in multiple joints. All patients underwent multiple orthopedic surgical interventions as early as the second or third decade of life, of which total hip replacement (THR) was the most common procedure (61% of patients). Carpal tunnel syndrome (CTS) was found in twelve patients (92%) and in eight patients (61%) CTS release was performed.

Conclusions: Severe skeletal abnormalities, resulting from abnormal bone development and severe progressive osteoarthritis, are the hallmark of ML III, necessitating surgical orthopedic interventions early in life. Future therapies for this disease should focus on improving cartilage and bone quality, preventing skeletal complications and improving mobility.

INTRODUCTION

Mucopolidoses type II/III α/β or γ (ML II OMIM#252500, ML III α/β MIM# 252600, ML III γ OMIM#252605) are rare autosomal recessive diseases [1-6]. In these conditions, activity of the membrane bound hexameric enzyme UDP-*N*-acetyl glucosamine-1-phosphotransferase (GlcNAc-PTase), consisting of three subunits named $\alpha 2$, $\beta 2$ and $\gamma 2$, is absent or reduced [3, 7-10]. The *GNPTAB* gene (chromosome 12q23.3; OMIM#607840) encodes for the α/β subunits and *GNPTG* gene (chromosome 16; OMIM#607838) for the γ subunits. GlcNAc-PTase is responsible for the first step in the phosphorylation of enzyme-conjugated mannose residues to mannose-6-phosphate in the Golgi apparatus. Mannose-6-phosphate serves as the recognition marker, targeting newly synthesized lysosomal enzymes to the lysosome. In the reduced presence or absence of this marker, lysosomal enzymes are secreted in plasma, where they are unable to execute their function [9] which results in the accumulation of several substrates such as glycosaminoglycans and (glyco)sphingolipids.

ML presents as a clinical spectrum. In the most severe form, ML II (OMIM#252500, I-cell disease), GlcNAc-PTase activity is completely deficient, leading to severe and rapidly progressive airway, cardiac, skeletal and nervous system disease, resulting in death in early childhood [1, 2, 5]. ML III α/β has a broader phenotypic range from severely affected patients that die in childhood, to milder affected patients displaying primarily skeletal symptoms, who survive into adulthood [2, 6, 11-15]. The patients with ML III γ that have been described so far all have milder phenotypes [3, 4, 16-18].

Clinical features that have been described in ML III are mild coarsening of the face, corneal clouding, mild retinopathy, cardiac valve abnormalities, restrictive pulmonary function, tracheal/ bronchomalacia, skeletal dysplasia, scoliosis, stiffness of the joints, short stature, claw hand deformity, carpal/tarsal tunnel syndrome and spinal cord compression [2, 4, 12-14, 18-29]. Reports on intellectual performance and learning abilities vary from normal to mild cognitive impairment [2, 4, 10, 15, 26, 27, 30-34]. Publications on the natural history of adult ML III patients are rare. Some single case studies or small case series of ML III patients reaching adulthood have been published, but they lack a systematic description of disease onset, progression over time, severity of the disease characteristics and surgical interventions [2, 4, 12-15, 34].

Currently, there are no curative treatments for ML II and III. From experience in other extremely rare disorders (e.g., the MPS's) for which therapy became available, we recognize the importance of natural history data collection, especially in milder cases, since the focus in medical literature is often on the severe phenotypes. Once treatment becomes available, the latter may lead to an overestimation of treatment effect as the course of the treated patients that are mildly affected is compared to severely affected patients reported in the literature. Natural history studies help to identify future therapeutic goals, aid counseling and provide the basis for tailored, standardized follow up of these patients. The aim of this study is to provide a detailed description of the disease characteristics of ML III and its natural course, by studying data from adult patients.

METHODS

Patients

In this retrospective medical record review, the clinical, biochemical and molecular findings from adult patients with a confirmed diagnosis of ML III from three specialist centers were collected (the Academic Medical Center (AMC), Amsterdam, the Netherlands; Erasmus MC, Rotterdam, the Netherlands and the National Hospital for Neurology and Neurosurgery, London, United Kingdom).

The diagnosis of ML III was established by measurement of plasma and/or fibroblast activity of several lysosomal enzymes including β -hexosaminidase A, β -hexosaminidase A+B, α -L-fucosidase, β -D-glucuronidase, α -D-mannosidase and β -D-galactosidase. In addition, in a subset of patients, GlcNAc-1-PTase activity in fibroblasts was measured, or DNA analysis of the *GNPTAB* or *GNPTG* gene was performed.

Data on demographic and general characteristics (age of initial/correct diagnosis and anthropometry), clinical symptoms, cognitive ability, highest education qualification, impairments in activities of daily living (ADL), wheelchair dependency, employment, imaging results (radiographs and MRI scans), number and types of orthopedic surgeries performed and echocardiography and pulmonary function tests, were collected from patient records.

RESULTS

Patient characteristics

Characteristics of the thirteen adult patients are outlined in table 1. The median age at last follow up was 30 years (range 18 to 68). Most patients were of Caucasian descent and both genders were equally represented. Patients 9, 11 and 10, 12 are siblings. Out of the 13 patients, one was initially misdiagnosed as MPS II and three as MPS IV. In one patient who was diagnosed with MPS IV at the age of 30, the correct diagnosis was as established as late as age 64.

Most patients developed clinical symptoms in the first decade of life. The diagnosis of ML was made in ten patients through the establishment of elevated levels of lysosomal enzymes in plasma, confirmed by a concomitant decreased lysosomal enzyme activity in fibroblast in four patients (in one patient, only enzyme measurements in fibroblasts were performed) and in one patient by a decreased activity of GlcNAc-1-PTase. In seven patients, DNA analysis was performed. Three patients had mutations in the *GNPTAB* gene and four patients in the *GNPTG* gene. The mutations and clinical features of patient 2 were published 13 years ago by Raas-Rotschild et al [4]. The *GNPTAB* gene c.1178A>G; p.(His393Arg) mutation (patient 1), the *GNPTG* gene homozygous variants c.409+11_411+35del (patient 3) and c.318-1G>C (patients 6 and 7) and the *GNPTG* gene heterozygous mutation c.122_138del; p.(Pro41fs) with the c.331 T>C variant (patient 5) have not been published before.

Clinical signs and functioning in daily life

Five patients had notably short statures (range 129-158 cm, median of 145 cm) (table 2), in patient 13 height could not be measured. Six patients needed help with activities of daily life (ADL) and/or were wheelchair dependent. All but one patient suffered from carpal tunnel syndrome (supplemental table 2).

Four patients had mild cognitive impairment (patients 4, 5, 10 and 13), while cognitive function was normal in the other nine patients (table 2). Ten patients were employed at any time during adult life. Pregnancies with healthy offspring were reported in two patients (patients 3 and 11).

Skeletal pathology

The most prominent clinical signs were the skeletal abnormalities. All patients had abnormally shaped bones (dysostosis multiplex) and progressive osteoarthritis, characterised by cartilage destruction in joints and areas of radiolucency in bones that may reflect erosive bone lesions (supplemental table 1). These abnormalities were found on X-rays

of the hand, feet, shoulders, elbows, hips, knees and spine [14, 20-22, 29, 35, 36]. In four patients, the carpal and/or tarsal bones were hypoplastic, with secondary osteoarthritic changes observed in the older patients (examples fig. 1A and supplemental table 1). In eleven patients, the same abnormalities were seen in the humeral/ femoral heads and femoral neck (examples fig. 1A and B). In all patients with available hip morphology data (n=9), hip dysplasia and altered pelvic shape were present (examples fig. 1B). Abnormalities of the spine were present in all patients. The most common findings were atypically shaped vertebrae (hypoplasia), subluxation and scoliosis (examples fig. 1A). The majority of patients reported pain of the glenohumeral joints and/or the hands, feet, hips, knees and the lumbar spine. In six patients, signs of spinal cord or nerve root compression were present (supplemental table 1).

Figure 1A shows exemplary radiographs of the skull, spine, shoulder, elbow, knee, hand, ankle and foot of three ML III patients (patients 4, 5 and 7) at the ages of 18, 28 and 65 years. The findings in these radiographs are described in the legend of fig. 1A. X-rays of the pelvis of four ML III patients (patients 1, 5, 6 and 7) over time are shown separately in figure 1B. In all patients, there is severe hip dysplasia, with flaring of iliac wings as well as significant ossification disorders of the femoral heads, with arthritic changes of the hips. In the most severely affected patient (patient 1), near total destruction of the femoral heads occurred by age 11. In contrast, in patient number 5, the femoral heads are hardly affected at the age of eight years old, but by the second decade of life, severe osteoarthritis of both hips had developed.

The oldest patient (patient 7) was completely wheelchair dependent from the age of 23 years onwards. In this patient, for unknown reasons, no surgical hip interventions have been performed. The femoral heads were abnormally shaped with severe secondary osteoarthritis. This is also seen on macroscopic and histopathological examination of the left hip, which was removed after her death at the age of 69 years (fig. 1B), when she succumbed to metastatic bladder cancer.

Table 1 Patient characteristics

Patient	Gender	Initial Diagnosis (years)	Age at correct diagnosis (years)	Age at last Follow up (years)	Mutations GNPTAB gene	
					Allele 1	Allele 2
1	M	MPS IV 8	11	23	NM_024312.4:c.1178A>G p.(His393Arg)	NM_024312.4:c.3503_3504del p.(Leu1168fs)[1]
2	M		7	27	NM_024312.4:c.196C>T p.(Gln66*)	NM_024312.4:c.366-1G>C p.?[2]
3	F	MPS II 4	7	48		
4	F		9	18	NM_024312.4:c.1090C>T p.(Arg364*)	NM_024312.4:c.2715+2T>G p.?
5	M		8	30		
6	M	MPS IV	46	48		
7	F	MSP IVB 30	64	68		
8	F		7	28	N.A.	N.A.
9 [^]	M		22	28	N.A.	N.A.
10#	M		8	39	N.A.	N.A.
11 [^]	F		17	32	N.A.	N.A.
12#	F		Unknown	35	N.A.	N.A.
13	F		3.5	27	N.A.	N.A.

*: GLCNAC1PT enzyme deficient in fibroblasts, N.A.: not available, #[^]; siblings

1.Kudo M, Bao M, D'Souza A, Ying F, Pan H, Roe BA, *et al*. The alpha- and beta-subunits of the human UDP-N-acetylglucosamine:lysosomal enzyme N-acetylglucosamine-1-phosphotransferase [corrected] are encoded by a single cDNA. *J Biol Chem* 2005; 280:36141-36149.

Mutations GNPTG gene		Multiple lysosomal enzyme activities	
Allele 1	Allele 2	Plasma	Fibroblasts
		Elevated	N.A.*
		N.A.	Reduced
NM_032520.4:c.409+11_411+35del p.?	NM_032520.4:c.409+11_411+35del p.?	Elevated	Reduced
		Elevated	N.A.
NM_032520.4:c.122_138del p.(Pro41fs)	NM_032520.4:c.331T>C p.(Trp111Arg)	Elevated	N.A.
NM_032520.4:c.318-1G>C p.?	NM_032520.4:c.318-1G>C p.?	N.A.	Reduced
NM_032520.4:c.318-1G>C p.?	NM_032520.4:c.318-1G>C p.?	Elevated	N.A.
N.A.	N.A.	N.A.	Reduced
N.A.	N.A.	Elevated	N.A.
N.A.	N.A.	Elevated	N.A.
N.A.	N.A.	Elevated	N.A.
N.A.	N.A.	Elevated	N.A.
N.A.	N.A.	Elevated	Reduced

2.Raas-Rothschild A, Bargal R, Goldman O, Ben-Asher E, Groener JE, Toutain A, *et al*. Genomic organisation of the UDP-N-acetylglucosamine-1-phosphotransferase gamma subunit (GNPTAG) and its mutations in mucopolipidosis III. *J Med Genet* 2004; 41:e52.

Table 2 Anthropometry, cognitive involvement and functioning in daily life

Patient	Height (cm) BMI (kg/m ²) at last follow-up	Cognitive impairment (Y/N)
1	129 (16)	N.
2	171 (24)	N.
3	144 (28)	N
4	170 (24)	Y, Mild, [IQ 65]
5	170 (22)	Y, Mild.
6	176 (33)	N
7	150 (52)	N
8	145 (24)	N
9	179 (23)	N
10	169 (29)	Y, Mild, [IQ 70]
11	158 (21)	N
12	160(20)	N (OCD, depression)
13	+	Y, Mild

Y; yes, N; no, IQ: intelligence quotient, ADL: activities of daily living, *can walk 400 meters without a wheelchair

#: was previously employed, ^: rollator dependent, + height could not be measured (wheelchair dependent for many years), weight 45 kg.

Supplemental table 1 Skeletal abnormalities

Patient	Shoulders and Hands	Pelvis	Femur
1		Severe hip dysplasia. Os ilium: neo-acetabulum formation and flaring wings (19 yr.)	Dislocation/luxation femur to cranial in relation to the acetabulum. Absence of femoral heads. Shaft: osteopenia (19 yr.)
2		Acetabula steep, barely covering femoral heads (24 yr.)	Epiphyseal dysplasia (6 yr.) Femoral heads subluxation to cranial L>R, subchondral areas of radiolucency (24 yr.) Secondary osteoarthritis femoral heads after femoral osteotomy, L>R (25 yr.)
3		Flaring os ileum and dysplasia (42 yr.)	

Highest Education qualifications	Impairment in ADL/ Wheelchair user (Y/N)	In employment (Y/N)
Secondary education	N/Y*	Y
Academic education	N/N	Y
Secondary education	N/N	y
Secondary education	N/N	Y
Special need education	Y/N	N#
Professional education	Y/N^	Y
N.A.	Y/Y (from age 23 yrs onwards)	Y
University	Y/Y	Y
University	N/N	Y
Secondary school	N/N	N
College	N/N	Y
Secondary school	N/N	N
College (assisted)	Y/Y	N

Knees and feet	Spine, spinal cord compression
	Flattened vertebral bodies, hypoplastic dens, cervical pannus around dens-atlas area, thoracic, lumbar spondylosis Cranio-cervical compression spinal cord (20 yr.)
Irregular aspect dorsal side patella, slight intra-articular effusion (24 yr.) Upper ankle joints early signs of secondary osteoarthritis L/R (27 yr.)	S shape scoliosis L1 to L5: secondary osteoarthritis degenerative changes with multiple Schmorl nodules L2-L3, L3-L4, L4-L5: slight bulging disc (24 yr.)
Secondary osteoarthritis L knee joint abnormal aspect of the bones, tibiofemoral joint space slightly narrowed medial, areas of radiolucency medial condyle and R tibia (36 yr.)	Thoracolumbar severe convex left sided scoliosis, osteopenia, secondary osteoarthritis, degeneration L1-L2 Flattened vertebral bodies, mainly cervical increased anteroposterior diameter Sclerosis SI-joint (42 yr.)

Supplemental table 1 Continued

Patient	Shoulders and Hands	Pelvis	Femur
4		Mild horizontal acetabulum roof R (18 yr.)	Mild coxa recta L/R (18 yr.)
5	Glenoid deformation L/R Madelung's deformity L/R (28 yr.) Caput MCP: deformities, secondary osteoarthritis with collapse and areas of radiolucency Os lunatum L/R: hypoplasia proximal pool. Os scaphoid L/R: absence proximal pool (30 yr.)	Hip dysplasia L/R (28 yr.)	Secondary osteoarthritis femoral heads L/R (28 yr.)
6	Glenoids hypoplasia and secondary osteoarthritis (38 yr.) Severe secondary osteoarthritis of the wrist bones and MCPJ L/R: (44 yr.)	Flaring iliac wings, acetabulum (45 yr.)	Secondary osteoarthritis femoral heads L/R (25 yr.)
7	Severe secondary osteoarthritis humeral heads (subcortical areas of radiolucency, sclerosis) (65 yr.) Distal part ulna, os scaphoid, os lunatum, MCPJ-III and IPJ: deformities, destruction, osteoarthritis (60 yr.)	Hip dysplasia (60 yr.)	Dysplasia, flattening and cranial subluxations. Severe secondary osteoarthritis (subchondral sclerosis and areas of radiolucency) femoral heads with joint space narrowing Coxa valga L/R (60 yr.) Flattening and lateralization femoral heads Distal femur shaft fracture (65 yr.)
8	Secondary osteoarthritis glenohumeral joint PIPJ dig II R: secondary osteoarthritis (30 yr.)	Hip dysplasia	

Knees and feet	Spine, spinal cord compression
Multiple abnormalities feet R>L (dysostosis multiplex) (17 yr.)	Mild convex right sided scoliosis, with increased kyphosis and increased interpedicular distance Secondary osteoarthritic changes of the endplates of the corpus vertebrae (18 yr.)
Osteopenia, secondary osteoarthritis tibiofemoral and patella with femoral joint space narrowing Secondary osteoarthritis knees (50 yr.) Abnormal talus, tibia and caput MT-I (sclerosis) Flat caput metatarsalia with secondary osteoarthritis (44 yr.)	Hypoplasia of dens and vertebral bodies C3 to C7 C4-C5 and C5-C6: bilateral narrowing intervertebral foramina Spinal cord compression C3 -C5 Radicular syndrome C6 L (50 yr.)
Knee joint; severe secondary osteoarthritis (narrowing of the medial compartment, deformation of the tibia plateau with lateral hook formation/bone formation) Secondary osteoarthritis (hook formation at the lateral femur condyles) with deformed aspect femur condyles L/R (65 yr.)	Altered vertebral shape, flattened (most prominent TH9/TH10). L3 and L4: anterior displacement Mild convex right sided scoliosis, with increased kyphosis and increased interpedicular distance Severe secondary osteoarthritis endplates of the corpus vertebrae L3-L4 and L4-L5: decreased diameter of the spinal canal (66 yr.)
Avascular necrosis ankles (10 yr.) Secondary osteoarthritis with degenerative changes ankles, some collapse talus. Bilateral valgus knee deformities (25 yr.) Hammer toe R (30 yr.) Ankle secondary osteoarthritis R, predominant anterior wear and slight anterior subluxation (34 yr.)	Atlantoaxial subluxation os odontoid Loss of cervical lordosis C2, C3: grade 2 Anterolisthesis C4-C5 and C5-C6: Grade 1 retrolisthesis Multiple osteophyte bars C4 to C7: several multilevel bilateral neural foraminal narrowing with indentation of the cervical cord L5: spinal cord compression resulting in weakness of the right side (30 yr.) T10/T11: severe stenosis resulting in clonus on leg L/R (34 yr.)

Supplemental table 1 Continued

Patient	Shoulders and Hands	Pelvis	Femur
9		Unknown	
10		Unknown	Secondary osteoarthritis femoral head L (35 yr.)
11	IPJ: fixed flexion and deformities, secondary osteoarthritis		
12		Hip joint L/R: Loss of height, secondary osteoarthritis (subchondral sclerosis, changes acetabular margins) (24 yr.)	Sclerosis, osteophytes, progressive secondary osteoarthritis femoral heads L/R (24 yr.) Extensive secondary osteoarthritis femoral heads L/R (26 yr.)
13	Hypoplastic poorly formed glenoid fossae Varus positioning of both humeral heads (22 yr.)	Very shallow acetabula Incomplete fusion of right pubic ramus Widening and erosion of joints and growth plates (18 yr.)	Flat and deformed femoral heads (18 yr.)

MCP: metacarpal, L: left, R: Right, yr.=years, SI-joint: sacroiliac joint, MCPJ: metacarpal joint, IPJ: Interphalangeal joint, PIPJ: proximal interphalangeal joint, Dig: digitus, THR: total hip replacement, MT: metatarsals.

Knees and feet**Spine, spinal cord compression**

Cervical spine loss of normal lordosis and secondary osteoarthritis; degenerative change of the intervertebral discs, cervical, thoracic, lumbar regions
Some narrowing of the neural exit foramina at C2-3, C3-4 bilaterally
At the cranial cervical junction there is a Chiari I malformation with the right cerebellar tonsil extending inferiorly to the lower edge of the C1 arch
(23 yr.)

Secondary osteoarthritis whole spinal cord.
Decreased diameter of the spinal canal at multiple levels
(30 yr.)
Severe marked cervical spondylosis, multiple disc bulges
Some nerve root compression
(34 yr.)

Loose fragments in the articular surfaces of patellae (associated with fissuring and chondral flaps) L/R
(32 yr.)

Mild convex right side lumbar scoliosis
C2-C3: grade 1 anterolisthesis
(30 yr.)
C6-7 (and to a lesser degree C7-T1): secondary osteoarthritis (degenerative bone and disc changes)
C5-6: modest degree of foraminal compromise
(32 yr.)

Hallux valgus with deformed hammer toes L
(29 yr.)

Intractable right sided L5 radiculopathy and is stuck in forward flexion
Cervical, thoracic and lumbar spine: multilevel secondary osteoarthritis (degenerative disc changes)
(30 yr.)

Loss of vertebral body height and end-plate changes throughout
Severe narrowing of and compression of spinal cord at cranio-cervical junction (pre-laminoplasty)
(19 yr.)

For each finding, the age at which this was written down in the medical chart is depicted, this does not necessarily correspond with the age of onset of the symptom or sign. If no age is given, the symptom or sign was noted in the chart undated.

Figure 1A Skeletal radiographs

Fig.1A. Examples of three ML III patients, aged 18, 28 and 65 years (patients 4, 5 and 7). Skeletal radiographs of the skull (anterior posterior and lateral), spine (thoracic/lumbar vertebrae AP and lateral), left shoulder (AP), left elbow (lateral), left knee (AP), left hand (AP) and left ankle/foot (AP and or lateral). In general, the developmental bone abnormalities were present in all patients, but presence and severity of osteoarthritic changes were more prominent in the older patients.

Skull: In all patients thickened cortical bones and a prominent sella turcica were observed. Open skull sutures in patients 4 and 5. Dens aspect of the skull vault in patient 7.

Spine: Mild convex right sided scoliosis, with increased kyphosis and increased interpedicular distances in all three patients. Flattened corpora vertebrae on several levels (cervical, thoracic and lumbar) in all three patients. Osteoarthritic changes of the endplates of the corpora vertebrae, most prominent in the oldest patient (patient 7). In patient 7 there is anterior displacement of vertebrae L3 and L4 with a decreased diameter of the spinal canal.

Shoulder and elbows: In patient 4, no abnormalities of these joints were observed. Osteoarthritic changes in the humeral head, glenoid and elbow deformation were seen in patients 5 and 7.

Knee: No lateral left knee radiograph was available for patient 4. In patient 5 there is a patella baja and signs of osteochondral abnormalities of the patella with osteophyte formation. In patient 7 (X ray performed at age 60 years) osteoarthritic changes were observed with lateral hook formation/bone formation of the tibia plateau and at the lateral femur condyle.

Hand: Abnormal shaped phalanges in all three patients (subtle in patient number 4). Osteoarthritic changes of the phalangeal joints (proximal and distal) in patients 5 and 7. Abnormal shaped metacarpal bones (hypoplasia and collapse) with secondary osteoarthritis (patients 5 and 7).

Feet/ankle: In patient 4, no abnormalities of the joints were observed. In patient 5, there is osteoarthritis of the distal fibula. Suggestion for bifida talus or talus bipartite. Severe osteoarthritis of the ankle is seen in patient 7.

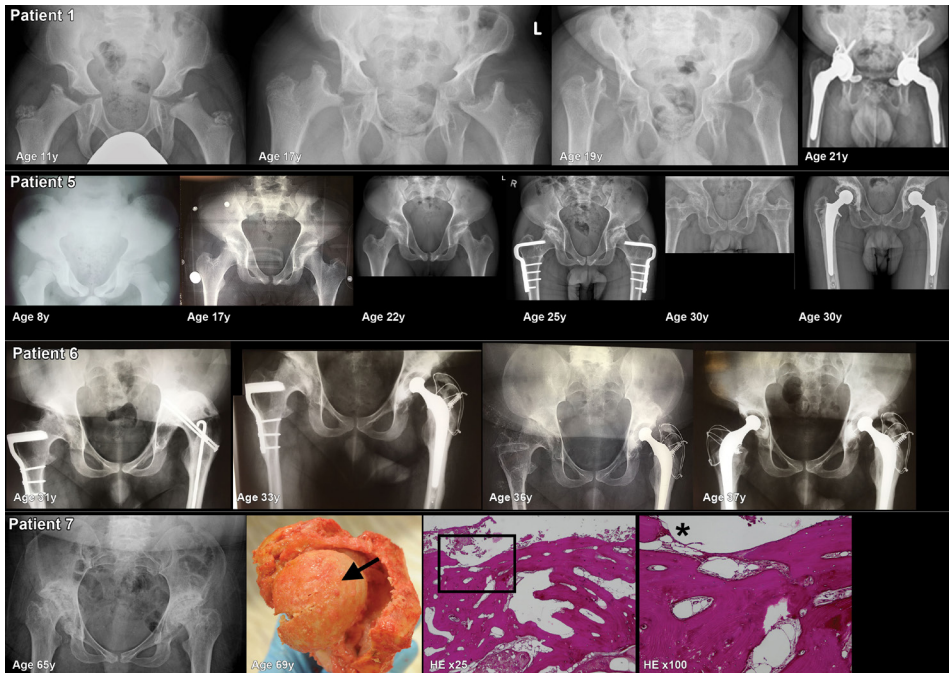
Figure 1B Radiographs, macroscopy and histopathology of the hip bones

Fig. 1B. X-rays of the hips of patients 1, 5, 6 and 7 over different ages. Macro- and microscopic photographs of the left hip of patient 7 are shown. This patient died at the age of 69 from metastatic bladder cancer.

Most prominent findings on radiographs:

Pelvis: in all patients, pelvic bones are abnormally shaped with flared iliac wings with hypoplasia of the inferior part of the ilea. The acetabula are severely dysplastic, very steep and shallow. Neoacetabula formation occurred in patients 5, 6 and 7. Impingement of the coxofemoral spaces was also seen in patient 7.

Femoral heads, neck shaft angle: Severe ossification disorders and severe secondary osteoarthritis of the femoral heads (with subchondral cysts, sclerosis and flattening in patients 5, 6 and 7) were present in all patients. In patient 1, at age 11, there was near total absence of the femoral heads. Femoral shaft angle abnormalities: in patient 1, the shaft angle over time develops from coxa valga to coxa vara. In patient 5 there is a coxa valga and in patient 7, coxa vara. On autopsy in patient 7, part of the left femur, femoral head and part of the acetabulum were removed (as shown on the macroscopic photo). The femoral head (shown from above): severe osteoarthritis is present, with complete destruction of the cartilage. An arrow on the top of the femoral head shows yellow collared bone tissue and not the normal, glossy blue-white in appearance, cartilage. Total destruction of cartilage is also illustrated by the histological slides of the upper part of the femoral head, coloured with HE, magnification X25 and X100. A square on the X25 magnification indicates the place of the X100 magnification. No cartilage is left at the place of the asterisk on the 100X magnification.

Orthopedic surgical interventions and medical treatment

For all patients, the type of orthopedic surgeries and the age at which these surgeries were performed, are depicted in fig. 2. Details of the specific surgical procedures can be found in supplemental table 2. The most frequent intervention was hip surgery, performed in eight patients, with the first interventions in the second or third decade of life. In all of these patients, total hip replacement (THR) was eventually required.

Eight patients underwent bilateral CTS release, mostly in the second decade of life. In one patient, this intervention was performed more than once. Less frequently, surgical interventions of the knees, feet and spinal cord were performed. Several patients were treated with repeated corticosteroid injections in the glenohumeral or knee joint to reduce pain. Two patients were treated with bisphosphonates at their last outpatient visit (patients 8 and 10).

Cardiac and pulmonary examinations

Echocardiography was performed in 12 patients (supplemental table 3). In patient 4, there were limited signs of cardiac hypertrophy, with thickening of the posterior left ventricular wall. Systolic ventricular function was normal in all patients. A mildly dilated right ventricle with normal systolic function was seen in patient 10. Five patients (patients 1, 4, 5, 10 and 13) had mild regurgitation of one or more valves (mitral, aortic, pulmonary, or tricuspid) and one patient had moderate stenosis and regurgitation of the aortic valve (patient 5). None of the patients required valve replacement at the time of their last follow up. Pulmonary function tests were performed in 6 patients (supplemental table 3) and two patients had mild to moderate restrictive lung disease (patients 1 and 4).

Figure 2 Orthopedic surgical interventions

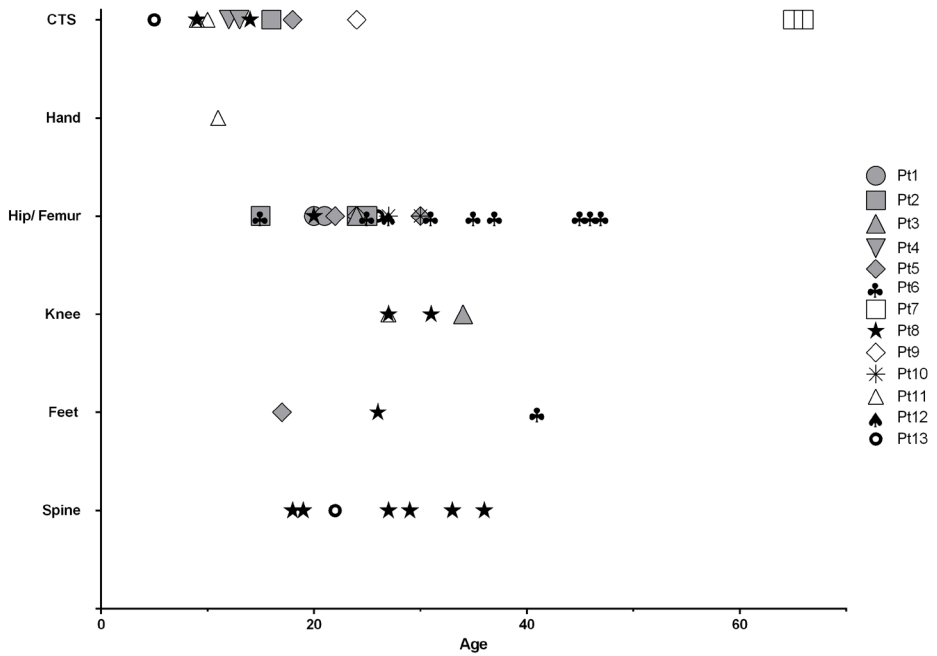


Fig.2. All orthopedic surgical interventions of thirteen ML III patients and the age at which they were performed, are shown. In some patients, the same surgical intervention was performed more than once.

Supplemental table 2 Orthopedic surgeries

Patient	CTS Age (years)	Pelvis, Femur Age (years)	
1		20& 21	Custom-made THR L, THR R with distal tenotomy hamstring R
2	16	CTS release L/R	Femoral varus osteotomy and endorotating osteotomy proximal femur L/R
		24& 25	THR (sequential) L/R
3	#	24	THR (sequential) L/R
4	12&13	CTS release R/L	
5	18	CTS release L/R	Femoral varus osteotomy (sequential) L/R
		22& 24	THR (sequential) R/L
		30	
6		15	Femoral varus osteotomy R
		25	Arthrodesis L hip
		31	THR L (Charnley)
		35	Removal of bridge plate R
		37	THR trochanter osteotomy R
		45	Osteosynthesis femur R (femur fracture R)
		45	Bridge plate failure, reposition, fixation fracture distal femur R with plate osteosynthesis
		46& 47	Re-osteosynthesis femur R, allograft bone grafting
		47	Drainage abscess (R femur)
		47	Removing osteosynthesis material, resection pseudarthrosis part R femur, placement angle blade plate R femur condyle
7	65&66	CTS release L/R	
8	9-14	Multiple CTS releases	THR (sequential) L/R
9	24	CTS release L/R	
10	#	27& 30	Uncemented THR (sequential) R/ L
11	9&10	CTS release L/R	
12	#	27	Uncemented Ceramic THR (sequential) L/R
13	5	Bilateral CTS release	Excision arthroplasty of R hip

CTS; carpal tunnel syndrome, # CTS present bilateral, no surgical intervention, THR; total hip replacement, L: left, R: right; PIP; proximal interphalangeal, dig: digits

Hands, knees and feet		Spine, spinal cord	
Age (Years)		Age (Years)	
34	Total knee prosthesis R		
17	Bunioectomy metatarsalia, PIP resection dig. V L/R feet		
41	Arthrodesis upper ankle joint		
		18	C1/C2 fusion secondary to cervical fracture
		19	Trans articular screws os odontoid
26	Arthroscopic debridement ankle R	27	L4/L5 and sacral fusion
27	Arthroscopy knee L	29	L4-S2 anterior fusion
31	Total knee replacement L	29	C4/5, C5/6, C6/7 bilateral foraminoplasties
		33	T10-11 post. decompressive laminectomy, extension of the posterior fixation to T10
		36	Occipito-cervico-thoracic spine fusion
11	Surgery for trigger fingers, tendon release bilaterally (ring finger)		
27	Knee arthroscopy and washout L/R		
		22	C3-T1 laminoplasty

Supplemental table 3 Cardiac and pulmonary evaluations

A. Cardiac evaluation				
Patient	Age cardiac evaluation (years)	LVH	LV function	Other abnormalities
1	20	No	Normal	Mild AR and MR
2	21	No	Normal	No
3	43	No	Normal	Myxomatous mitral valve with redundant tissue, minor billowing, no insufficiency
4	16	No	Normal	Mild MR. Posterior left ventricular wall slightly thickened
5	29	No	Normal	Bicuspid aortic valve, mild AS, moderate AR, mild MR and TR
6	N.A.	N.A.	N.A.	N.A.
7	65	No	Normal	No
8	32	No	Normal	No
9	28	No	Normal	No
10	35	No	Normal	Mild/ moderate TR. Mildly dilated RV with normal systolic function
11	30	No	Normal	No
12	35	No	Normal	No
13	26	No	Normal	Moderate/ severe AR, mild MR, PR and TR

Supplemental table 3 Continued

B. Pulmonary evaluation					
Patient	Age at spirometry (years)	FVC (% predicted)	FEV1 (% predicted)	FEV1/VC (% predicted)	Comments
1	23	60	52	96	Moderate restrictive spirometry without obstructive characteristics
3	46	116	121	105	No restriction, no obstruction
4	17	74	78	78	Mild Restriction
5	30	101	85	85	
7	66	89	88	72	No airway restriction or obstruction, normal flow-volume curve
13	24	36	37	105	

N.A.: not available, LVH: left ventricle hypertrophy; LV: left ventricle; RV: right ventricle; N.A.: not available, AR: aortic regurgitation, MR: mitral regurgitation, AS: aortic stenosis, TR: tricuspid regurgitation, PR: pulmonary regurgitation, FVC: forced vital capacity; FEV1: Forced expiratory volume in 1 second; VC: vital capacity

DISCUSSION

This multi-center retrospective medical record review describes the clinical course of adult forms of ML III. About half of the patients experienced significant physical limitations, being either wheelchair dependent and/or needing help with activities of daily living. Pain was reported by all patients. Approximately one third of the patient group had mild cognitive impairment. Three fourths of the patient group had been employed at any time during adulthood.

All patients have extensive skeletal pathology, requiring orthopedic surgical interventions as early as the second or third decade of life. Total hip replacement (THR) was the most common intervention, performed in 67% of all patients. In three patients, this was preceded by femoral varus osteotomy, but despite this position correction, these patients still needed THR some ten years later (fig. 1B, supplemental table 2).

As is seen in the different forms of MPS, abnormal bone development (dysostosis multiplex) [6] is uniformly present in ML III patients. Clinically, the earliest disabling feature is hip disease, characterized by pain and limited mobility. Abnormal hip morphology (acetabula, iliac bones and femoral heads) have been observed in very young ML III patients (at birth, at age four and six years [2, 14, 20]), suggesting early developmental alterations such as seen in MPS VI for example [37].

In addition to the dysostosis multiplex, the joints in ML III patients are affected throughout their lifespan by rapidly progressive osteoarthritis, resulting in cartilage destruction and bone lesions (areas of radiolucency and sclerosis). Clinically all patients suffer from bone and joint pain.

Bone disease in ML III may arise from an imbalance between bone forming osteoblasts and bone resorbing osteoclasts caused by the increased presence of osteoclastic enzymes in the bone-resorbing zone in osteoclasts [38]. Mannose-6-phosphate is important for the trafficking of these enzymes along the exocytic pathway to the apical membrane, where they are secreted in the bone-resorbing compartment [39]. The absence of mannose-6-phosphate on the osteoclastic enzymes may lead to increased secretion of these enzymes, resulting in uncontrolled bone and cartilage degradation [22, 40]. However, this hypothesis still needs to be substantiated by pathophysiological studies.

CTS was highly prevalent in our ML III patient population (present in 11 out of 13 patients) and bilateral CTS release was performed in eight patients. Cardiac valve abnormalities were found in six patients although there were no signs of cardiac dysfunction. Six

patients underwent formal pulmonary function assessment and two patients had moderate to mild restriction, most likely due to thoracic skeletal abnormalities. No remarks concerning airway infections or pulmonary complaints were present in the medical records. This distinguishes this condition from the different forms of MPS (e.g. type I, II, IV and VI) in which cardiac and pulmonary problems are more frequent, often with severe clinical implications, also seen in the milder adult forms of these disorders [41-43].

Future therapies

Future therapies for ML III should aim to improve bone metabolism in order to reduce bone pain, delay the need for surgical intervention and improve mobility. Bisphosphonates are given in ML III patients to decrease osteoclastic activity, with variable outcomes [22, 26, 27, 44]. Since long term use of these drugs suppresses bone turnover and may have a negative effect on length growth, they may be of limited use in ML III. A newer anti-bone resorption drug, Denosumab (blocking the osteoclast activating cytokine receptor activator of NF κ B ligand) may hold promise for the treatment of ML and has already been used with some success in osteogenesis imperfecta, improving both growth and vertebral shape [45-47]. Another option for treatment may be reduction of inflammation using drugs such as pentosan polysulfate (PPS), which has been shown to improve range of motion and reduce pain in MPS I patients [48]. Future pathophysiological studies on the characteristics of bone metabolism in ML III will be needed to establish the most promising therapeutic option for this disease.

CONCLUSION

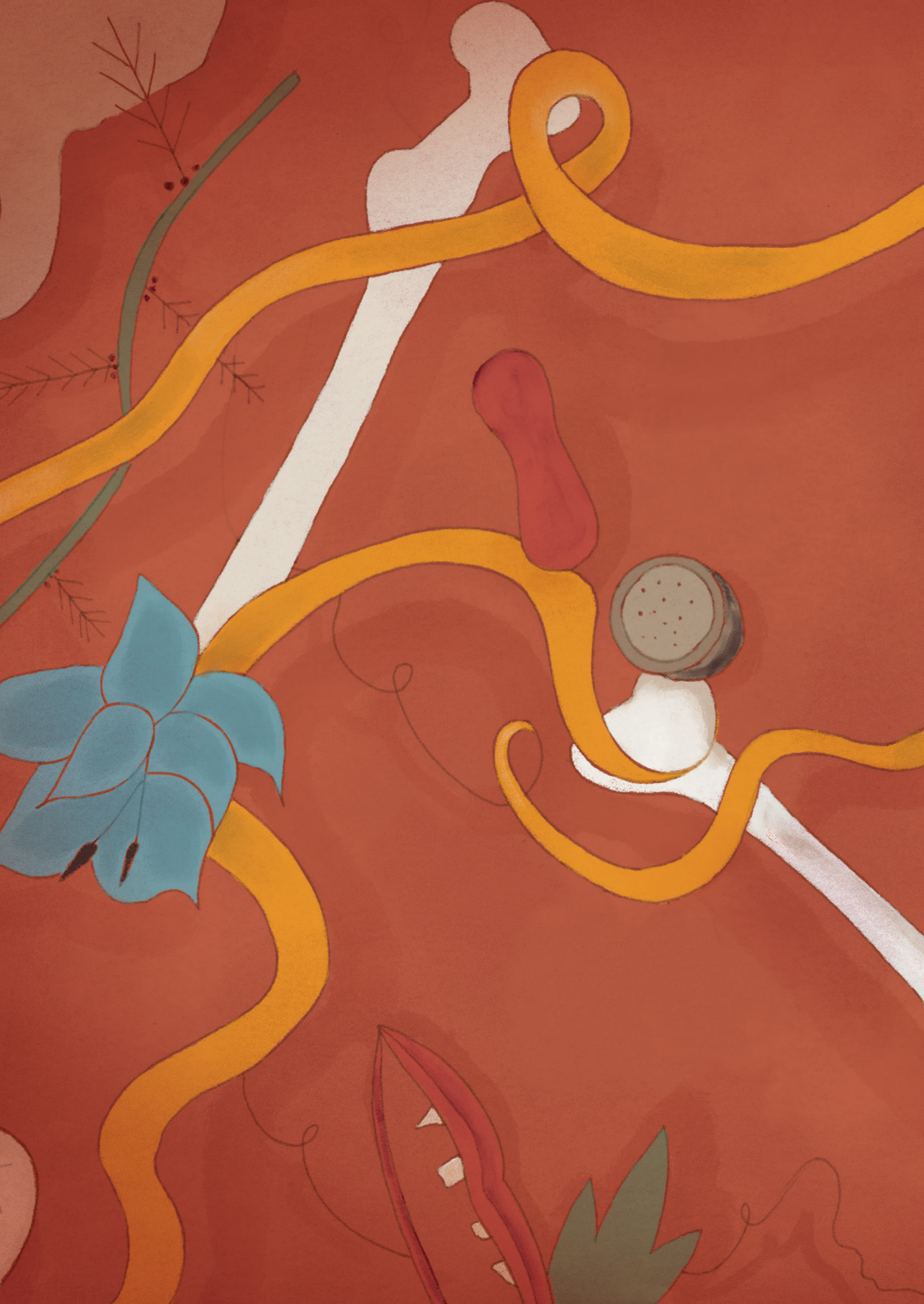
Severe skeletal abnormalities resulting from abnormal bone development and severe progressive osteoarthritis, are the hallmarks of ML III, necessitating surgical orthopedic interventions early in life. Future therapies for this disease should focus on improving cartilage and bone quality, preventing skeletal complications and improving mobility.

REFERENCES

- [1] S.S. Cathey, M. Kudo, S. Tiede, A. Raas-Rothschild, T. Braulke, M. Beck, H.A. Taylor, W.M. Canfield, J.G. Leroy, E.F. Neufeld, V.A. McKusick, Molecular order in mucopolipidosis II and III nomenclature, *Am J Med Genet A*, 146A (2008) 512-513.
- [2] S.S. Cathey, J.G. Leroy, T. Wood, K. Eaves, R.J. Simensen, M. Kudo, R.E. Stevenson, M.J. Friez, Phenotype and genotype in mucopolipidoses II and III alpha/beta: a study of 61 probands, *J Med Genet*, 47 (2010) 38-48.
- [3] A. Raas-Rothschild, V. Cormier-Daire, M. Bao, E. Genin, R. Salomon, K. Brewer, M. Zeigler, H. Mandel, S. Toth, B. Roe, A. Munnich, W.M. Canfield, Molecular basis of variant pseudo-hurler polydystrophy (mucopolipidosis IIIC), *J Clin Invest*, 105 (2000) 673-681.
- [4] A. Raas-Rothschild, R. Bargal, O. Goldman, E. Ben-Asher, J.E. Groener, A. Toutain, E. Stemmer, Z. Ben-Neriah, H. Flusser, F.A. Beemer, M. Penttinen, T. Olender, A.J. Rein, G. Bach, M. Zeigler, Genomic organisation of the UDP-N-acetylglucosamine-1-phosphotransferase gamma subunit (GNPTAG) and its mutations in mucopolipidosis III, *J Med Genet*, 41 (2004) e52.
- [5] J.G. Leroy, J.J. Martin, Mucopolipidosis II (I-cell disease): present status of knowledge, *Birth Defects Orig Artic Ser*, 11 (1975) 283-293.
- [6] P. Maroteaux, M. Lamy, [Hurler's pseudo-polydystrophy] La pseudo-polydystrophie de Hurler, *Presse Med*, 74 (1966) 2889-2892.
- [7] M. Bao, J.L. Booth, B.J. Elmendorf, W.M. Canfield, Bovine UDP-N-acetylglucosamine:lysosomal-enzyme N-acetylglucosamine-1-phosphotransferase. I. Purification and subunit structure, *J Biol Chem*, 271 (1996) 31437-31445.
- [8] M. Kudo, M. Bao, A. D'Souza, F. Ying, H. Pan, B.A. Roe, W.M. Canfield, The alpha- and beta-subunits of the human UDP-N-acetylglucosamine:lysosomal enzyme N-acetylglucosamine-1-phosphotransferase [corrected] are encoded by a single cDNA, *J Biol Chem*, 280 (2005) 36141-36149.
- [9] M.L. Reitman, S. Kornfeld, UDP-N-acetylglucosamine:glycoprotein N-acetylglucosamine-1-phosphotransferase. Proposed enzyme for the phosphorylation of the high mannose oligosaccharide units of lysosomal enzymes, *J Biol Chem*, 256 (1981) 4275-4281.
- [10] S. Tiede, N. Muschol, G. Reutter, M. Cantz, K. Ullrich, T. Braulke, Missense mutations in N-acetylglucosamine-1-phosphotransferase alpha/beta subunit gene in a patient with mucopolipidosis III and a mild clinical phenotype, *Am J Med Genet A*, 137A (2005) 235-240.
- [11] R. Bargal, M. Zeigler, B. Abu-Libdeh, V. Zuri, H. Mandel, Z. Ben Neriah, F. Stewart, N. Elcioglu, T. Hindi, M. Le Merrer, G. Bach, A. Raas-Rothschild, When Mucopolipidosis III meets Mucopolipidosis II: GNPTA gene mutations in 24 patients, *Mol Genet Metab*, 88 (2006) 359-363.
- [12] M. Encarnacao, L. Lacerda, R. Costa, M.J. Prata, M.F. Coutinho, H. Ribeiro, L. Lopes, M. Pineda, J. Ignatius, H. Galvez, A. Mustonen, P. Vieira, M.R. Lima, S. Alves, Molecular analysis of the GNPTAB and GNPTG genes in 13 patients with mucopolipidosis type II or type III - identification of eight novel mutations, *Clin Genet*, 76 (2009) 76-84.
- [13] T. Otomo, T. Muramatsu, T. Yorifuji, T. Okuyama, H. Nakabayashi, T. Fukao, T. Ohura, M. Yoshino, A. Tanaka, N. Okamoto, K. Inui, K. Ozono, N. Sakai, Mucopolipidosis II and III alpha/beta: mutation analysis of 40 Japanese patients showed genotype-phenotype correlation, *J Hum Genet*, 54 (2009) 145-151.
- [14] G. David-Vizcarra, J. Briody, J. Ault, M. Fietz, J. Fletcher, R. Savarirayan, M. Wilson, J. McGill, M. Edwards, C. Munns, M. Alcausin, S. Cathey, D. Silience, The natural history and osteodystrophy of mucopolipidosis types II and III, *J Paediatr Child Health*, 46 (2010) 316-322.

- [15] M. Yang, S.Y. Cho, H.D. Park, R. Choi, Y.E. Kim, J. Kim, S.Y. Lee, C.S. Ki, J.W. Kim, Y.B. Sohn, J. Song, D.K. Jin, Clinical, biochemical and molecular characterization of Korean patients with mucopolipidosis II/III and successful prenatal diagnosis, *Orphanet J Rare Dis*, 12 (2017) 11.
- [16] T.C. Falik-Zaccai, M. Zeigler, R. Bargal, G. Bach, Z. Borochowitz, A. Raas-Rothschild, Mucopolipidosis III type C: first-trimester biochemical and molecular prenatal diagnosis, *Prenat Diagn*, 23 (2003) 211-214.
- [17] E. Persichetti, N.A. Chuzhanova, A. Dardis, B. Tappino, S. Pohl, N.S. Thomas, C. Rosano, C. Balducci, S. Paciotti, S. Dominissini, A.L. Montalvo, M. Sibilio, R. Parini, M. Rigoldi, M. Di Rocco, G. Parenti, A. Orlacchio, B. Bembi, D.N. Cooper, M. Filocamo, T. Beccari, Identification and molecular characterization of six novel mutations in the UDP-N-acetylglucosamine-1-phosphotransferase gamma subunit (GNPTG) gene in patients with mucopolipidosis III gamma, *Hum Mutat*, 30 (2009) 978-984.
- [18] S. Liu, W. Zhang, H. Shi, Y. Meng, Z. Qiu, Three novel homozygous mutations in the GNPTG gene that cause mucopolipidosis type III gamma, *Gene*, 535 (2014) 294-298.
- [19] F.S. Haddad, D.H. Jones, A. Vellodi, N. Kane, M.C. Pitt, Carpal tunnel syndrome in the mucopolysaccharidoses and mucopolipidoses, *J Bone Joint Surg Br*, 79 (1997) 576-582.
- [20] C. Hetherington, N.J. Harris, T.W. Smith, Orthopaedic management in four cases of mucopolipidosis type III, *J R Soc Med*, 92 (1999) 244-246.
- [21] F.S. Haddad, R.A. Hill, A. Vellodi, Orthopaedic manifestations of mucopolipidosis III: an illustrative case, *J Pediatr Orthop B*, 9 (2000) 58-61.
- [22] C. Robinson, N. Baker, J. Noble, A. King, G. David, D. Sillence, P. Hofman, T. Cundy, The osteodystrophy of mucopolipidosis type III and the effects of intravenous pamidronate treatment, *J Inherit Metab Dis*, 25 (2002) 681-693.
- [23] R.A. Steet, R. Hullin, M. Kudo, M. Martinelli, N.U. Bosshard, T. Schaffner, S. Kornfeld, B. Steinmann, A splicing mutation in the alpha/beta GlcNAc-1-phosphotransferase gene results in an adult onset form of mucopolipidosis III associated with sensory neuropathy and cardiomyopathy, *Am J Med Genet A*, 132A (2005) 369-375.
- [24] L.H. Cripe, S.M. Ware, R.B. Hinton, Replacement of the aortic valve in a patient with mucopolipidosis III, *Cardiol Young*, 19 (2009) 641-643.
- [25] I. Smuts, D. Potgieter, F.H. van der Westhuizen, Combined tarsal and carpal tunnel syndrome in mucopolipidosis type III. A case study and review, *Ann N Y Acad Sci*, 1151 (2009) 77-84.
- [26] D.A. Kerr, V.A. Memoli, S.S. Cathey, B.T. Harris, Mucopolipidosis type III alpha/beta: the first characterization of this rare disease by autopsy, *Arch Pathol Lab Med*, 135 (2011) 503-510.
- [27] H. Kobayashi, J. Takahashi-Fujigasaki, T. Fukuda, K. Sakurai, Y. Shimada, K. Nomura, M. Ariga, T. Ohashi, Y. Eto, T. Otomo, N. Sakai, H. Ida, Pathology of the first autopsy case diagnosed as mucopolipidosis type III alpha/beta suggesting autophagic dysfunction, *Mol Genet Metab*, 102 (2011) 170-175.
- [28] S. Liu, W. Zhang, H. Shi, F. Yao, M. Wei, Z. Qiu, Mutation Analysis of 16 Mucopolipidosis II and III Alpha/Beta Chinese Children Revealed Genotype-Phenotype Correlations, *PLoS One*, 11 (2016) e0163204.
- [29] L. Pantoja Zarza, C. Diez Morrondo, Skeletal deformities in mucopolipidosis III, *Reumatol Clin*, 10 (2014) 340-341.
- [30] C. Ward, R. Singh, C. Slade, A.H. Fensom, A. Fahmy, A. Semrin, A. Sjøvall, A. Talat, A. Hasilik, I. Klein, et al., A mild form of mucopolipidosis type III in four Baluch siblings, *Clin Genet*, 44 (1993) 313-319.
- [31] W.C. Cavalcante, L.C. Santos, J.N. Dos Santos, S.J. de Vasconcellos, R.A. de Azevedo, J.N. Dos Santos, Oral findings in patients with mucopolipidosis type III, *Braz Dent J*, 23 (2012) 461-466.
- [32] F. Umehara, W. Matsumoto, M. Kuriyama, K. Sukegawa, S. Gasa, M. Osame, Mucopolipidosis III (pseudo-Hurler polydystrophy); clinical studies in aged patients in one family, *J Neurol Sci*, 146 (1997) 167-172.
- [33] M. Hara, T. Inokuchi, T. Taniwaki, T. Otomo, N. Sakai, T. Matsuishi, M. Yoshino, An adult patient with mucopolipidosis III alpha/beta presenting with parkinsonism, *Brain Dev*, 35 (2013) 462-465.

- [34] B. Tuysuz, O. Kasapcopur, D.U. Alkaya, S. Sahin, B. Sozeri, G. Yesil, Mucopolipidosis type III gamma: Three novel mutation and genotype-phenotype study in eleven patients, *Gene*, (2017).
- [35] P. Freisinger, J.C. Padovani, P. Maroteaux, An atypical form of mucopolipidosis III, *J Med Genet*, 29 (1992) 834-836.
- [36] A. Kadar, B. Elhassan, S.L. Moran, Manifestations of Mucopolipidosis III in the hand: avascular necrosis of multiple carpal bones, *J Hand Surg Eur Vol*, 42 (2017) 645-646.
- [37] E. Oussoren, J. Bessems, V. Pollet, J.C. van der Meijden, L.J. van der Giessen, I. Plug, A.S. Devos, G.J.G. Ruijter, A.T. van der Ploeg, M. Langeveld, A long term follow-up study of the development of hip disease in Mucopolysaccharidosis type VI, *Mol Genet Metab*, 121 (2017) 241-251.
- [38] K. Kollmann, J.M. Pestka, S.C. Kuhn, E. Schone, M. Schweizer, K. Karkmann, T. Otomo, P. Catala-Lehnen, A.V. Failla, R.P. Marshall, M. Krause, R. Santer, M. Amling, T. Braulke, T. Schinke, Decreased bone formation and increased osteoclastogenesis cause bone loss in mucopolipidosis II, *EMBO Mol Med*, 5 (2013) 1871-1886.
- [39] R. Baron, L. Neff, W. Brown, P.J. Courtoy, D. Louvard, M.G. Farquhar, Polarized secretion of lysosomal enzymes: co-distribution of cation-independent mannose-6-phosphate receptors and lysosomal enzymes along the osteoclast exocytic pathway, *J Cell Biol*, 106 (1988) 1863-1872.
- [40] J.G. Barriocanal, J.S. Bonifacino, L. Yuan, I.V. Sandoval, Biosynthesis, glycosylation, movement through the Golgi system, and transport to lysosomes by an N-linked carbohydrate-independent mechanism of three lysosomal integral membrane proteins, *J Biol Chem*, 261 (1986) 16755-16763.
- [41] M.M. Brands, I.M. Frohn-Mulder, M.L. Hagemans, W.C. Hop, E. Oussoren, W.A. Helbing, A.T. van der Ploeg, Mucopolysaccharidosis: cardiologic features and effects of enzyme-replacement therapy in 24 children with MPS I, II and VI, *J Inherit Metab Dis*, 36 (2013) 227-234.
- [42] B.M. Clark, J. Sprung, T.N. Weingarten, M.E. Warner, Anesthesia for patients with mucopolysaccharidoses: Comprehensive review of the literature with emphasis on airway management, *Bosn J Basic Med Sci*, (2017).
- [43] D.M. Rapoport, J.J. Mitchell, Pathophysiology, evaluation, and management of sleep disorders in the mucopolysaccharidoses, *Mol Genet Metab*, (2017).
- [44] Z. Zolkipli, L. Noimark, M.A. Cleary, C. Owens, A. Vellodi, Temporomandibular joint destruction in mucopolipidosis type III necessitating gastrostomy insertion, *Eur J Pediatr*, 164 (2005) 772-774.
- [45] J.L. Shaker, C. Albert, J. Fritz, G. Harris, Recent developments in osteogenesis imperfecta, *F1000Res*, 4 (2015) 681.
- [46] D.A. Hanley, J.D. Adachi, A. Bell, V. Brown, Denosumab: mechanism of action and clinical outcomes, *Int J Clin Pract*, 66 (2012) 1139-1146.
- [47] D.A. Hanley, M.R. McClung, K.S. Davison, L. Dian, S.T. Harris, P.D. Miller, E.M. Lewiecki, D.L. Kendler, A. Writing Group for the Western Osteoporosis, Western Osteoporosis Alliance Clinical Practice Series: Evaluating the Balance of Benefits and Risks of Long-Term Osteoporosis Therapies, *Am J Med*, 130 (2017) 862 e861-862 e867.
- [48] J.B. Hennermann, S. Gokce, A. Solyom, E. Mengel, E.H. Schuchman, C.M. Simonaro, Treatment with pentosan polysulphate in patients with MPS I: results from an open label, randomized, monocentric phase II study, *J Inherit Metab Dis*, 39 (2016) 831-837.



A stylized illustration on a reddish-brown background. At the top left is a light-colored fetus in a curled position. Below it is a white skull with a yellow band wrapped around it. To the right of the skull is a red flower with green leaves. Further right is a white egg-like shape with a yellow band wrapped around it. At the bottom left is a white bone and a small circular object with holes. The background is filled with swirling yellow and orange lines.

CHAPTER 6

CRANIOSYNOSTOSIS
AFFECTS THE MAJORITY OF
MUCOPOLYSACCHARIDOSIS
PATIENTS AND CAN CONTRIBUTE
TO INCREASED INTRACRANIAL
PRESSURE

E. Oussoren, I.M.J. Mathijssen, M. Wagenmakers, R.M. Verdijk,
H.H. Bredero-Boelhouwer, M.L.C. van Veelen-Vincent, J.C. van der Meijden,
J.M.P. van den Hout, G.J.G. Ruijter, A.T. van der Ploeg, M. Langeveld

J Inherit Metab Dis. 2018;Aug 6

ABSTRACT

Introduction: The mucopolysaccharidoses are multisystem lysosomal storage diseases characterized by extensive skeletal deformities, including skull abnormalities. The objective of this study was to determine the incidence of craniosynostosis in the different MPS types and its clinical consequences.

Methods: In a prospective cohort study spanning 10 years, skull imaging and clinical evaluations were performed in 47 MPS patients (type I, II, VI and VII). A total of 215 radiographs of the skull were analyzed. The presence and type of craniosynostosis, the sutures involved, progression over time, skull shape, head circumference, fundoscopy and ventriculoperitoneal shunt (VPS) placement data were evaluated.

Results: Craniosynostosis of at least one suture was present in 77% of all 47 MPS patients (≤ 6 years in 40% of all patients). In 32% of all MPS patients, premature closure of all sutures was seen (≤ 6 years in 13% of all patients). All patients with early closure had a more severe MPS phenotype, both in the neuronopathic (MPS I, II) and non-neuronopathic (MPS VI) patient groups. Because of symptomatic increased intracranial pressure, a VPS was placed in six patients, with craniosynostosis as a likely or certain causative factor for the increased pressure in four patients. One patient underwent cranial vault expansion because of severe craniosynostosis.

Conclusion: Craniosynostosis occurs in the majority of the MPS patients. Since the clinical consequences can be severe and surgical intervention is possible, skull growth and signs and symptoms of increased intracranial pressure should be monitored in both neuronopathic and non-neuronopathic patients with MPS.

INTRODUCTION

Mucopolysaccharidoses are lysosomal storage diseases caused by deficiencies of glycosaminoglycan (GAG) degrading enzymes. The mucopolysaccharidoses are multisystem disorders with a broad range of clinical manifestations, including extensive skeletal abnormalities (dysostosis multiplex, joint contractures) and hydrocephalus [1, 2]. Neurological decline due to GAG accumulation in the brain is seen in a subset of patients with mucopolysaccharidosis (MPS) type I, II, III and VII [1, 3].

In healthy individuals, the skull expands by growth from the sutures up to the age of six years. After the age of six, both sutural and appositional growth takes place [4, 5]. The metopic suture closes between the age of 3 and 9 months [6]. The sagittal, coronal and lambdoid sutures begin to close much later, around ages 22, 24 and 26 respectively [4]. If one or more suture(s) close(s) at an earlier age, this can result in growth stagnation and/or an abnormal skull shape. This premature fusion (craniosynostosis) can be classified as simple (one fused suture), or complex (multiple sutures involved); primary (sutural biology abnormality), or secondary (due to external influences) and as part of a syndrome or isolated [7].

Early closure of each suture results in a different shape of the skull. For example, early closure of the sagittal suture results in an elongated and narrow skull (scaphocephaly) and early closure of the lambdoid sutures results in occipital flattening (pachycephaly) [8]. Early onset craniosynostosis, defined as closure of sutures before the age of 6 years, can restrict skull growth and can cause elevated intracranial pressure (ICP) which can result in visual impairment [9]. Therefore, early recognition of craniosynostosis is of great importance. Timely surgical intervention can provide space for the brain to grow, thus preserving development and vision [10].

Up till now, only two small cross-sectional studies investigated the prevalence of craniosynostosis in MPS patients. They found secondary craniosynostosis in 19% (7 out of 36) of severe MPS II patients and 11% (2 out of 18) of MPS IVA patients. Additionally, three case reports describe the presence of craniosynostosis in MPS (type I and type VI) [4, 11-16]. The incidence and type of craniosynostosis in MPS, the development over time, severity and clinical consequences have not been studied. In our prospective study, this was systematically evaluated in a relatively large cohort of patients with MPS I, II, VI and VII.

METHODS

Patients

From 2007 onwards all pediatric patients with mucopolysaccharidosis (type I, II, VI and VII) treated in the Center for Lysosomal and Metabolic diseases of the Erasmus MC Rotterdam, were included in a prospective cohort study. In all patients, the diagnosis of MPS had been confirmed by measurement of enzyme deficiency in leucocytes or fibroblasts and by DNA analysis. Yearly evaluation was done according to a standardized follow-up protocol which included taking the patients' medical history, physical and neurological examination, skull radiographs and ophthalmological examinations. Available data from 2002 to 2007 was added retrospectively. The study was approved by the Medical Ethical Review board at the Erasmus MC.

Radiographic evaluation of sutures and skull shape

Skull radiographs (anterior posterior (AP) and lateral) were obtained yearly up to the age of 18 years. Radiographs of patients with a ventriculoperitoneal shunt (VPS) were excluded after drain placement, as the drain itself can induce secondary closure of one or more sutures in proximity to the drain [17]. Furthermore, the postoperative radiographs of a patient who underwent cranial surgery were excluded from the analysis.

Each radiograph was evaluated by two independent observers (craniosynostosis expert and plastic surgeon professor I. M. and lysosomal expert and metabolic pediatrician E.O.). In each radiograph, three sutures (coronal, sagittal and lambdoid) were scored as open, partially closed, or closed. The metopic suture was not analyzed as it closes physiologically between the age of 3 and 9 months and for most patients, radiographs were not available at such an early age [6].

For each MPS type (I, II, VI and VII) the proportion of patients with craniosynostosis was determined. Furthermore, the proportion of patients with one closed suture, as well as those with two or more closed sutures was determined and the order in which the sutures closed was analyzed. For each patient, the shape of the skull was described using the last available radiograph. Of three patients with craniosynostosis, three dimensional CT scans of the skull were available.

Head circumferences, ophthalmological and physical examination

Head circumference was measured at least yearly and the measurements closest to the evaluated radiographs of the skull were used for analysis. At physical examination, head shape and facial features were examined.

The presence of raised ICP was evaluated by fundoscopy during yearly ophthalmological assessments unless fundoscopy could not be reliably performed due to corneal clouding or behavioral problems.

Ventriculoperitoneal shunt (VPS) placement

Of the MPS patients who received a VPS, the following parameters at the time of placement were determined: age, VPS indication (clinical features, brain imaging and cerebrospinal fluid pressure (CSF)), head circumference, head shape, presence or absence of craniosynostosis and result of fundoscopy.

Statistics

All data are presented as median and range unless otherwise stated.

RESULTS

Patients data and characteristics

Forty-seven patients with MPS (type I, II, VI and VII) were included in this study (72% were male patients). The median age at diagnosis was 2.8 (range 0-12) years. Table 1 shows disease type and severity, mutation(s), gender, age at diagnosis, age at first and last radiograph and skull shape for each patient.

Skull radiographs

A total of 215 skull radiographs were analyzed. The first available radiograph was taken at 4.2 (0-12.4) years of age for the entire MPS patient group. The follow-up period was 3.4 (0.1-9.1) years (table 1).

Prevalence of craniosynostosis in MPS

Craniosynostosis of at least one suture was present in 77% of all 47 MPS patients and in 40% of patients this occurred before the age of 6 years (fig. 1 and 2). Table 2 shows the prevalence of craniosynostosis, the number of sutures involved and the resulting head shape for each MPS type.

Sutures involved, progression over time and severity

In all MPS patients, 9% had premature (partial) closure of only one suture. In 66% of all MPS patients, two or three sutures partially or fully closed prematurely (fig. 1 and table 2). The longitudinal data on the closure of each suture in each individual MPS patient are depicted in figure 2. In most cases, two or three sutures were already (partially) closed at the time the first radiograph was made (fig. 2). The coronal suture was never the first to close (fig. 1). In 32% of all MPS patients, premature closure of all sutures was seen (≤ 6 years in 13% of all patients; table 2). All these patients with early closure (≤ 6 year) had a more severe MPS phenotype.

Skull shape

No specific skull shape abnormality (normocephaly) could be detected in 51% of all MPS patients (table 1, 2). Despite a normal skull shape in two patients, all sutures had closed before age 6 (MPS VI, patients 1 and 5). This is also referred to as pansynostosis [18].

Scaphocephaly was seen in 26% of all MPS patients. In 8 of these 12 patients, closure of the sagittal suture had occurred around or before age 6. Pachycephaly was detected in 23% of all MPS patients. Pachycephaly with scaphocephaly was seen in one patient (MPS I, patient 2). Plagiocephaly at the right anterior side of the head was seen in one MPS II patient (fig. 3A, patient 10).

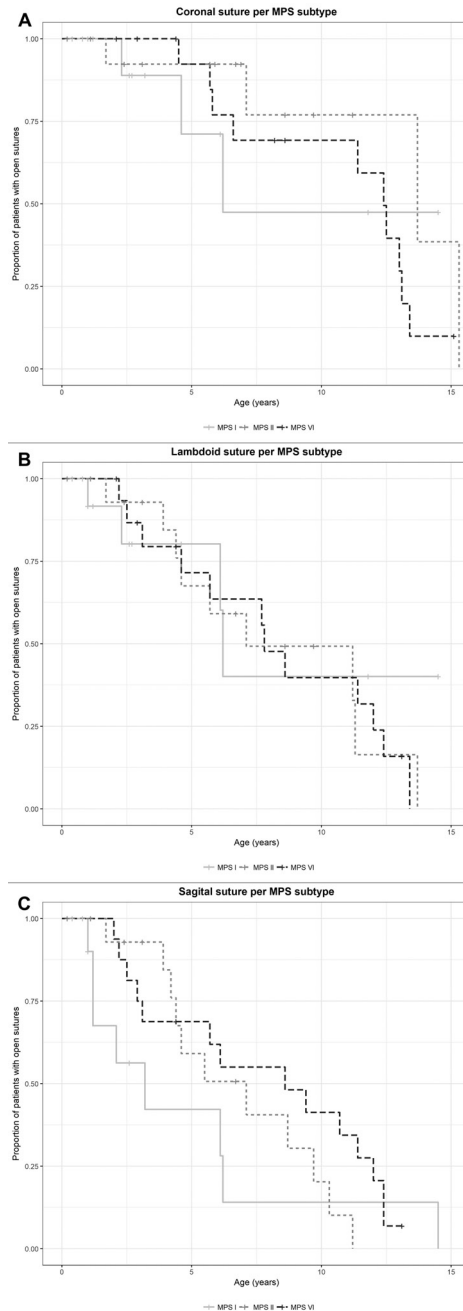
Figure 1 Suture closure in the different MPS types

Fig. 1. Kaplan-Meier curves of open suture(s) (coronal: **A**, lambdoid: **B** and sagittal: **C**) by MPS subtype (type I, II, VI). 1.0 means 100% of patients with open or partially closed suture, 0 means suture closed in all patients. MPS VII patients were not included in the graph because of the low number (n=2).

Table 1 Patients characteristics

MPS I Pt nr.	Hurler (H) / Hurler/Scheie (HS) / Scheie (S)	IDUA gene Protein	Gender Male (M) / Female (F)
1	H	p.Q70X/p.L218P	M
2	H	p.Q70X/p.W402X	F
3	H	p.Q70X/p.L218P	M
4	H	p.Q70X/p.L218P	M
5	H	p.Q70X/p.A327P	M
6#	H	p.Q70X/p.Q70X	F
7	H	p.Q70X/p.L218P	M
8	H	p.A327P/p.A327P	F
9	H	c.1273dup, p.H425fs/ c.1273dup, p.H425fs	F
10#	H	p.Q70X / Q70X	M
11	H	c.1893del, p.F632fs/ c.1893del, p.F632fs	F
12	H/S	p.W402X/p.W402X	M
13	S	p.W402X/n.i.	M
14	S	p.R383H/c.474-2A>G	F
MPS II	Neuropatic (N) / Nonneuropatic (NN)	IDS gene Protein	Gender Male (M) / Female (F)
1	N	p.S349R	M
2	N	p.E521K	M
3	N	p.P86L	M
4	N	p.E459*	M
5	N	p.S333L	M
6	N	p.S117del	M
7	N	c.1511del, p.G504fs	M
8	N	c.544del, p.L182fs	M
9	N	Total IDS del^	M
10	N	p.S333L	M
11	N	p.L522P	M
12	Unknown	p.H229R	M
13\$	NN	p.F137S	M
14\$	NN	p.F137S	M
15	NN	p.Y225D	M
MPS VI	Rapidly progressive (R) / Slowly progressive (S)	ARSB gene Protein	Gender Male (M) / Female (F)
1	R	c.1142+2T>C, p?/ c.1142+2T>C, p?	F
2	R	p.P313S/p.P313S	M
3	R	p.V332G/p.V332G	M
4	R	p.P313S/p.P313S	F
5	R	p.N301K/p.N301K	F
6	R	p.G324V/p.G324V	M
7€	R	p.P313A/p.P313A	F

Age at diagnosis (years)	Age first X skull (years)	Age last X skull (years)	Skull shape last radiograph
2.4	11.8		normal
2	6.1		scaphocephaly, pachycephaly
1.7	6.2	8.1	pachycephaly
0.9	1		scaphocephaly
1	0.8		pachycephaly
1	1.2	2.2	scaphocephaly
0.9	1.0	3.2	pachycephaly
1.3	1		scaphocephaly
0.7	2.7		scaphocephaly
0	0	4.6	normal
1.2	1.2		scaphocephaly
1	0.4		pachycephaly
5	7.9	14.5	normal
2.3	2.6		normal
Age at diagnosis (years)	Age first X skull (years)	Age last X skull (years)	Skull shape last radiograph
3	10.3	15.3	normal
3	11.2		pachycephaly
6	9.7		pachycephaly
2	8.7	13.7	normal
3	3.1		normal
0	0.2		normal
4.7	5.5	8.6	normal
2	2.4		normal
4	7.1	7.7	normal
2	0.2	1.7 (CT scan)	plagiocephaly anterior right
1	1.1		normal
5	6.7		normal
3.3	3.5	6.9	scaphocephaly
3.3	3.5	7.2	scaphocephaly
4.1	4.2	5.7	pachycephaly
Age at diagnosis (years)	Age first X skull (years)	Age last X skull (years)	Skull shape last radiograph
2.9	5.7	14.8	Normal
12	12	13	scaphocephaly
2.7	2.9		pachycephaly
6.5	8.6		scaphocephaly
1.9	2.5	8.6	normal
1.4	2.2	8.2	scaphocephaly
4.6	4.6	6.6	normal

Table 1 Continued

MPS VI	Rapidly progressive (R) / Slowly progressive (S)	ARSB gene Protein	Gender Male (M) / Female (F)
8	R	Unknown	F
9£	R	p.P313A/p.P313A	M
10	R	p.H141P/p.L321P	M
11	S	p.R152W/p.R152W	F
12	S	p.Y210C/p.P313A	M
13	S	p.R152W/p.R152W	M
14&	S	p.Y210C/p.R327X	F
15&	S	p.Y210C/p.R327X	M
16	S	p.Y210C/p.R327X	M
MPS VII	Mild / severe	GUSB gene Protein	Gender Male (M) / Female (F)
1α	Mild	p.V99M/p.V99M	M
2α	Mild	p.V99M/p.V99M	M

#, \$, £, & and α: siblings

Patient numbering is the same as in figure 2.

Table 2 Frequency of premature suture closure in MPS

	Total MPS	MPS I
≥ 1 Suture closed; n/total (%)	36/47 (77%)	10/14 (71%)
≥ 1 Suture closed ≤6 year; n/total (%)	19/47 (40%)	6/14 (43%)
1 Suture closed; n/total (%)	4/47 (9%)	2/14 (14%)
> 2 Sutures closed; n/total (%)	31/47 (66%)	7/14 (50%)
All sutures closed; n/total (%)	15/47 (32%)	2/14 (14%)
All sutures closed ≤6 year; n/total (%)	6/47 (13%)	2/14 (13%)
All sutures open; n/total (%)	11/47 (23%)	4/14 (29%)
Skull shape; n/total (%)*	N 24/47 (51%)	N 4/14 (29%)
	S 12/47 (26%)	S 6/14 (43%)#
	P 11/47 (23%)	P 5/14 (36%)#

*N; Normocephalic, S; Scaphocephalic, P; Pachycephalic. # one patient had both scaphocephalic and pachycephalic head shape. ^ one patient had only plagiocephaly at the right anterior side of the head and therefor data of one patient is missing

Age at diagnosis (years)	Age first X skull (years)	Age last X skull (years)	Skull shape last radiograph
3.1	3.1	4.5 (CT scan)	scaphocephaly
2.2	2.4	4.4	normal
1.9	2.0	2.1 (CT scan)	pachycephaly, brachycephaly
7.5	7.8	14	normal
10.3	12.4	14.4	normal
0.7	7.7	15.1	normal
6.4	7.3	15.3	normal
5	5.3	14.3	normal
5.9	5.8	13.1	normal
Age at diagnosis (years)	Age first X skull (years)	Age last X skull (years)	Skull shape last radiograph
8.4	8.4		normal
6.7	6.7		pachycephaly

MPS II	MPS VI	MPS VII
10/15 (67%)	15/16 (94%)	1/2 (50%)
6/15 (40%)	7/16 (44%)	0/2 (0%)
0/15 (0%)	1/16 (6%)	1/2 (50%)
10/15 (67%)	14/16 (88%)	0/2 (0%)
4/15 (27%)	9/16 (56%)	0/2 (0%)
1/15 (7%)	3/16 (19%)	0/2 (0%)
5/15 (33%)	1/16 (6%)	1/2 (50%)
N 9/15 (60%) [^]	N 10/16 (63%)	N 1/2 (50%)
S 2/15 (13%) [^]	S 4/16 (25%)	S 0/2 (0%)
P 3/15 (20%) [^]	P 2/16 (13%)	P 1/2 (50%)

Figure 2 Craniosynostosis by MPS type in individual patients

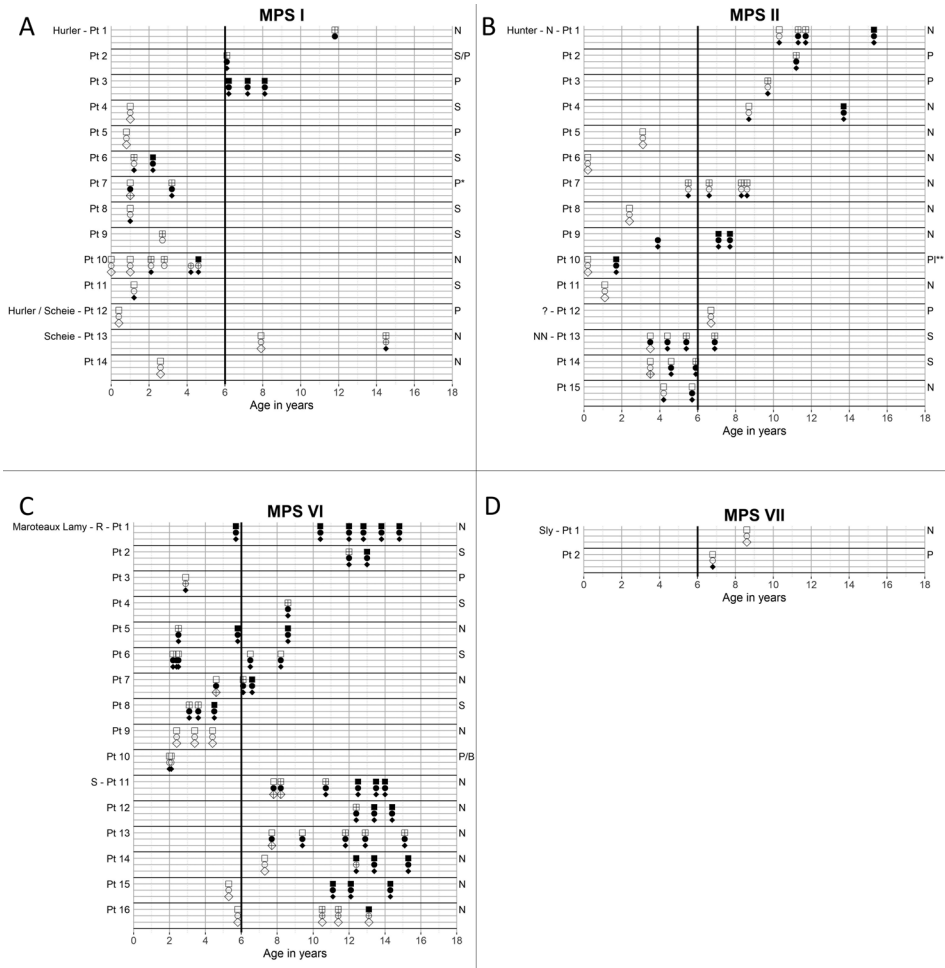


Fig.2. For each MPS type, the suture closure over time is shown. Each suture is depicted by a symbol: coronal: square, lambdoid: circle, sagittal: diamond. Closure status is indicated by the filling of the symbol: transparent: open suture(s), shaded: partial closure, black: completely closed. For MPS I, II and VI, the most severe phenotypes are at the top and the least severe phenotypes at the bottom of the graph. Abbreviations in the graph: Pt.: patient, N: neuronopathic, NN: non-neuronopathic, R: rapidly progressive, S: slowly progressive
 Right: skull shape, N: normocephaly, S: scaphocephaly, P: pachycephaly, B: brachycephaly, Pl*: plagiocephaly
 A black line is drawn at age 6 years. If suture closure occurs before the age of six, this is regarded as early onset craniosynostosis.

Illustrative cases of craniosynostosis in MPS

Figure 3 shows photographs, skull X-rays, 3D CT scans and MRI cerebrum of a MPS II patient (patient 10) (fig. 3A) with bulging anterior fontanel due to craniosynostosis, a MPS VI patient (patient 8) (fig. 3B), with frontal bossing and scaphocephaly due to craniosynostosis and an adult MPS VI patient (brother of patient 4) (fig. 3C). This adult patient died unexpectedly at 25 years of age as a result of a respiratory tract infection in an already highly compromised respiratory setting. Figure 3C shows macroscopic pictures from the brain autopsy, with an impression of the sinus transversus in the skull (X-skull) and an impression of the brain gyri in the frontal bone, the result of raised ICP earlier in life.

Head circumferences

Data from at least one head circumferences measurement was available for 94% of all MPS patients. Only two patients had a head circumference outside the normal reference range (-2SD). Both were MPS VI patients (patients 1 and 5) in whom all sutures closed before age 6, with stagnation (arrest) of skull growth. After age 6, their head circumferences started to increase again, in line with appositional growth of the skull. Supplemental figure 1 shows skull and height growth curves and photo- and radiographs of one of these patients (MPS VI patient 1).

Ophthalmic examination

Fundoscopy data was available for 85% of all MPS patients. Two patients had papilledema. In one of them, craniosynostosis was recognized at that time as the cause of increased ICP. Occipital cranial vault expansion with fronto-supraorbital remodulation surgery was performed at the age of 1 year and 9 months (MPS II, patient 10, fig. 3A). In the second patient (MPS VI, patient 7), edema was mild, there were no clinical signs of increased ICP and skull growth was normal. Therefore, an intervention was deemed unnecessary.

Table 3 Characteristics of MPS patients with ventricular peritoneal shunt

	MPS I (Patient 2)	MPS I (Patient 4)
Age at VPS placement	7.5	2
Reason for VPS placement		
- Clinical	Neurological decline	Neurological decline; headaches
- Brain imaging	CT: mild progression triventricular hydrocephalus	CT: progression hydrocephalus, bulging fontanel
- CSF pressure*	NP	NP
Head circumferences in SD values at the time of VPS placement	+1½SD	+2½SD
Head shape[§]	S/P	S
Craniosynostosis present before VPS placement	Yes	Highly susceptible (bulging fontanel)
Papilledema (fundoscopy)	No	NP

MPS: mucopolysaccharidosis; VPS: Ventriculoperitoneal shunt; NP: Not Performed; SD: Standard Deviation; CSF: Cerebrospinal Fluid

*CSF pressure of >25 to 30 cm H₂O (18-22 mmHg) an indication for VPS

§ S: scaphocephaly; P: pachycephaly; N: normocephaly

Ventriculoperitoneal shunt (VPS) placement

In six patients, a VPS was placed at a median age of 5.4 (range 2-7.5) years because of suspected elevated ICP (table 3). Fundoscopy was performed or attempted in three patients before VPS placement. Two patients had no papilledema and in the other patient, fundoscopy was not possible due to corneal clouding or abnormal behavior. In five of the six patients, CT or MRI scan of the brain prior to VPS placement showed progressive hydrocephalus. They had clinical symptoms caused by the increased ICP such as neurological decline (faster than the expected decline due to GAG accumulation in the brain), headache and epilepsy. In four patients, the SD value of the head circumferences increased before VPS placement. In one patient (MPS II, patient 6), this occurred in a relatively short time (increase from 1 to 4SD), with only slightly elevated CSF pressure measured at the time of VPS placement. In one patient (MPS VI, patient 3), head circumferences SD value declined prior to drain placement. This patient had partial closure of the lambdoid suture and complete closure of the sagittal suture with elevated CSF pressure (30-45 cm H₂O) at the time of VPS placement (fig. 2). We concluded that craniosynostosis, in combination with hydrocephalus, most likely contributed to the increased ICP in four out of the six patients with a VPS (table 3; MPS I, patients 2, 4 and 6; MPS VI, patient 3). In the fifth patient, craniosynostosis was not present (MPS II, patient 5) and in the sixth patient (MPS II, patient 6), no radiograph had been taken in the two years before shunt placement occurred. One year after VPS placement, all sutures were closed in this patient (fig. 2) suggesting this had already occurred, at least partially, before drain placement.

MPS I (Patient 6)	MPS II (Patient 5)	MPS II (Patient 6)	MPS VI (Patient 3)
5.3	7.5	2.5	5.5
Reduced concentration	Neurological decline; epilepsy	Neurological decline	Headaches
MRI: progression hydrocephalus	MRI: hydrocephalus	MRI: mild progression quadriventricular hydrocephalus	MRI: no signs hydrocephalus
NP	NP	20 mmHg	30-45 cm H ₂ O
+2SD	+2½SD	+4SD	-1SD
S	N	N	S
Yes	No	NP	Yes
Not possible: corneal clouding	NP	NP	No

Figure 3 Three illustrative cases of craniosynostosis in MPS

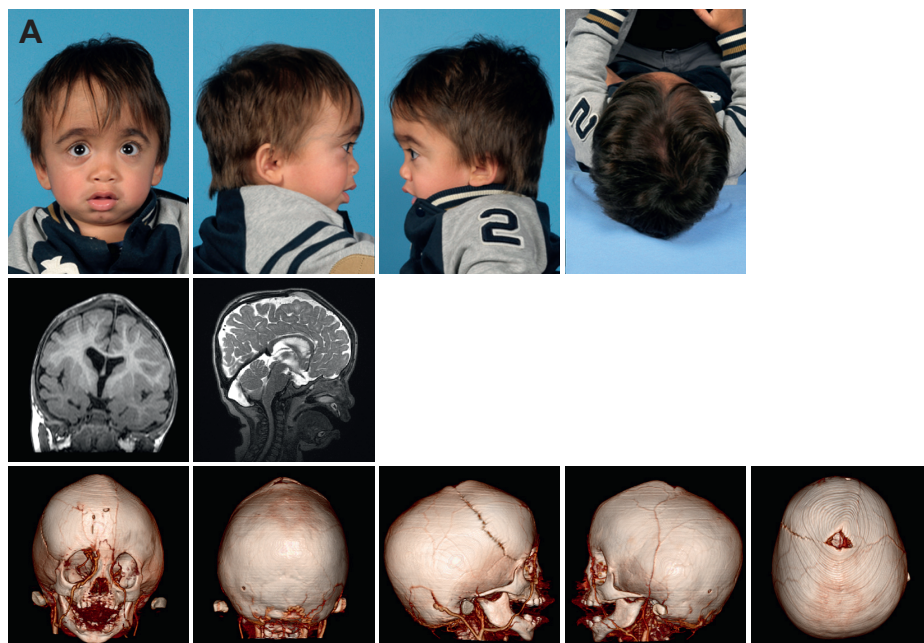


Fig. 3A) Patient 10, MPS II, 1.5 years old. Photographs show the distinct facial features, MRI T2 flair and 3D CT scan shows the bulging anterior fontanel (volcano sign) with plagiocephaly at the right anterior site of the head. 3D CT scan shows the premature closure of the left coronal suture, the sagittal suture and both lambdoid sutures.

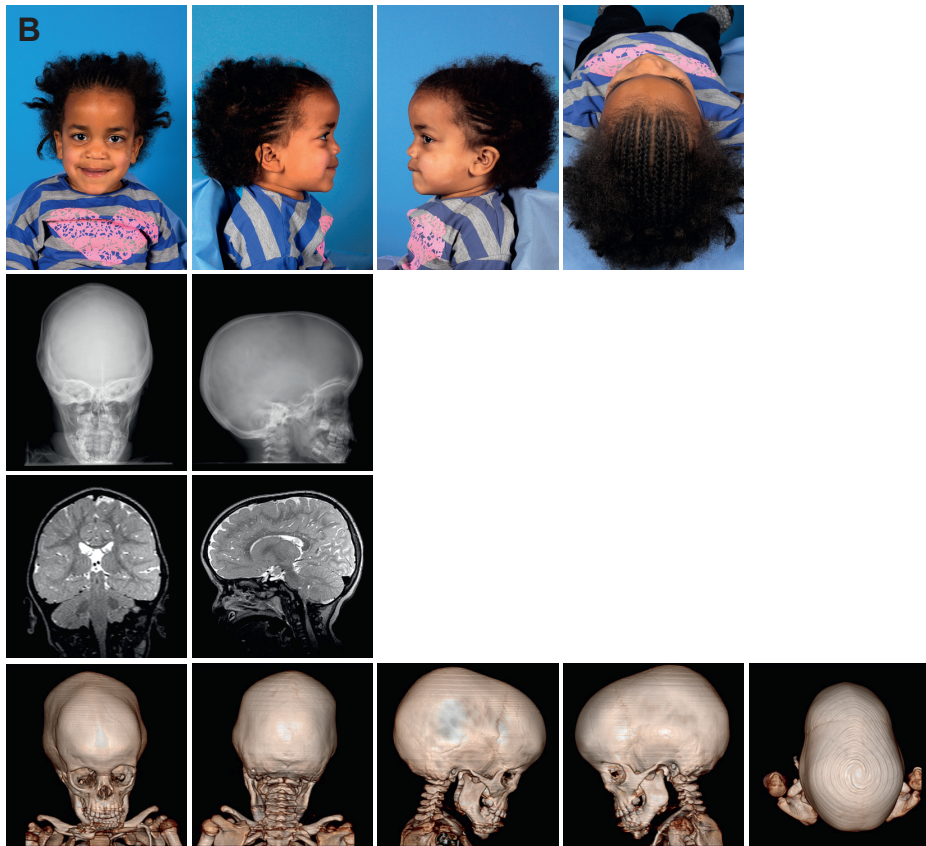
Figure 3 Continued

Fig. 3B) Patient 8, MPS VI 3.3 years old. Skull X ray shows frontal bossing and scaphocephaly. X-skull and 3D-CT scan show craniosynostosis of the metopic, both lambdoid and sagittal sutures. On MRI T2/FLAIR cerebrum there are no signs of increased ICP.

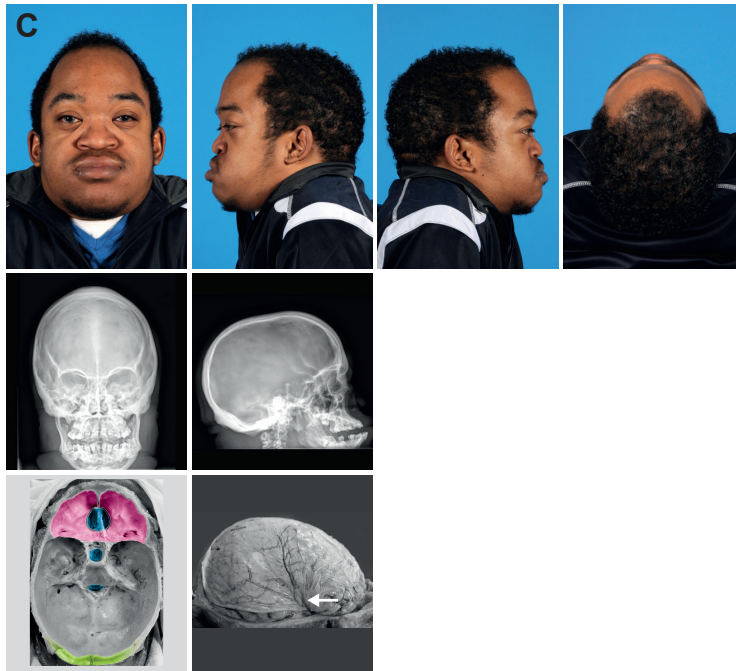
Figure 3 Continued

Fig. 3C) MPS VI patient, 24 years old. Photographs and skull X rays show distinct facial features, scaphocephaly and sinus transversus impression in the skull.

Macroscopic pictures from the autopsy at age 25 years show in red impressions of the brain gyri in the frontal bones and an abnormally thin bone layer. In blue (top to bottom), abnormally deep olfactory furrow, sella tursica and severe narrow foramen magnum. In green; thickened skull. The white arrow shows where there is an impression of the skull in the brain.

DISCUSSION

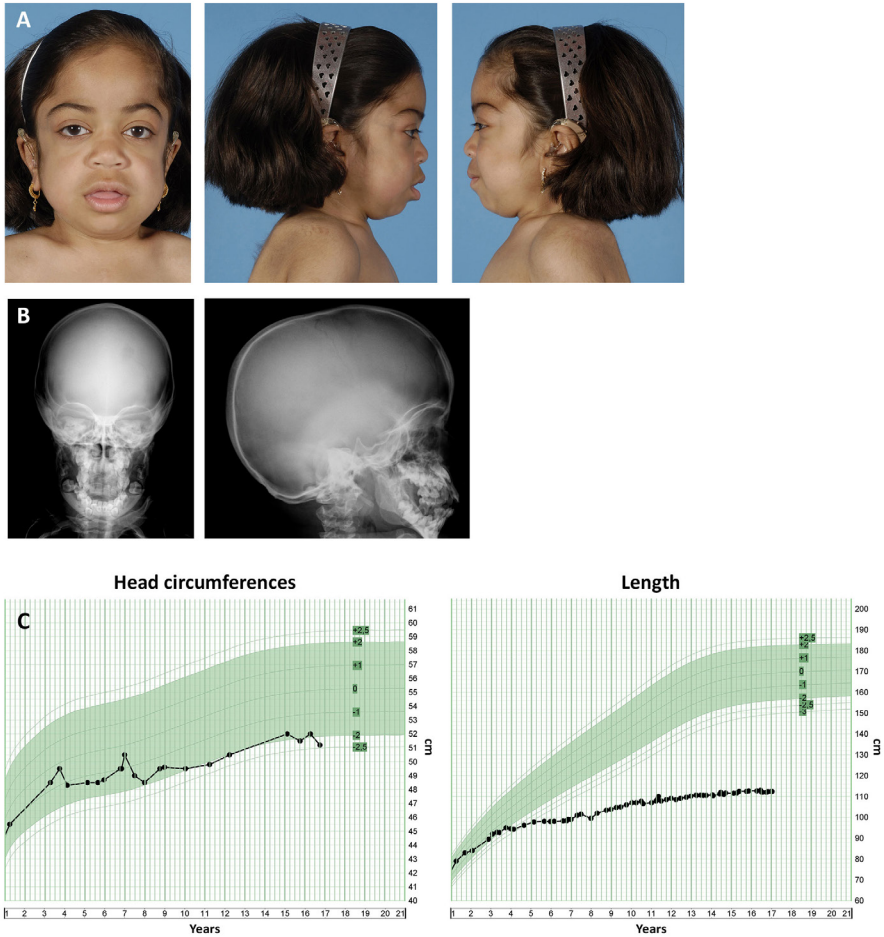
This is the first long-term prospective study assessing skull suture closure and its consequences in patients with MPS I, II, VI and VII. Our results show that craniosynostosis occurs at a very high frequency in these different types of MPS. Premature closure of at least one suture was present in 77% of patients, with suture closure occurring before age 6 in 40% of patients. In the general population, non-syndromic craniosynostosis occurs with a frequency between 0.4 and 1.0 per 1000 live births and syndromic craniosynostosis is even rarer [19-23]. The incidence found in the current study may even be an underestimation, because only one skull radiograph was available for 43% of our patients. In addition, the median follow-up was relatively short (3.4 years).

Consistent with syndromic craniosynostosis, the majority of MPS patients (66%) had early closure of more than one suture, with involvement of the lambdoid and coronal sutures [24].

An abnormal head shape resulting from early suture closure was seen in about half of all studied MPS patients with scaphocephaly and pachycephaly being the most frequently observed abnormalities. The trichonocephalic head shape resulting from early closure of the metopic suture was not present in our MPS population.

Scaphocephaly due to premature closure of the sagittal suture was often (21%) seen in the severely affected MPS I (6 patients) and MPS VI (4 patients) patients. In 13% of all MPS patients, all sutures closed at an early age (pansynostosis), with normal head shape in two patients. Pansynostosis can easily be overlooked in these children, as their small head size can be interpreted as normal due to the fact that they are often small in stature. In MPS patients in whom growth stagnation of the head occurs (example in supplemental fig. 1), further investigation is warranted regardless of whether or not this is in line with their body length growth.

In MPS, evaluation of the consequences of craniosynostosis is complicated because increased ICP in this condition is often multifactorial. Hydrocephalus in MPS arises from accumulation of GAGs in cells of the brain (ventricles, arachnoid villi), in supporting structures (meninges or spinal column), or results from venous hypertension related to the flow limiting morphological changes in the skull base (fig. 3C) and craniocervical junction [2, 25]. Moreover, the detection of clinical symptoms of raised ICP, such as visual decline or headache and nausea, can be difficult to detect, especially in the cognitively impaired patients.

Supplemental figure 1 Example of early pansynostosis in a MPS VI patient**Supplemental fig.1.** Patient 1, MPS VI, 9 years old.**A)** Photographs show the distinct facial features and the normal shape of the skull**B)** X-skull at age 6 years shows closure of all sutures.**C)** The growth curve shows the stagnation of the skull growth (from -1SD to -2SD at around the age of 6 years). Decline in height (0SD to -8.8SD) from age of 1.5 till age 17 years old.

Another pitfall in evaluation of the consequences of craniosynostosis in MPS is the assessment of increased ICP in these disorders. Papilledema is not always present in MPS patients with increased ICP (for example MPS VI patients pt. no. 3). While conversely, it can be present in patients with normal ICP as a result of GAG accumulation in the sclera or optic nerve [26, 27]. Expansion of the ventricles in response to increased ICP is often not present in MPS patients as the ventricles are stiff due to the GAG accumulation, while enlarged ventricles can be present without raised ICP in the neuronopathic MPS patients due to brain atrophy [25]. Therefore, in cases where clinical suspicion of increased ICP in MPS patients is high, thorough examination using different diagnostic modalities (including lumbar puncture and/or 24 hours ICP monitoring) should be carried out before dismissing this diagnosis.

When hydrocephalus and craniosynostosis occur in the same MPS patient, this can result in severely elevated ICP since expansion of the skull in response to increase in pressure cannot take place. This is illustrated by the examples in our studied cohort. Patient 6 with MPS II did not have craniosynostosis and his skull could, therefore, expand to +4SD in response to the occurring hydrocephalus, resulting in near normal ICP. In contrast, high ICP was found in patient 3 with MPS VI. In this patient, all sutures closed at a young age leading to skull growth stagnation. The high ICP was potentially the result of a combination of a CSF drainage problem and craniosynostosis.

In our patient cohort, craniosynostosis resulting in increased ICP also occurred in the non-neuronopathic MPS VI patients. This is demonstrated in the adult MPS VI patient in figure 3C, where the indentations of the brain in the skull, observed upon autopsy, indicate raised ICP earlier in life. In non-neuronopathic MPS patients, extensive GAG accumulation in the brain is not observed and neurocognitive development is usually described as normal [1, 28]. Interestingly, we previously described mild cognitive impairment in three MPS VI patients [29]. In this study it is shown that two of these patients had pansynostosis and one had closure of two sutures before the age of six (patients 1, 5 and 6). Whether craniosynostosis did indeed contribute to the cognitive disturbances in these patients remains to be determined by studying larger numbers of non-neuronopathic patients.

In other craniosynostosis syndromes such as Apert and Pfeiffer syndrome, suture closure occurs in utero which results in increased ICP very early in life [30, 31]. In these cases, guidelines for treatment in the form of surgical cranial vault expansion are clear [32]. In MPS, suture closure seems to occur in early childhood, thus the clinical consequences are likely to be less severe. Increased ICP in MPS can be multifactorial therefore, treatment decisions should be made on a case-by-case basis with all aspects of the disorder being taken into account. In the non-neuronopathic MPS patients, surgical cranial vault expansion

sion might be an option in early childhood. In the neuronopathic patients, placement of a VPS to decrease ICP may be the treatment of choice since ongoing neurocognitive decline due to intracerebral GAG accumulation is to be expected and surgery for craniosynostosis imposes a large burden on the child.

In order to prevent complications of craniosynostosis, we recommend monitoring skull growth by measuring head circumferences and performing radiographs of the skull yearly in both neuronopathic and non-neuronopathic MPS patients until at least the age of 6 years.

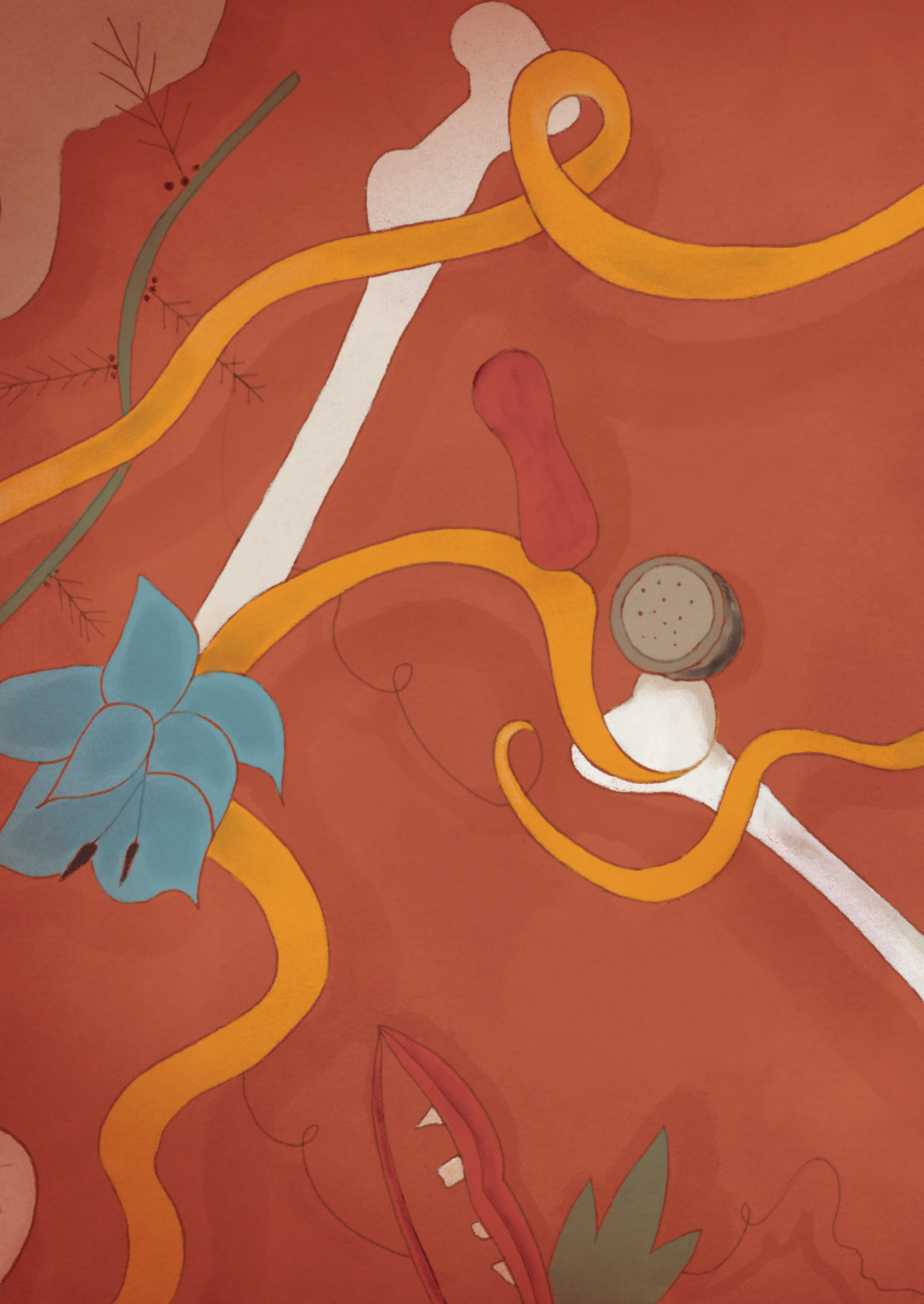
CONCLUSION

Craniosynostosis occurs in the majority of the MPS patients. Since the clinical consequences can be severe and surgical intervention is possible, skull growth and signs and symptoms of increased intracranial pressure should be monitored in both neuronopathic and non-neuronopathic patients with MPS.

REFERENCES

- [1] E.F. Neufeld, J. Muenzer, "The Metabolic Bases of Inherited Disease," McGraw-Hill, New York, 2001.
- [2] A. Dalla Corte, C.F.M. de Souza, M. Anes, R. Giuliani, Hydrocephalus and mucopolysaccharidoses: what do we know and what do we not know?, *Childs Nerv Syst*, 33 (2017) 1073-1080.
- [3] E.G. Shapiro, S.A. Jones, M.L. Escolar, Developmental and behavioral aspects of mucopolysaccharidoses with brain manifestations - Neurological signs and symptoms, *Mol Genet Metab*, 122S (2017) 1-7.
- [4] M.M. Cohen, Jr., Sutural biology and the correlates of craniosynostosis, *Am J Med Genet*, 47 (1993) 581-616.
- [5] M.M. Cohen, Jr., Craniosynostosis update 1987, *Am J Med Genet Suppl*, 4 (1988) 99-148.
- [6] H.L. Vu, J. Panchal, E.E. Parker, N.S. Levine, P. Francel, The timing of physiologic closure of the metopic suture: a review of 159 patients using reconstructed 3D CT scans of the craniofacial region, *J Craniofac Surg*, 12 (2001) 527-532.
- [7] S. Moosa, B. Wollnik, Altered FGF signalling in congenital craniofacial and skeletal disorders, *Semin Cell Dev Biol*, 53 (2016) 115-125.
- [8] J.A. Persing, J.A. Jane, M. Shaffrey, Virchow and the pathogenesis of craniosynostosis: a translation of his original work, *Plast Reconstr Surg*, 83 (1989) 738-742.
- [9] T. de Jong, N. Bannink, H.H. Bredero-Boelhouwer, M.L. van Veelen, M.C. Bartels, L.J. Hoeve, A.J. Hoozeboom, E.B. Wolvius, M.H. Lequin, J.J. van der Meulen, L.N. van Adrichem, J.M. Vaandrager, E.M. Ongkosuwito, K.F. Joosten, I.M. Mathijssen, Long-term functional outcome in 167 patients with syndromic craniosynostosis; defining a syndrome-specific risk profile, *J Plast Reconstr Aesthet Surg*, 63 (2010) 1635-1641.
- [10] M.L. Speltz, K.A. Kapp-Simon, M. Cunningham, J. Marsh, G. Dawson, Single-suture craniosynostosis: a review of neurobehavioral research and theory, *J Pediatr Psychol*, 29 (2004) 651-668.
- [11] R. Manara, E. Priante, M. Grimaldi, L. Santoro, L. Astarita, R. Barone, D. Concolino, M. Di Rocco, M.A. Donati, S. Fecarotta, A. Ficcadenti, A. Fiumara, F. Furlan, I. Giovannini, F. Lilliu, R. Mardari, G. Polonara, E. Procopio, A. Rampazzo, A. Rossi, G. Sanna, R. Parini, M. Scarpa, Brain and spine MRI features of Hunter disease: frequency, natural evolution and response to therapy, *J Inherit Metab Dis*, 34 (2011) 763-780.
- [12] J.L. Brisman, Y. Niimi, A. Berenstein, Sinus pericranii involving the torcular sinus in a patient with Hunter's syndrome and trigonocephaly: case report and review of the literature, *Neurosurgery*, 55 (2004) 433.
- [13] K. Bhattacharya, S. Balasubramaniam, Y.S. Choy, M. Fietz, A. Fu, D.K. Jin, O.H. Kim, M. Kosuga, Y.H. Kwun, A. Inwood, H.Y. Lin, J. McGill, N.J. Mendelsohn, T. Okuyama, H. Samion, A. Tan, A. Tanaka, V. Thamkunanon, T.H. Toh, A.D. Yang, S.P. Lin, Overcoming the barriers to diagnosis of Morquio A syndrome, *Orphanet J Rare Dis*, 9 (2014) 192.
- [14] J. Ziyadeh, M. Le Merrer, M. Robert, E. Arnaud, V. Valayannopoulos, F. Di Rocco, Mucopolysaccharidosis type I and craniosynostosis, *Acta Neurochir (Wien)*, 155 (2013) 1973-1976.
- [15] N. Sadashiva, P.S. Bindu, V. Santosh, B.I. Devi, D. Shukla, Mucopolysaccharidosis type I with craniosynostosis, *Neurol India*, 63 (2015) 612-615.
- [16] H.R. Taylor, F.C. Hollows, J.J. Hopwood, E.F. Robertson, Report of a mucopolysaccharidosis occurring in Australian aborigines, *J Med Genet*, 15 (1978) 455-461.
- [17] H.G. Ryoo, S.K. Kim, J.E. Cheon, J.Y. Lee, K.C. Wang, J.H. Phi, Slit ventricle syndrome and early-onset secondary craniosynostosis in an infant, *Am J Case Rep*, 15 (2014) 246-253.

- [18] R. Foo, L.A. Whitaker, S.P. Bartlett, Normocephalic panocraniosynostosis resulting in late presentation of elevated intracranial pressures, *Plast Reconstr Surg*, 125 (2010) 1493-1502.
- [19] Y. Tahiri, S.P. Bartlett, M.S. Gilardino, Evidence-Based Medicine: Nonsyndromic Craniosynostosis, *Plast Reconstr Surg*, 140 (2017) 177e-191e.
- [20] L.R. French, I.T. Jackson, L.J. Melton, 3rd, A population-based study of craniosynostosis, *J Clin Epidemiol*, 43 (1990) 69-73.
- [21] A. Shuper, P. Merlob, M. Grunebaum, S.H. Reisner, The incidence of isolated craniosynostosis in the newborn infant, *Am J Dis Child*, 139 (1985) 85-86.
- [22] S. Singer, C. Bower, P. Southall, J. Goldblatt, Craniosynostosis in Western Australia, 1980-1994: a population-based study, *Am J Med Genet*, 83 (1999) 382-387.
- [23] S.L. Boulet, S.A. Rasmussen, M.A. Honein, A population-based study of craniosynostosis in metropolitan Atlanta, 1989-2003, *Am J Med Genet A*, 146A (2008) 984-991.
- [24] S.R. Twigg, A.O. Wilkie, New insights into craniofacial malformations, *Hum Mol Genet*, 24 (2015) R50-59.
- [25] T.D. Alden, H. Amartino, A. Dalla Corte, C. Lampe, P.R. Harmatz, L. Vedolin, Surgical management of neurological manifestations of mucopolysaccharidosis disorders, *Mol Genet Metab*, 122S (2017) 41-48.
- [26] M.L. Collins, E.I. Traboulsi, I.H. Maumenee, Optic nerve head swelling and optic atrophy in the systemic mucopolysaccharidoses, *Ophthalmology*, 97 (1990) 1445-1449.
- [27] M. Beck, G. Cole, Disc oedema in association with Hunter's syndrome: ocular histopathological findings, *Br J Ophthalmol*, 68 (1984) 590-594.
- [28] V. Valayannopoulos, H. Nicely, P. Harmatz, S. Turbeville, Mucopolysaccharidosis VI, *Orphanet J Rare Dis*, 5 (2010) 5.
- [29] B.J. Ebbink, M.M. Brands, J.M. van den Hout, M.H. Lequin, R.R. Coebergh van den Braak, R.L. van de Weitgraven, I. Plug, F.K. Aarsen, A.T. van der Ploeg, Long-term cognitive follow-up in children treated for Maroteaux-Lamy syndrome, *J Inherit Metab Dis*, 39 (2016) 285-292.
- [30] I.M. Mathijssen, J. van Splunder, C. Vermeij-Keers, H. Pieterman, T.H. de Jong, M.P. Mooney, J.M. Vaandrager, Tracing craniosynostosis to its developmental stage through bone center displacement, *J Craniofac Genet Dev Biol*, 19 (1999) 57-63.
- [31] E. Lajeunie, S. Heuertz, V. El Ghouzzi, J. Martinovic, D. Renier, M. Le Merrer, J. Bonaventure, Mutation screening in patients with syndromic craniosynostoses indicates that a limited number of recurrent FGFR2 mutations accounts for severe forms of Pfeiffer syndrome, *Eur J Hum Genet*, 14 (2006) 289-298.
- [32] I.M. Mathijssen, Guideline for Care of Patients With the Diagnoses of Craniosynostosis: Working Group on Craniosynostosis, *J Craniofac Surg*, 26 (2015) 1735-1807.





ADDENDUM

SUMMARY

SUMMARY

Mucopolysaccharidosis (MPS) and mucopolipidosis (ML II and III) are lysosomal storage disorders with multisystem involvement. Several intra- and extracellular processes are activated and altered by intralysosomal glycosaminoglycan (GAG) accumulation. Skeletal abnormalities are common in MPS and ML patients and originate from GAG storage in cells of the cartilage, bones and ligaments. At present, only part of the processes involved in cartilage and bone disease in MPS and ML are well understood and there are still many uncertainties and unanswered questions regarding the mechanisms (**chapter 2 and 7**). Some of the most pressing of these questions and options for future studies to provide answers have been described in this thesis.

The pathophysiology of cartilage and bone disease in MPS and ML patients is immensely complex. Intracellularly, lysosomal GAG accumulation causes loss of cellular function by disturbed autophagy, polyubiquitination, mitochondrial dysfunction, inflammation, apoptosis and loss of lysosomal membrane integrity, followed by tissue damage and organ dysfunction (**chapter 2**).

Altered cartilage and deformed bones are the result of dysfunctional chondrocytes, bone cells and extra cellular matrix (ECM). Then, pathological processes such as abnormal biomechanical forces on deformed bones, with inflammation, finally lead to early secondary osteoarthritis, often necessitating orthopedic surgical interventions early in life (**chapter 2, 4, 5 and 7**). Clinical aspects of skeletal pathology in MPS and ML III patients, such as hip disease and craniosynostosis, are described in **chapters 4-6**.

Currently, available treatments for the MPS's do not prevent and ameliorate the abnormalities in bones and cartilage as a result of these disorders (**chapter 1 and 2**). There are no therapeutic options for ML at this time. This disease is very complicated as no lysosomal enzymes are able to enter the lysosome. Development of new, targeted treatment, or improving existing therapies is vital for both diseases.

In **chapter 2** the histological and biochemical abnormalities in bones, joints, teeth and extracellular matrix (ECM) in MPS patients are reported against the background of normal tissue-specific processes. Cellular dysfunction by intralysosomal GAG storage in connective-tissue-forming cells directly affects the composition and metabolism of the ECM. These primary events create a cascade of pathological processes that have local effects on tissue and organ function, and distant effects on systemic functions. Clinically, these pathological processes lead to growth retardation, dysostosis multiplex, osteopenia/osteoporosis, stiff joints and abnormal teeth.

Chapter 3 describes the correlation between residual IDUA activity in cultured fibroblasts and the phenotype of MPS I patients. This may provide a tool for the early prediction of the phenotype of MPS I patients when the genotype is uninformative, for instance, after detection of a novel mutation with unknown effect. This would be very helpful for patients who will be picked up at an early age through newborn screening in the near future.

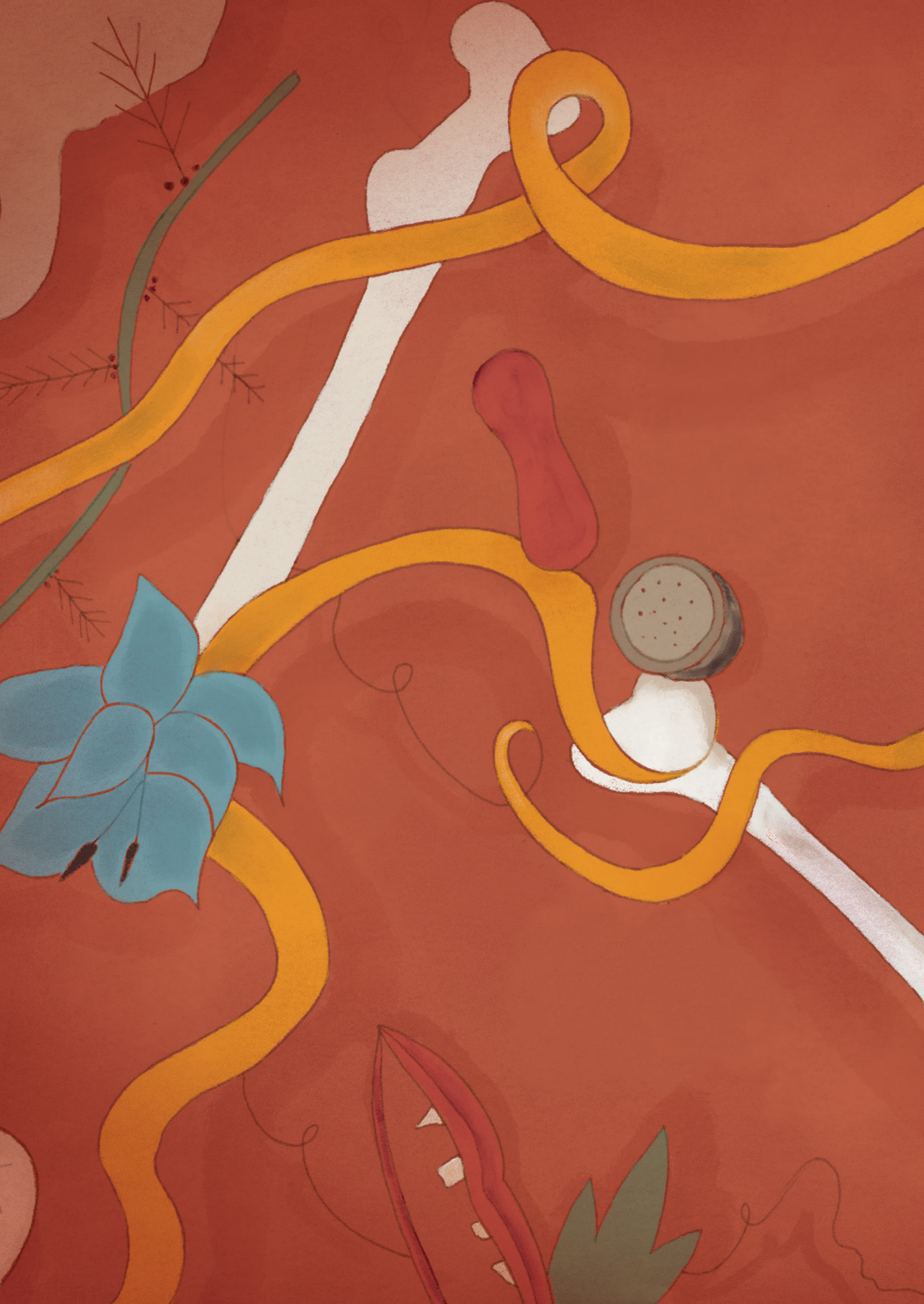
The most frequently and most severely affected part of the skeleton in MPS and ML is the hip, often from early childhood onwards. Abnormal hip development in MPS VI and adult ML III patients is described in **chapters 4 and 5**. The hip problems in all MPS VI and in almost all ML III patients finally lead to pain and to severe limitations in mobility. In MPS VI patients, clinically significant hip abnormalities develop very early in life, starting with deformities of the os ilium and acetabulum. Femoral head abnormalities occur later, most likely due to altered mechanical forces in combination with epiphyseal abnormalities due to GAG storage. The final shape and angle of the femoral head differs between individual MPS VI patients and is difficult to predict; therefore, hip surgery, both in terms of timing and type of intervention, still remains a challenge with these patients. In adult ML III patients, abnormal bone development and severe progressive osteoarthritis lead to other severe skeletal abnormalities. These patients often undergo surgical orthopedic interventions early in life (**chapter 5**).

Future therapies for ML III should focus on improving cartilage and bone quality in these patients in order to prevent skeletal complications and improve mobility.

Another severe complication of bone and cartilage disease in MPS patients is early cranial suture closure (craniosynostosis) which is described in **chapter 6**. In our study, craniosynostosis occurred in the majority of the MPS I, II, VI and VII patients. Early recognition of craniosynostosis is important as closure of cranial sutures before the age of 6 may restrict skull growth, which can lead to elevated intracranial pressure (ICP), with visual and developmental impairment. Monitoring skull growth and the signs and symptoms of increased ICP in both neuronopathic and non-neuronopathic patients with MPS is necessary, as surgical interventions are possible.

Finally, **Chapter 7** discusses and summarizes the findings of the studies, and provides new hypotheses and insights into the development of cartilage and bone disease in MPS and ML, which are relevant for future therapeutic strategies.

The pathological changes involved in cartilage and bone disease in MPS and ML starts very early in development. The fetal origin of the cartilage and bone pathology in MPS and ML patients presents a great hurdle for adequate treatment and explains the limited effects of existing therapies on skeletal complications. Besides development of innovative therapeutic strategies, future therapies should also focus on reducing pain and maintaining patient independence.



A stylized illustration on a red background. A yellow ribbon winds through the scene. In the upper left, a light-colored fetus is curled. In the lower left, a white skull is shown. In the center, a red flower with green leaves is depicted. In the lower right, a white bone is visible. The overall style is graphic and artistic.

ADDENDUM

SAMENVATTING

SAMENVATTING

Mucopolysaccharidose (MPS) en mucopolipidose (ML II en ML III) zijn lysosomale stapelingsziekten, waarbij meerdere weefsels zijn aangedaan. Verschillende intra- en extracellulaire processen worden geactiveerd of verlopen anders door glycosaminoglycanen (GAGs) stapeling in het lysosoom. Skelet afwijkingen komen vaak voor in MPS en ML patiënten en ontstaan door GAG stapeling in kraakbeencellen, botcellen en in ligamenten. Op dit moment begrijpen we slechts een deel van de betrokken processen in kraakbeen en botziekte in MPS en ML en zijn er nog steeds veel lacunes in onze kennis met betrekking tot de pathofysiologie (**hoofdstukken 2 en 7**).

Dit proefschrift beantwoordt een aantal van de meest urgente van deze vragen en opties voor toekomstige studies. De pathofysiologie van kraakbeen en botziekte in MPS en ML patiënten is immens complex.

Lysosomale GAG stapeling veroorzaakt functieverlies van cellen, verstoorde autofagie, polyubiquitinatie, mitochondriële disfunctie, inflammatie, apoptose en verlies van lysosomale membraan integriteit, gevolgd door weefsel schade en orgaan dysfunctie (**hoofdstuk 2**).

Veranderd kraakbeen en vervormde botten zijn het resultaat van disfunctie van kraakbeen- en botcellen en van de extracellulaire matrix (ECM). Daarna leiden pathologische processen, zoals abnormale biomechanische krachten op vervormde botten, en inflammatie uiteindelijk tot vroege secundaire osteoartrose, waarvoor orthopedische chirurgische ingrepen vaak al op jonge leeftijd nodig zijn (**hoofdstukken 2, 4, 5 en 7**). Klinische aspecten van skeletpathologie, zoals heupziekte en craniosynostose, in de verschillende vormen van MPS en ML III, worden beschreven in de **hoofdstukken 4 t/m 6**.

De op dit moment beschikbare therapieën voor MPS kunnen de afwijkingen in kraakbeen en botten bij deze ziekten niet voorkomen of genezen (**hoofdstuk 1 en 2**). Voor ML zijn er nog geen therapeutische opties. Deze ziekte is erg gecompliceerd, omdat vrijwel alle lysosomale enzymen niet in het lysosoom kunnen komen. De ontwikkeling van nieuwe doelgerichte therapieën of verbetering van bestaande therapieën is essentieel voor beide ziekten.

In **hoofdstuk 2** worden de histologische en biochemische afwijkingen in botten, gewrichten, tanden en ECM van MPS patiënten besproken, tegen de achtergrond van normale weefsel specifieke processen. Cellulaire disfunctie door intra-lysosomale GAG stapeling in bindweefselvormende cellen, beïnvloedt direct de samenstelling en het metabolisme

van de ECM. Deze primaire gebeurtenissen veroorzaken een cascade van pathologische processen die lokale effecten hebben op weefsels en orgaan functie en effecten op afstand op systemische functies. Klinisch leiden deze processen tot groeiachterstand, dysostosis multiplex, osteopenie/osteoporose, stijve gewrichten en abnormale tanden.

Hoofdstuk 3 beschrijft de correlatie tussen restactiviteit van iduronidase in gekweekte fibroblasten en het fenotype van MPS I patiënten. Dit kan een hulpmiddel zijn voor de vroege voorspelling van het fenotype van MPS I patiënten, wanneer het genotype niet informatief is, bijvoorbeeld na detectie van een nieuwe mutatie met onbekend effect. Dit zou in de nabije toekomst heel erg kunnen helpen voor de patiënten die op een jonge leeftijd worden opgepikt door de neonatale screening.

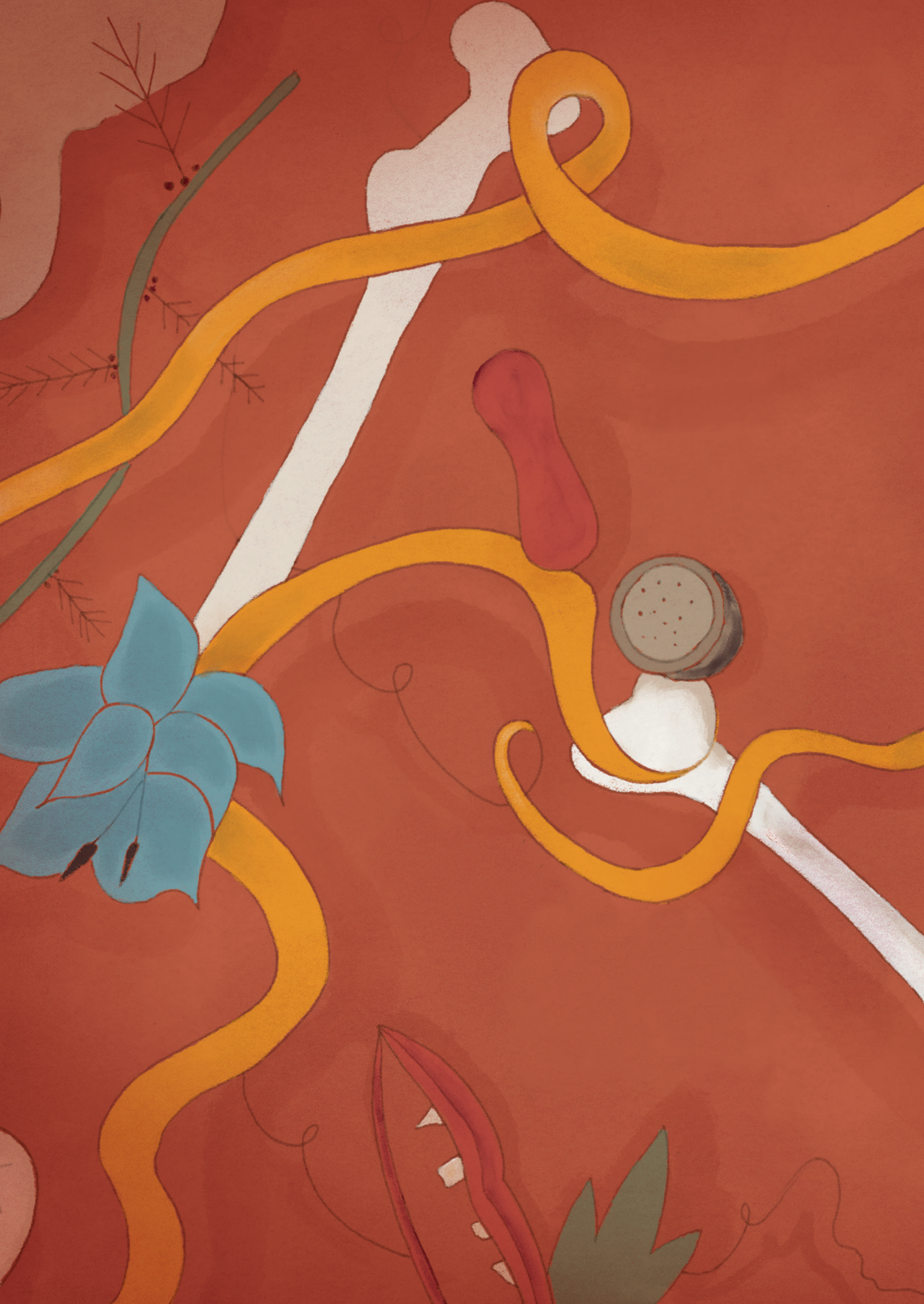
Het meest frequente en meest ernstig aangedane deel van het skelet in MPS en ML is de heup, vaak al vanaf vroege kinderleeftijd. Abnormale heupontwikkeling in MPS VI en volwassen ML III patiënten is beschreven in **hoofdstuk 4 en 5**. De heupproblemen in alle MPS VI en in bijna alle ML III patiënten leiden uiteindelijk tot pijn en tot ernstige beperkingen van de mobiliteit. In MPS VI patiënten ontwikkelen de klinisch significante heupafwijkingen zich zeer vroeg in het leven, beginnend met vervormingen van het os ileum en acetabulum. De heupkop afwijkingen volgen later, waarschijnlijk door de veranderde mechanische krachten in combinatie met epifysaire afwijkingen door GAG stapeling. De uiteindelijke vorm en hoek van de heup kop verschilt tussen de individuele MPS VI patiënten en is moeilijk te voorspellen. Daardoor blijven heupoperaties, zowel moment als type van interventie, nog steeds een uitdaging in deze patiënten.

In de volwassen ML III patiënten abnormale botontwikkeling en ernstige progressieve osteoartrose geven andere ernstige skeletafwijkingen. Vaak ondergaan deze patiënten op jonge leeftijd orthopedische operaties (**hoofdstuk 5**). Toekomstige therapieën voor ML III zouden gericht moeten zijn op verbetering van kraakbeen en botkwaliteit in deze patiënten, om zo skelet complicaties te voorkomen en mobiliteit te verbeteren.

Een andere ernstige complicatie van kraakbeen en botziekte in MPS patiënten is vroege sluiting van schedelnaden (cranosynostose) en wordt beschreven in **hoofdstuk 6**. In onze studie bleek cranosynostose voor te komen in de meeste van de MPS I, II VI en VII patiënten. Vroege herkenning van cranosynostose is belangrijk, omdat sluiting van de schedelnaden vóór de leeftijd van 6 jaar de groei van de schedel kan remmen. Dit kan leiden tot verhoogde intracraniale druk, met als gevolg visuele- en ontwikkelingsbeperking. Het monitoren van de groei van de schedel en signalen en symptomen van verhoogde intracraniale druk in zowel niet-neuronopatische als neuronopatische patiënten met MPS is noodzakelijk, omdat chirurgische interventies mogelijk zijn.

Uiteindelijk worden in **hoofdstuk 7** de resultaten van de studies bediscussieerd en samengevat en worden nieuwe hypothesen en inzichten gepresenteerd in de ontwikkeling van kraakbeen en botziekte in MPS en ML, die mogelijk van belang zijn voor toekomstige therapeutische strategieën.

De pathologische veranderingen in kraakbeen- en bot in MPS en ML ontstaan al heel vroeg tijdens de embryonale ontwikkeling. De foetale oorsprong van de kraakbeen- en botpathologie in MPS en ML patiënten zorgt voor een grote belemmering in de behandeling en verklaard de geringe effecten van de bestaande therapieën op de skeletcomplicaties. Toekomstige behandelingen zullen zich naast het ontwikkelen van vernieuwde therapeutische strategieën zich ook moeten focussen op het verminderen van pijn en het handhaven van zelfstandigheid van de patiënten.





ADDENDUM

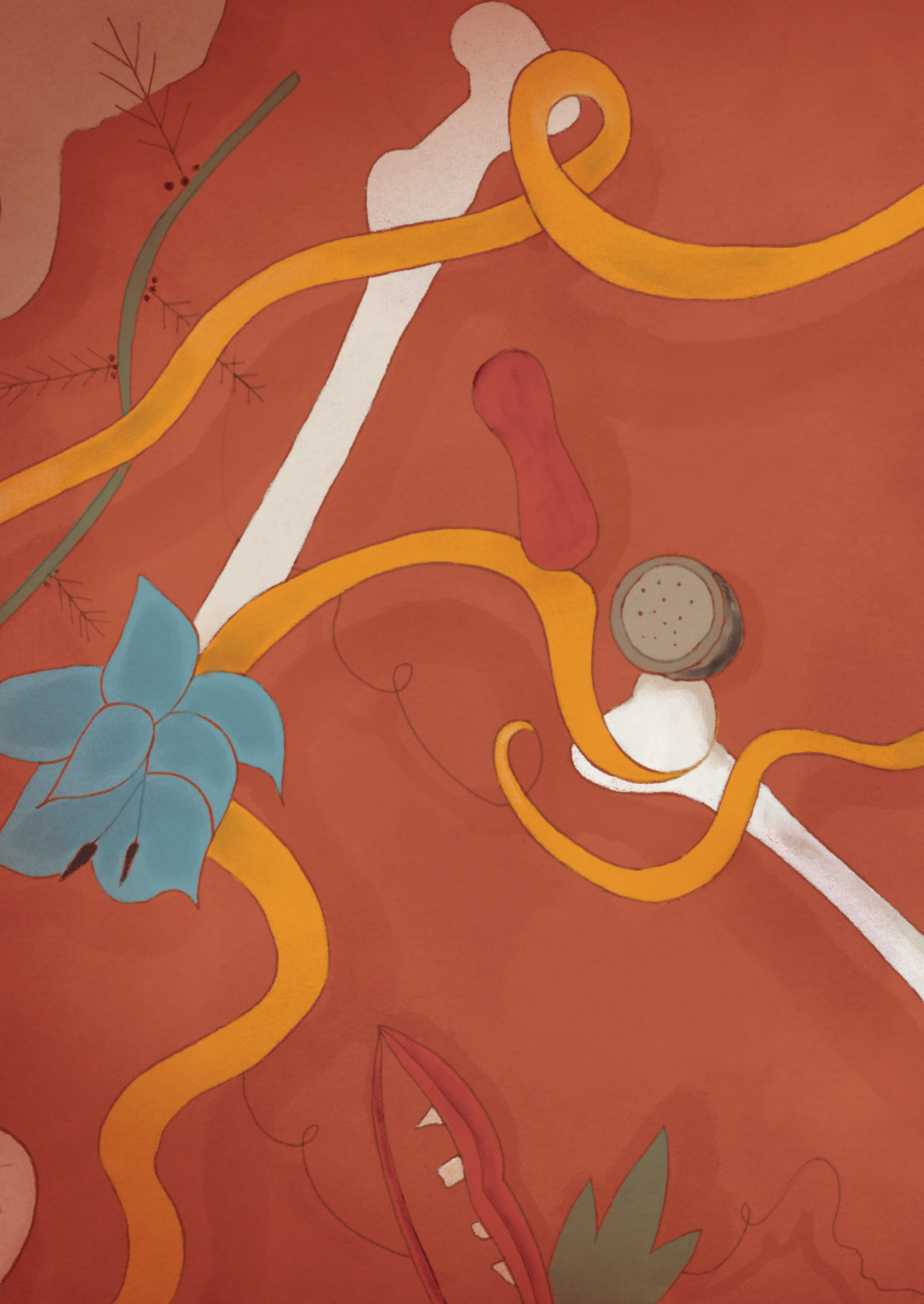
DANKWOORD



**WAAROM
MOEILIK DOEN**

**ALS HET
SAMEN KAN**

- Loesje -





ADDENDUM

PORTFOLIO

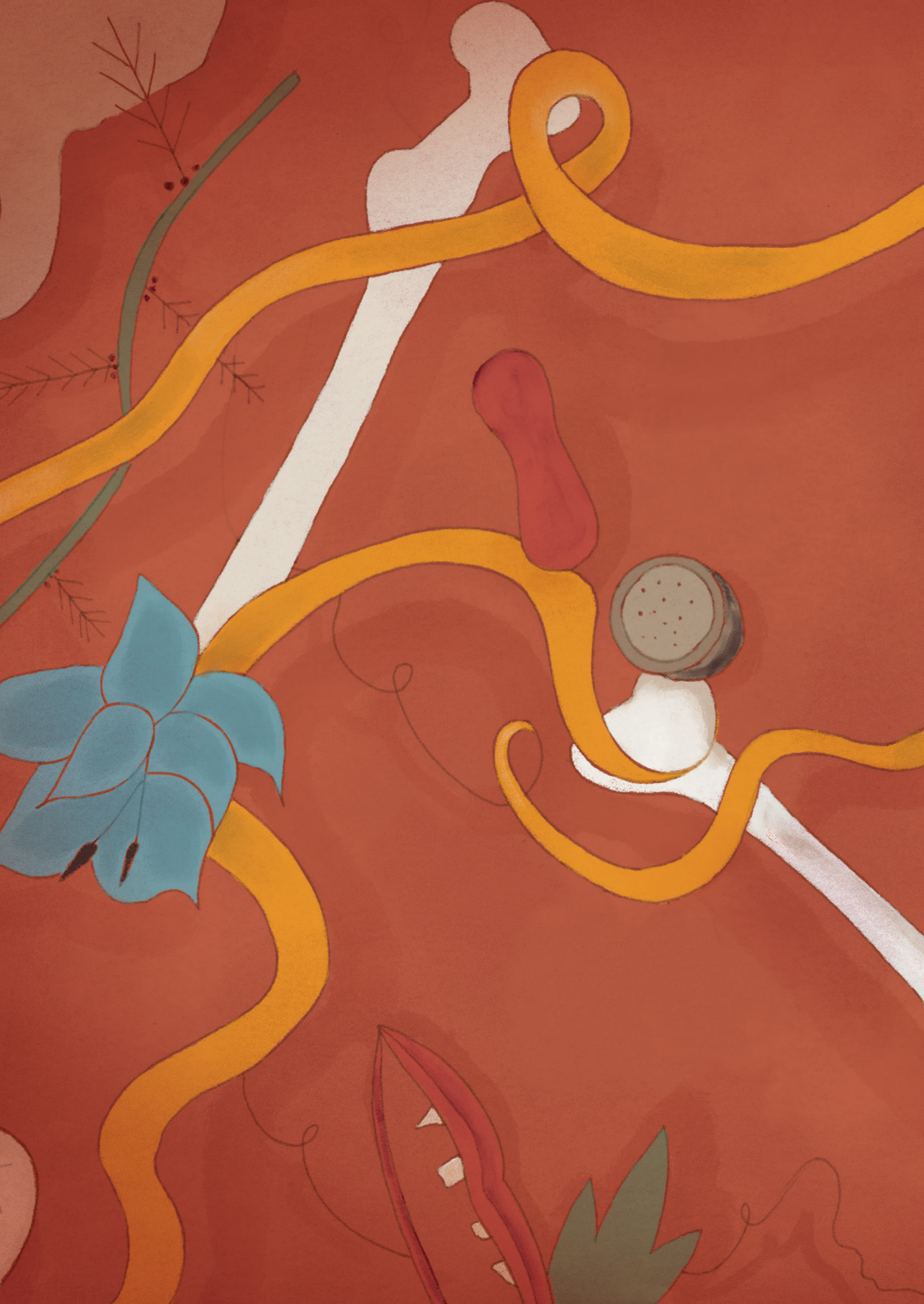
PORTFOLIO

PhD training		
	Year	Workload (ECTS)
Courses - general		
Basis cursus regelgeving en management (BROK)	2017	0.9
Integrity in Medical Research	2016	2.0
Courses - other		
Pompe disease expert day, Rotterdam	2010	0.5
11 th Postgraduate Course on LSD's Nierstein	2010	1.2
Orphan lysosomal storage disease 2e advanced level: European metabolic course 4 th inborn errors in neonatology	2010	1.0
SSIEM academy	2011	0.5
Updates On Neurometabolic Disorders	2014	0.5
17 th Postgraduate Course on LSD's Nierstein	2018	0.3
Presentations and International conferences		
MPS patient day Amersfoort (oral presentation)	2011	1.0
MPS patient day Amersfoort (oral presentation)	2012	1.0
12 th international Symposium on Mucopolysaccharide and Related Diseases, Noordwijkerhout (1e price poster presentation)	2012	0.5
13 th international Symposium on Mucopolysaccharide and Related Diseases, Brazil (poster presentation)	2014	1.0
Bot congress van de NVCB	2014	0.5
Grandround 2014 Erasmus MC-Sophia (oral presentation)	2014	1.0
14 th international Symposium on Mucopolysaccharide and Related Diseases, Bonn, Germany (poster presentation)	2016	1.0
11 th Scientific symposium on Niemann-Pick disease Type C (NP-C): Continuing our 10-year voyage of discovery	2018	0.5
17 th Postgraduate Course on LSD's (oral presentation)	2018	1.0
14 th annual WORLD symposium, San Diego (poster presentation)	2018	0.3
SSIEM annual meeting Athens	2018	0.5

Teaching tasks		
Lysosomal storage disease education for nursing staff (yearly)	2011-2018	1.0
Lysosomal storage disease education for junior doctors throughout the year (roughly 1-2 hours a week)	2009-2018	1.0
Lecture on recognition of lysosomal storage diseases for child orthopedics	2013	0.5
Voordracht AMC 'Craniostenosis affects the majority of mucopolysaccharidosis patients and can contribute to increased intracranial pressure'	2018	0.5
Onderwijs arts-assistenten over metabole ziekten	2018	0.5
Other tasks		
The PhD project was combined with my duties as a metabolic pediatrician	2012-2018	
Involved in the palliative care team of the ErasmusMC-Sophia weekly 3 hours	2017	2.0
Training kinderpalliatieve zorg	2017	0.5
Research skills		
Certified Biologist, University of Amsterdam	1992-1997	
Research at the Department of Neurogenetics Academic Medical Centrum at Amsterdam	1998-1999	
Fellowship Inborn Errors of Metabolism Department Metabolic Diseases Erasmus MC-Sophia Rotterdam	2009-2012	
Research meetings		
Internal Research meetings, Department Clinical Genetics	2011-2018	2.0
De Vereniging tot bevordering onderzoek Erfelijke Stofwisselingsziekten (ESN)	2010-2018	8.0

ECTS European Credit Transfer and Accumulation System

1 ECTS= 28 hours



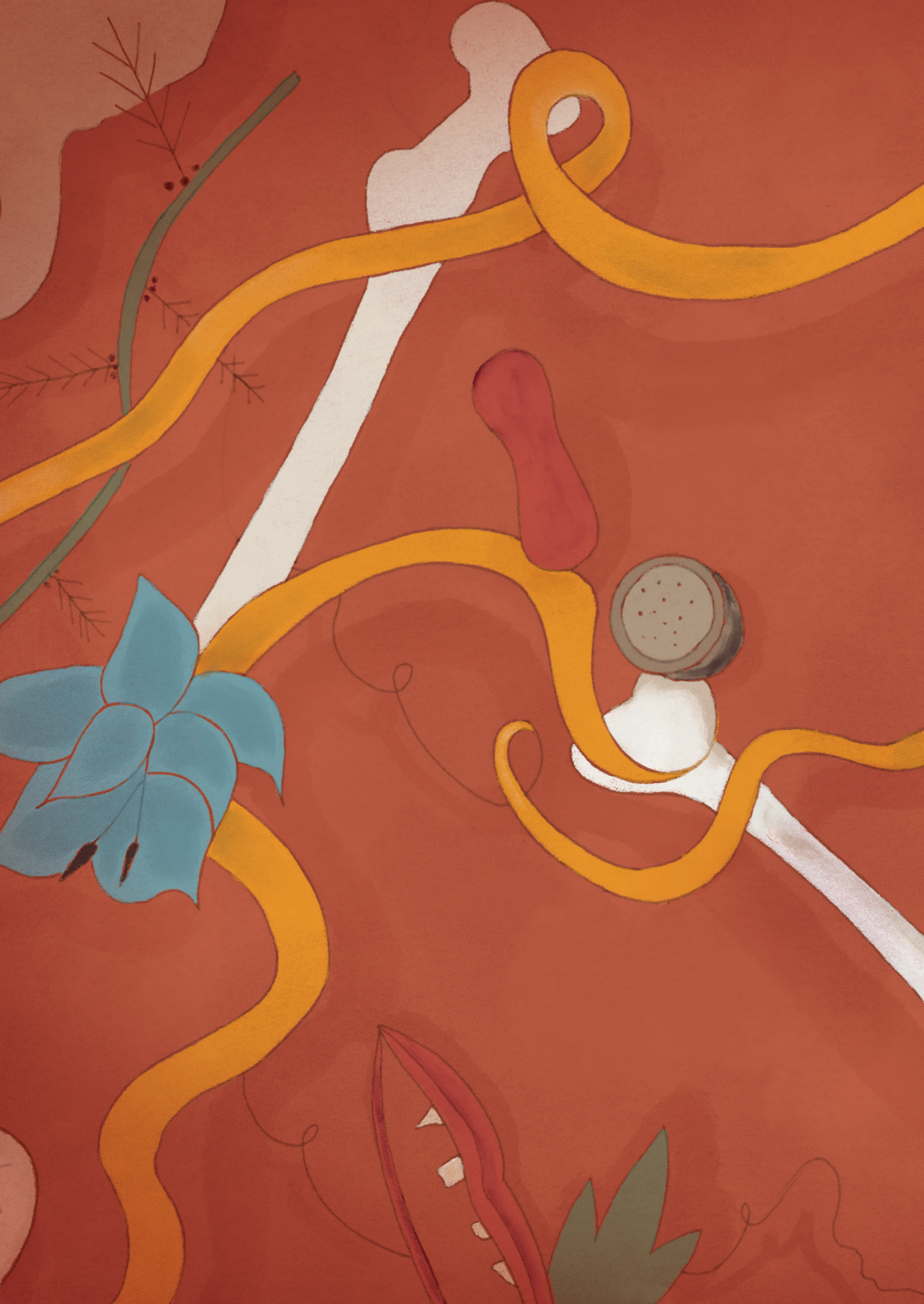


ADDENDUM

CURRICULUM VITAE

CURRICULUM VITAE

Esmee Oussoren is geboren op 7 mei 1973 in Zaandam. In Haarlem doorliep ze haar school-carrière op het Eerste Christelijk Lyceum. Hier haalde zij in 1992 haar VWO diploma. Hierna ging zij Biologie studeren aan de Anna 's Hoeve aan de Universiteit van Amsterdam. Na het derde studie jaar ging zij geneeskunde studeren aan de Universiteit van Amsterdam. In 1997 voltooide ze haar Biologie studie. Voor deze studie deed zij in 1995 haar wetenschappelijke stage bij de vakgroep van de Kindergastroenterologie in het Academisch Medisch Centrum (AMC) in Amsterdam. Tijdens haar geneeskunde studie deed ze wetenschappelijk onderzoek bij de Neurogenetica afdeling in het AMC. Meerdere publicaties volgden, waar zij ook medeauteur op was. In 2002 ronde zij haar geneeskunde studie af. Hierna werkte zij in het Spaarne ziekenhuis in Haarlem bij de afdeling Interne en als ANIOS kindergeneeskunde in het Bronovo ziekenhuis in de Haag. In 2003-2004 was zij ANIOS kindergeneeskunde in het Erasmus MC-Sophia kinderziekenhuis. In dit ziekenhuis vervolgde zij haar opleiding tot kinderarts tot en met 2009 en werkte daarna 1 jaar als supervisor op de kinderafdeling. Vanaf deze tijd startte zij met haar fellowship als kinderarts bij de afdeling metabole ziekten, bij het Centrum voor Metabole en Lyosomale ziekten, onder leiding van Prof. Dr. A.T. van der Ploeg. In 2012 beëindigde zij haar fellowship en kreeg zij een plek als stafarts op dezelfde afdeling. Vanaf 2012 is zij gestart met haar promotie traject bij dezelfde afdeling onder begeleiding van Prof. Dr. A.T. Van der Ploeg (promotor), dr. G.J.G. Ruijter (copromotor) klinisch chemicus bij de afdeling Klinische Genetica in het Erasmus MC en dr. M. Langeveld (copromotor) internist, bij de afdeling Endocrinologie en Metabolisme, Amsterdam Universiteit Medisch Centrum locatie AMC. Hiervan hebben jullie het resultaat in handen.



A stylized illustration on a red background. In the upper left, a light-colored fetus is curled. A thick yellow ribbon winds across the scene. In the lower left, a white skull is shown. To the right, a red flower with green leaves is depicted. Further right, a white egg with a crack is visible. In the bottom left corner, there is a small circular object with holes and a white bone. The overall style is graphic and artistic.

ADDENDUM

LIST OF PUBLICATIONS

LIST OF PUBLICATIONS

Deden AC, van Slegtenhorst MA, Ruijter GJG, Schoonderwoerd GC, Huidekoper HH, **Oussoren E**, Brooks AS, Demirdas S: Molecular characterization of MPS IIIA, MPS IIIB and MPS IIIC in Tunisian patients. *Clin Chim Acta* 2018, Sep;484:231.

Oussoren E, Mathijssen IMJ, Wagenmakers M, Verdijk RM, Bredero-Boelhouwer, van Veelen-Vincent, van der Meijden JC, van den Hout JMP, Ruijter GJG, van der Ploeg AT, Langeveld M: Craniosynostosis affects the majority of mucopolysaccharidosis patients and can contribute to increased intracranial pressure. *J Inherit Metab Dis* Online: 06 August 2018.

Oussoren E, van Eerd D, Murphy E, Lachmann R, van der Meijden JC, Hoefsloot LH, Verdijk R, Ruijter GJG, Maas M, Hollak CEM, Langendonk JG, van der Ploeg AT, Langeveld M: Mucopolipidosis type III, a series of adult patients. *J Inherit Metab Dis* 2018, 41(5):839-848.

Haskovic M, Poot WJ, van Golde RJT, Benneheij SH, **Oussoren E**, de Wert G, Krumeich A, Rubio-Gozalbo ME: Intrafamilial oocyte donation in classic galactosemia: ethical and societal aspects. *J Inherit Metab Dis* 2018, 41(5):791-797.

Oussoren E, Bessems J, Pollet V, van der Meijden JC, van der Giessen LJ, Plug I, Devos AS, Ruijter GJG, van der Ploeg AT, Langeveld M: A long term follow-up study of the development of hip disease in Mucopolysaccharidosis type VI. *Mol Genet Metab* 2017, 121(3):241-251.

Ardemani G, Govaert P, **Oussoren E**, Dorresteijn E, Wildschut E, Lequin M, Dudink J: Crystal clear cerebral ultrasound images mimicking acute asphyxia in an infant with primary hyperoxaluria. *Eur J Paediatr Neurol* 2017, 21(5):792-794.

Vollebregt AAM, Hoogeveen-Westerveld M, Kroos MA, **Oussoren E**, Plug I, Ruijter GJ, van der Ploeg AT, Pijnappel W: Genotype-phenotype relationship in mucopolysaccharidosis II: predictive power of IDS variants for the neuronopathic phenotype. *Dev Med Child Neurol* 2017, 59(10):1063-1070.

Rutten M, Ciet P, van den Biggelaar R, **Oussoren E**, Langendonk JG, van der Ploeg AT, Langeveld M: Severe tracheal and bronchial collapse in adults with type II mucopolysaccharidosis. *Orphanet J Rare Dis* 2016, 11:50.

Langereis EJ, Wagemans T, Kulik W, Lefeber DJ, van Lenthe H, **Oussoren E**, van der Ploeg AT, Ruijter GJ, Wevers RA, Wijburg FA *et al*: A Multiplex Assay for the Diagnosis of Mucopolysaccharidoses and Mucolipidoses. *PLoS One* 2015, 10(9):e0138622.

Hagen J, te Brinke H, Wanders RJ, Knecht AC, **Oussoren E**, Hoogeboom AJ, Ruijter GJ, Becker D, Schwab KO, Franke I *et al*: Genetic basis of alpha-aminoacidic and alpha-ketoadipic aciduria. *J Inherit Metab Dis* 2015, 38(5):873-879.

Brands MM, Gungor D, van den Hout JM, Karstens FP, **Oussoren E**, Plug I, Boelens JJ, van Hasselt PM, Hollak CE, Mulder MF *et al*: Pain: a prevalent feature in patients with mucopolysaccharidosis. Results of a cross-sectional national survey. *J Inherit Metab Dis* 2015, 38(2):323-331.

Brands MM, Frohn-Mulder IM, Hagemans ML, Hop WC, **Oussoren E**, Helbing WA, van der Ploeg AT: Mucopolysaccharidosis: cardiologic features and effects of enzyme-replacement therapy in 24 children with MPS I, II and VI. *J Inherit Metab Dis* 2013, 36(2):227-234.

Brands MM, **Oussoren E**, Ruijter GJ, Vollebregt AA, van den Hout HM, Joosten KF, Hop WC, Plug I, van der Ploeg AT: Up to five years experience with 11 mucopolysaccharidosis type VI patients. *Mol Genet Metab* 2013, 109(1):70-76.

Oussoren E, Keulemans J, van Diggelen OP, Oemardien LF, Timmermans RG, van der Ploeg AT, Ruijter GJ: Residual alpha-L-iduronidase activity in fibroblasts of mild to severe Mucopolysaccharidosis type I patients. *Mol Genet Metab* 2013, 109(4):377-381.

Oussoren E, Brands MM, Ruijter GJ, van der Ploeg AT, Reuser AJ: Bone, joint and tooth development in mucopolysaccharidoses: relevance to therapeutic options. *Biochim Biophys Acta* 2011, 1812(11):1542-1556.

Oussoren E, Bindels-de Heus GC: [Diagnostic image (395). A girl with failure to thrive and abdominal distension] Diagnose in beeld (395). Een meisje met groeivertraging en een bolle buik. *Ned Tijdschr Geneesk* 2008, 152(45):2456.

de Haas T, **Oussoren E**, Grajkowska W, Perek-Polnik M, Popovic M, Zdravec-Zaletel L, Perera M, Corte G, Wirths O, van Sluis P *et al*: OTX1 and OTX2 expression correlates with the clinicopathologic classification of medulloblastomas. *J Neuropathol Exp Neurol* 2006, 65(2):176-186.

Michiels EM, **Oussoren E**, Van Groenigen M, Pauws E, Bossuyt PM, Voute PA, Baas F: Genes differentially expressed in medulloblastoma and fetal brain. *Physiol Genomics* 1999, 1(2):83-91.

Van Klinken BJ, Van Dijken TC, **Oussoren E**, Buller HA, Dekker J, Einerhand AW: Molecular cloning of human MUC3 cDNA reveals a novel 59 amino acid tandem repeat region. *Biochem Biophys Res Commun* 1997, 238(1):143-148.

van Klinken BJ, **Oussoren E**, Weenink JJ, Strous GJ, Buller HA, Dekker J, Einerhand AW: The human intestinal cell lines Caco-2 and LS174T as models to study cell-type specific mucin expression. *Glycoconj J* 1996, 13(5):757-768.

Van Klinken BJ, **Oussoren E**, Weenink JJ, Buller HA, Dekker J, Einerhand AW: Mucin expression in colon adenocarcinoma cell lines. *Biochem Soc Trans* 1995, 23(4):529S.